2015-03-01

Reducing Drifts in Buckling Restrained Braced FramesThrough Elastic Stories

Jennifer Lorraine Craft
Brigham Young University - Provo

Reducing Drifts in Buckling Restrained Braced Frames Through Elastic Stories

Jennifer Lorraine Craft

A thesis submitted to the faculty of
Brigham Young University
in partial fulfillment of the requirements for the degree of

Master of Science

Paul W. Richards, Chair
Fernando S. Fonseca
Richard J. Balling

Department of Civil and Environmental Engineering

Brigham Young University

March 2015

ABSTRACT

Reducing Drifts in Buckling Restrained Braced Frames
Through Elastic Stories

Jennifer Lorraine Craft
Department of Civil and Environmental Engineering, BYU
Master of Science

It is possible to reduce residual and maximum drifts in buildings by adding "elastic stories" that engage gravity columns in seismic response. An elastic story is a story wherein the buckling restrained brace frame (BRBF) size is increased to prevent yielding when an earthquake occurs. Buildings ranging from 4–16 stories were designed with various elastic story brace sizes and locations to determine the optimal combination to best reduce drifts. Gravity column stiffnesses were also varied in elastic story buildings to determine the effects on drifts. Computer models were used to analyze these buildings under a suite of earthquakes.

Adding elastic stories reduce residual drifts 34% to 65% in 4- to 16-story BRBF buildings. General recommendations are made to achieve optimal reductions in drifts. For buildings with six or more stories, drifts were generally reduced most when an elastic story was added to every 4^{th} story starting at level 1 (the bottom story). The most effective size for the braces in the elastic story appears to be three times the original brace size. For buildings with less than six stories, adding a three times elastic story to the bottom level was observed to reduce drifts the most. Further research is also recommended to confirm the optimal location and size of elastic stories for buildings with differing number of stories. Increasing gravity column stiffnesses in buildings with elastic stories helps to further reduce drifts, however it may not be economical. Residual drifts were observed to decrease significantly more than maximum drifts when elastic stories were added to buildings. Maximum drifts generally decreased at some levels, but also increased at others when elastic stories were used.

Keywords: residual drift, buckling restrained braced frame, elastic story, gravity column

ACKNOWLEDGEMENTS

I wish to convey my gratitude for the many people who have assisted in the completion of my thesis project. First, to my graduate advisor, Dr. Richards, I would like to express my deepest gratitude for his encouragement, patience, understanding, and continual motivation to contribute quality work. Additionally, I would like to thank my graduate committee members Dr. Balling and Dr. Fonseca for their support. I would like to thank my peers for their continual support in encouraging, listening, and answering questions. Specifically, I would like to thank Joseph Eixenberger for his help in running parts of the analyses. Finally, I would like to express my deepest appreciation for my husband, Spencer Craft, for his unfailing love and support.

TABLE OF CONTENTS

LIST OF TABLES

LIST OF FIGURES

1 INTRODUCTION

1.1 Background

The intent of current building codes is to prevent building collapse during severe earthquakes, while allowing for some structural and nonstructural damage to occur. This controlled structural damage (yielding of the building) results in significant energy dissipation, which helps keep people safe. However, the inelastic response also results in residual drifts, or permanent horizontal displacements, of structural members. If residual drifts are greater than 0.5%, the building may not be repairable [1]. Therefore, it is desirable to develop economic building systems with minimal or no residual drifts.

Several lateral force resisting systems are available for use in steel buildings. Steel braced frames tend to be the most economical, but conventional braced frames have limited ductility because the braces buckle. Steel moment frames do not have braces, but tend to be more expensive because they require rigid connections (welded or bolted) and much more material. There are different classifications of steel moment frames: Special Moment Frames (SMFs), Intermediate Moment Frames (IMFs), and Ordinary Moment Frames (OMFs). The differences between the special, intermediate, and ordinary MFs are the detailing requirements [2]. Some buildings have dual systems that incorporate both braced and moment frames.

Buckling restrained braced frames (BRBFs) are a relatively new type of braced frame that have better ductility than conventional braced frames. BRBFs rely on special braces to withstand lateral forces caused by wind and earthquakes. These special braces have a special

encasement around a steel core that prevents the core from buckling or moving out of place. Figure 1-1a shows the inside casing of a buckling restrained brace and Figure 1-1b shows the outside of the brace [3].

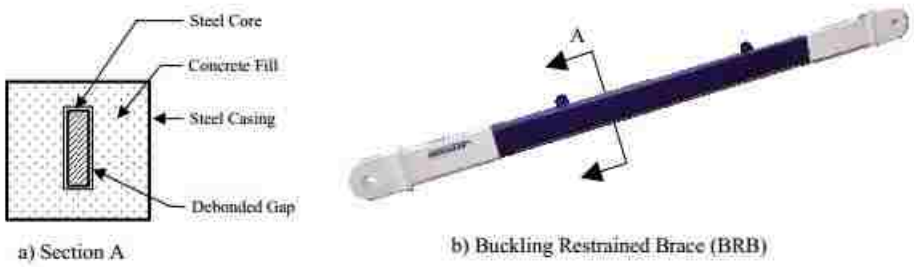

Figure 1-1. Typical buckling restrained braced frame[3].

Drifts are a common weakness of moment and braced frame systems. Moment frame beams and columns are often sized for drift control rather than strength, thus making them larger and heavier than most braced frame systems [2]. Still, braced frames as well as moment framed systems tend to have relatively high drifts. There are two types of drifts of interest to engineers: residual drifts, which are the permanent horizontal displacements from earthquakes or heavy winds, and maximum drifts, which are the maximum displacements that occur during the maximum considered earthquake (MCE). In buildings these drifts can cause the structure to be out of alignment on several floors, make people feel unsafe, and often jeopardize the structural integrity of the building.

Dual systems, which typically combine two types of lateral force resisting systems, can be used to reduce drifts in buildings. Previous studies [4][5][6], discussed in the literature review, have identified several benefits of steel dual systems. Most steel dual systems consist of braced frames [concentric braced frames (CBFs), eccentrically braced frames (EBFs), or

buckling restrained braced frames (BRBFs)] acting in parallel with secondary moment resisting frames (MRFs). The secondary moment frames help distribute inelastic demands over all stories, preventing concentrated drifts at any one story. In addition, inelastic response of the secondary frames can contribute to energy dissipation. Multiple studies [4][5][6] have shown that secondary moment frames reduce residual drifts in steel dual systems. Overall, steel dual systems control story drifts better than single braced frame systems, but large drifts are still expected during the maximum considered earthquake (MCE). Although dual systems decrease residual drifts better than single braced frame systems, the cost of dual systems is much more expensive.

Another type of dual system that has been explored utilizes gravity columns as a secondary system paired with BRBFs. Gravity columns are the columns in a steel structure that support the dead and live loads in the structure. Gravity columns have insignificant lateral stiffness and thus, have little contribution to the resistance of lateral loads. Therefore, they are not considered as part of the lateral force resisting system. However, gravity columns may be engaged as part of a dual system so that some lateral resistance can be obtained, helping reduce the amount of steel needed to resist lateral loads. Such systems may be more economical because they do not require special moment resisting connections and are more efficient because all of the columns in the building participate in the lateral response in all directions of loading. The redundancy of the system resembles more of a traditional seismic design, where all components are involved in the response.

Figure 1-2 shows the first type of dual system discussed herein: braced frames paired with MRFs. Figure 1-2a shows a plan view of a typical building with the bold lines representing the resisting bays of the dual system. The two outer bays are braced frames where the three middle bold bays are moment frames. Figure 1-2b shows a side view of how the dual system

works with the gravity columns (non-lateral resisting steel) of the building. The first system is the braced frames on the far left, the second system is the moment frames in the middle, and the third system is the gravity columns on the far right. Figure 1-2c shows the model being subject to lateral forces. In this system the gravity columns are essentially passive and do not contribute to the resistance of lateral loads [7].

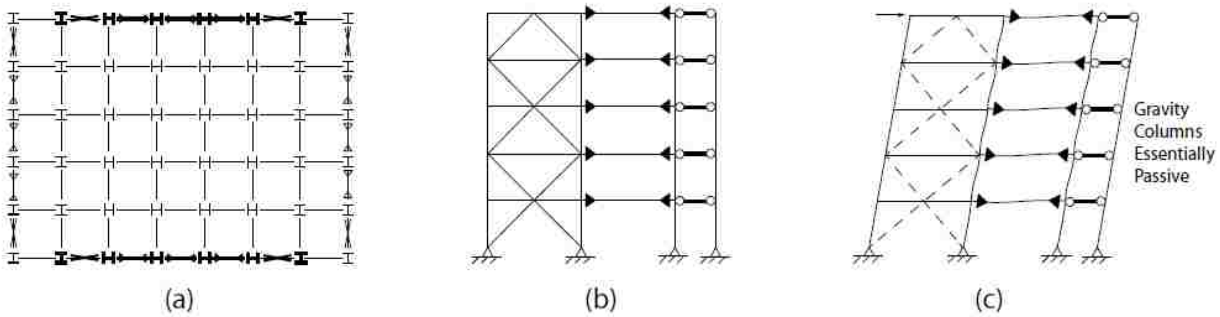

Figure 1-2. Dual system with braced frames and MRFs: (a) plan view indicating lateral force resisting bays; (b) 2-D model of braced frames paired with MRFs with gravity columns represented on right; (c) Model with lateral force acting on structure[7].

In order to activate the gravity columns to help contribute in lateral resistance, elastic stories are created by adding large braces to at least one story in the building as shown in Figure 1-3. An elastic story is a level that has oversized braces that are designed not to yield under lateral loads. Because they do not yield, the elastic stories have relatively little story deformation. In Figure 1-2(c), the gravity columns (represented by the element on the right), have no lateral stiffness because they are pinned at the base. The elastic story creates a constraint at two locations in the gravity columns [Figure 1-3(c)], the top and bottom of the elastic story. In essence, the continuous gravity column can cantilever from the elastic story and resist lateral forces through shear and bending. This process uses active lateral resisting gravity columns as a secondary system paired with braced frames to create a less expensive dual system.

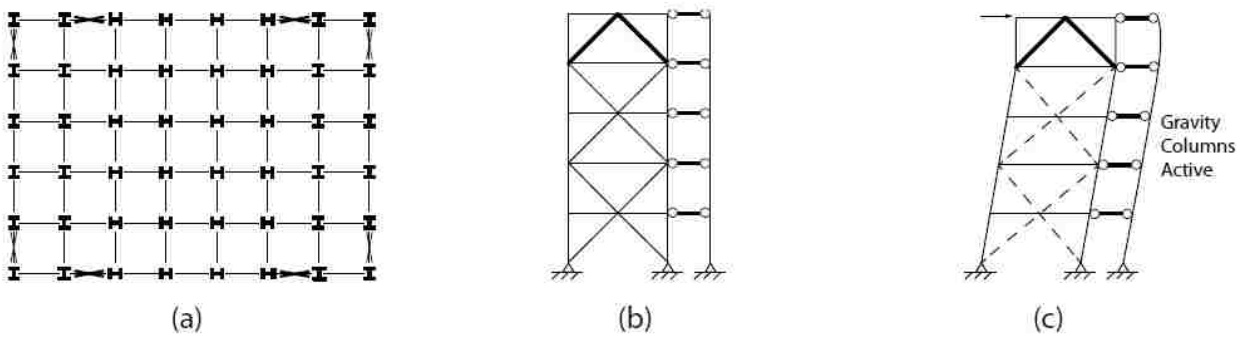

Figure 1-3. Proposed dual system with BRBF paired with gravity columns: (a) plan view all vertical elements are part of the lateral force resisting system; (b) 2-D model of BRBFs paired with gravity columns on right; (c) gravity columns are active in response to constraint at one or more elastic stories[7].

The research presented in this thesis investigated different configurations of elastic stories to determine the optimal location and size of elastic stories to best reduce drifts in BRBF buildings. Specifically, the effects of elastic stories were investigated on 4-, 6-, 8-, 12-, and 16-story buildings. For each of these buildings, various locations and sizes of elastic stories were explored. Additionally, differing sizes of gravity columns were explored to identify effective ways to help reduce residual and maximum drifts.

1.2 **Outline**

This thesis is organized into five chapters. This chapter has introduced the topic while Chapter 2 presents related studies from the literature. Topics reviewed include, residual drifts, buckling restrained braced frames, self-centering systems, and dual systems. Chapter 3 describes the methods used to complete this research, including frame and building design, frame modeling, procedures for analyses, and outputs from analyses. Chapter 4 presents results of this research. General trends are discussed for specific buildings analyzed (4-story, 6-story, etc.). Finally, chapter 5 summarizes overall conclusions and trends evident from this research.

2 LITERATURE REVIEW

Previous research on seismic resistant buildings gives further background for this research. Additionally, research completed on BRBFs provides insight into the importance of this research.

2.1 Residual Drifts

2.1.1 Permissible Residual Deformation Levels for Building Structures

McCormick et al. [8] researched residual deformation and determined that it needs to be considered as a limit state with performance-based seismic design. Permissible residual drift levels were developed based on functionality, construction tolerances, and safety. Also, an extensive literature review was conducted to confirm the importance of residual drifts, determine occupant's perspective of residual drifts, and determine approximate drift limits. In addition, floor inclinations and column tilt of an occupied 40 year old structure were investigated to confirm findings.

The main findings suggest that for all three categories (functionality, construction tolerances, and safety) a standard permissible residual drift level of 0.005 rad can be defined for both column tilt and beam inclination. This value can be used as a starting point for considering suitable residual deformation for performance based seismic design. The permissible residual

drift level of 0.005 rad was determined through the extensive literature review and confirmed by a building investigation [8].

The building investigated had two main studies conducted to confirm the standard permissible residual drift level. The building investigated was a currently occupied structure located on the Uji campus of Kyoto University. The first study focused on measuring inclinations of the 4th story corridor floors in all four sides of the building and column tilt of the 4th story east and west columns. The second study focused on measuring residual deformations on the occupied office space on the second floor of the south corridor. Figure 2-1 shows the laser level position and the 107 measuring points that were taken in this office space. This office space was chosen because the occupants felt the floor was inclined.

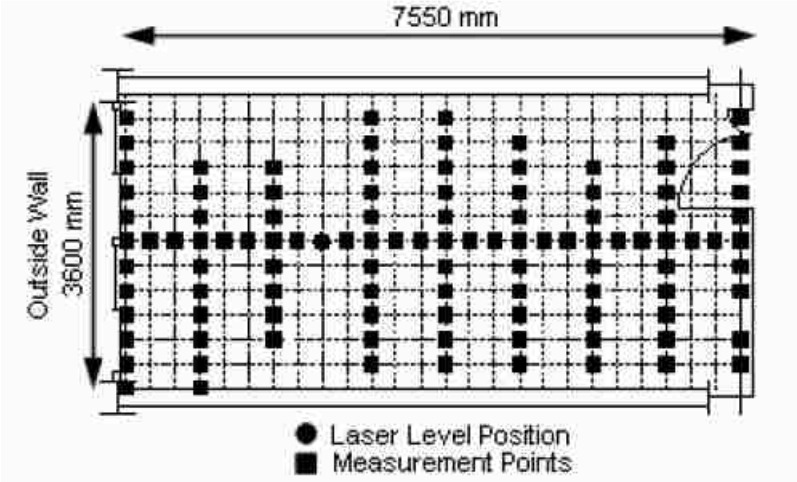

Figure 2-1. Plan view of the occupied office space and measuring points [8].

The main conclusion from the investigation confirmed the standard permissible residual drift level. As a whole, the building did not show a significant amount of residual deformation. However, local floor inclinations of 0.0067 rad were measured in the office space. This measurement is above the permissible residual deformation level of 0.005 rad. The occupant's

comment and the measurement of 0.0067 rad inclination confirms that a good permissible drift level could indeed be 0.005 rad as determined by the literature review [8].

McCormick et al. [8] work relates to this thesis by providing a target of the amount of residual drift that can be tolerated by occupants. Erochko et al. [1] also confirmed that residual drifts greater than 0.5% are noticed by occupants. These findings emphasize the importance of minimizing residual drifts in buildings.

2.1.2 Post-Yield Stiffness Influences Residual Drift

Christopoulos and Pampanin [9] studied the possibility of considering residual drifts in performance based seismic design. They studied several parameters that influence residual drifts, proposing a framework based on a combination of maximum and residual responses, and performing nonlinear time history analyses on single and multiple degrees of freedom systems. This research determined that post-yielding stiffness (amount of stiffness remaining in a building after members have yielded) influences residual deformations significantly. Authors also determined, through defining the framework and analyses, that residual displacements are significantly more sensitive to both higher mode effects and p-delta effects than they are to maximum displacements. These factors emphasize the importance of designing directly to minimize residual drifts.

MacRae and Kawashima [10] studied residual displacements of bilinear oscillators. The objectives of that study were to identify the parameters, explain reasons they control the residual displacements of single degree of freedom bilinear oscillators, and to develop a method for estimating the residual displacements of single degree of freedom structures. The authors subjected several bilinear single degree of freedom oscillators to 11 earthquake records from

various ground types. Oscillator's ductility, stiffness ratio, and fundamental periods were the variables.

The main finding of MacRae and Kawashima [10] was that the residual drift depends more on the amount of post yield stiffness than on the ground motion. Bilinear oscillators with positive stiffness ratios had small residual displacements, while those with negative stiffness ratios had larger residual displacements. Thus, increasing stiffness of members reduces residual drift. This finding agrees with Christopoulos and Pampanin [9] that post yield stiffness influences residual drifts significantly.

Hatzigeorgiou et al. [11] developed empirical equations to effectively determine the maximum seismic deformation from residual displacements. Post-earthquake performance level of structures provided imperative information in determining structural damage, response and rehabilitation. Performance level was described by the maximum deformation; therefore, it is very important to have suitable methods to link maximum residual deformations to obtain performance level. Hatzigeorgiou et al. [11] proposed an alternative method to determine post-earthquake performance levels of structures. Equations were developed after extensive dynamic inelastic analyses followed by a comprehensive nonlinear regression analysis were completed. In these analyses, seven different values for post-yield stiffness ratio were considered. This clearly shows that post-yield stiffness is one of the most important parameters controlling the magnitude of residual drifts. Hatzigeorgiou et al. [11] also determined that maximum displacements can be effectively evaluated for known residual displacements.

Borzi et al. [12] studied and introduced a new form of inelastic displacement spectra and displacement reduction factor, as well as residual displacement spectra. These were developed through nonlinear analyses. The purpose of these spectra and reduction factor is to help develop

displacement-based seismic design as potentially more rational than force-based techniques. Through this process the authors confirmed that residual drift is dependent on post-yield stiffness of the system and ductility requirements. These findings match previous research and help the development of possibilities to reducing residual drift.

2.1.3 Damage Assessment using Residual Displacements

Yazgan and Dazio [13] developed a post-earthquake damage assessment method that accounts for residual deformations incurred by the damaged structure. Figure 2-2 shows a basic schematic presentation of the method proposed. Notice that the probabilities $Pr(M_i|I)$ of M_i are conditional on the inspection results I. This method was analyzed and then applied to predict the maximum average drifts ratio attained by the WDH4 test unit by Lestuzzi et al. [14]. The results from this application example confirm the effectiveness of the method. The estimated maximum drift ratio distribution using the proposed method matched the actual drift measured during the test. Thus, the assessment method developed can be used to make rational decisions regarding functionality and repair of damaged structures [13]. As tools such as these are developed, it is clear that minimizing residual and maximum drifts is important in preventing structural damage and needed repairs.

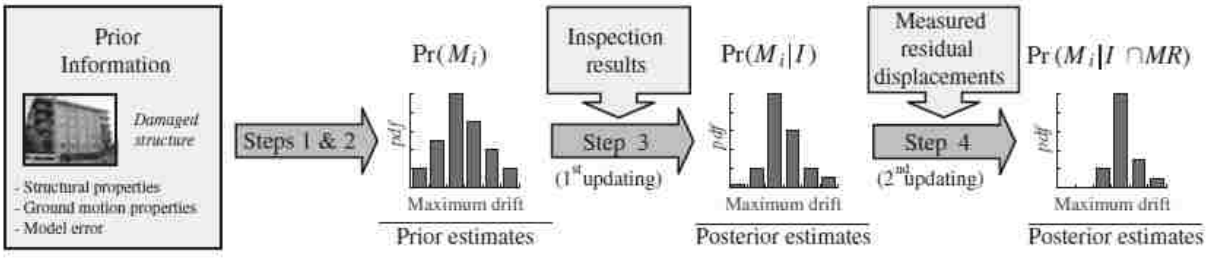

Figure 2-2. Schema of the proposed damage assessment method [13].

Christpoulos et al. [15] and Pampanin et al. [16] examined single and multiple degree of freedom systems and suggested a Residual Deformation Damage Index (RDDI) for evaluating a building after an earthquake. The RDDI only considers the maximum and residual deformations caused by an earthquake to assess the potential damage of the building. The RDDI is similar to the method discussed in Yazgan and Dazio's [13] paper. Both the RDDI and Yazgan and Dazio assessment method use residual and maximum displacement as performance parameters in assessing and predicting damage to buildings.

Ruiz-Garcia and Miranda [17] conducted an analytical study to evaluate residual displacement ratios which can be used to properly assess the performance of existing structures. Their research focused on estimating residual displacement ratios, the ratio of residual displacement to peak elastic displacement demand, using response time history analyses of single degree of freedom systems. The authors determined that mean residual displacement ratios are more sensitive to local firm site conditions than previously reported. After performing time history analysis, they determined that in the short period spectral region, periods less than 0.5 seconds, residual displacement demands of the system with constant relative strength are greater than peak elastic displacement demands. In the spectral region, the ratio is strongly dependent on the period of vibration, lateral strength ratio and type of hysteretic behavior. Finally, for periods longer than 1.0 second, ratios are not very sensitive to changes in period of vibration, but are primarily dependent on the lateral strength ratio and type of hysteretic behavior. Additionally, systems with positive post-yield stiffness ratios had smaller residual displacement and demands as compared with elastic plastic systems. These conclusions match those discussed previously.

2.2 Buckling-Restrained Braced Frames

Clark et al. [18] conducted large-scale tests of tension/compression yielding braces through restraint of compression buckling. Through the late 80s and 90s, a variety of "unbonded braces" were developed to dissipate energy through stable tension-compression yield cycles. The basic principle was to prevent Euler buckling of the steel core by encasing the brace over its length with a steel tube filled with mortar or concrete as shown in Figure 2-3. The right picture in Figure 2-3 shows the hysteric plots, highlighting their elasto-plastic behavior.

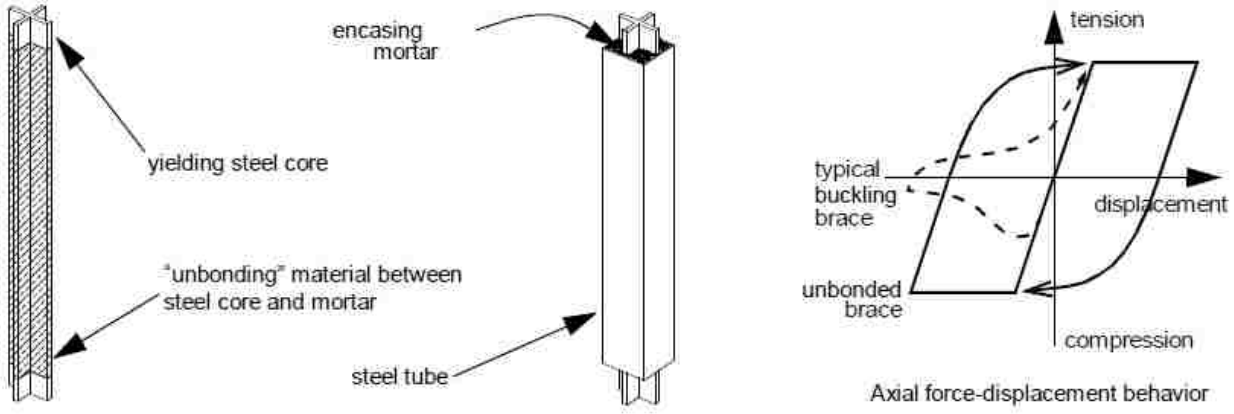

Figure 2-3. Schematic of mechanism of buckling-resistant unbonded braces [18].

The concrete and steel tube encasement is engineered to provide sufficient flexural strength and stiffness to prevent global buckling of the brace. This allows the steel core to undergo fully-reversed axial yield cycles without losing stiffness or strength (as shown in the right diagram in Figure 2-3). Clark et al. [18] performed large-scale testing of unbonded braces to determine their behavior. The tests resulted in predictable behavior and substantial over-strength in terms of displacement and energy dissipation capacity. One specimen had very stable force-displacement behavior over 17 fully-reversed displacement cycles at 2 percent axial strain.

These results showed the reliability of unbonded braces and helped lead to the use of what is now known as buckling restrained braced frames (BRBFs).

Sabelli et al. [19] researched the seismic response of concentrically braced steel buildings and determined that utilizing buckling restrained braces improved performance. Potential difficulties in using conventional concentrically braced frames are in the difference between the tensile and compressive capacity of the brace and the degradation of brace capacity under compressive cyclic loading. To achieve more ideal elasto-plastic behavior, buckling in compression is restrained by external casing. These buckling restrained braces were effective in overcoming problems associated with special concentric braced frames. Sabelli et al. [19] recommends further research to assess results of incorporating buckling-restrained braces into braced frame systems.

Trembley et al. [20] performed analysis on BRBFs and looked at drift results. Both incremental static analysis and nonlinear dynamic analysis were performed on BRBFs varying between 2 and 16 stories. Under static lateral loading, yielding of BRBFs occurred at deflections varied between 0.3% and 0.6% of the story height. The nonlinear dynamic analysis showed some pushover responses in a few stories not to be sufficient to reduce potential for the concentration of deformation. Thus, Trembley et al. [20] recommended that higher design seismic loads may be needed to improve collapse prevention. Another general trend observed was that permanent lateral deformations increased with the building height.

2.2.1 BRBF compared to SMRFs

Erochko et al. [1] performed a comparative study of residual drift response of Special Moment Resisting Frames (SMRFs) and BRBFs. This study included pushover and two-dimensional nonlinear time history analyses for two ground motion hazard levels. Buildings

between 2 and 12 stories in height were used for these analyses. The typical building design (height varies between 2 and 12 stories) is shown in Figure 2-4.

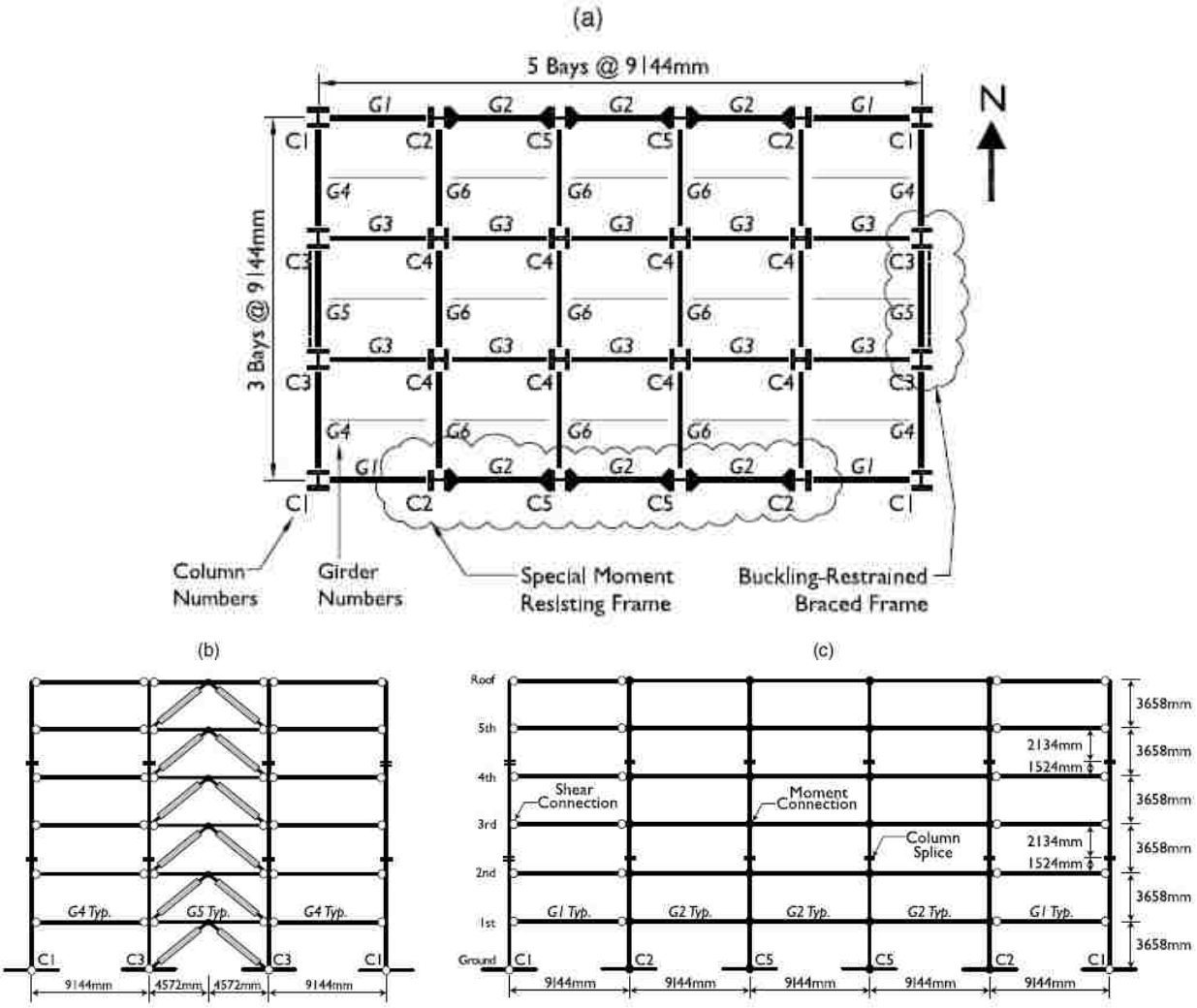

Figure 2-4. Typical building design: (a) building plan; (b) buckling-restrained braced frame typical north-south elevation; (c) special moment-resisting frame typical east-west elevation [1].

The results of this study were that BRBFs are more sensitive to residual drifts than SMRFs. On average BRBFs had between 0.8 and 1.8% permanent residual drifts after excitations and SMRFs had between 0.5 and 1.2% drifts. Both amounts of drifts are noticeable to occupants and would warrant repair. Erochko et al. [1] also determined that inter-story drift

response was larger in shorter SMRF buildings. BRBF systems were similar, except in 12-story structures where peak drift values were significantly worse, likely due to p-delta effects (response due to gravity forces). To help reduce residual drifts, it is important to understand the factors that influence them and what amount of drift affects occupants.

Choi et al. [21] also compared BRBFs and SMRFs seismic performance by performing pushover and nonlinear time history analyses. Results showed larger displacements and inter-story drifts in SMRFs compared to the braced frames. In the shorter buildings, there was a significant difference in these displacements. In taller buildings, however, displacements and inter-story drift responses worsened to the point where maximum values were higher than those experienced by SMRF systems, likely due to p-delta effects. Agreeing with previous research, BRBFs residual drifts were also determined to increase in taller buildings.

2.3 **Self-Centering Systems**

Self-centering systems are non-traditional systems that have been determined to have low residual drifts. Unlike traditional systems, self-centering systems have flag-shaped hysteretic behavior which limits damage to structural members causing low residual drifts. For this reason, self-centering systems have been heavily researched.

Christopoulos et al. [22] perform a study that investigated the inelastic response of flag-shaped hysteretic single degree of freedom (SDOF) systems and compared it to the responses of bilinear elasto-plastic hysteretic SDOF systems. Figure 2-5 shows examples of these two hysteretic plots. As indicated in the figure, flag-shaped hysteretic systems consist of a post-yielding stiffness parameter (α) and an energy-dissipation parameter (β).

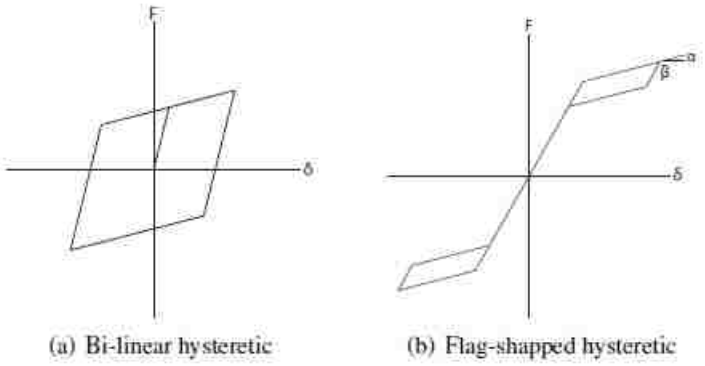

Figure 2-5. Examples of bi-linear and flag-shaped hysteretic systems compared by Christpoulos et al. [22] (figure from Boston [31]).

These SDOF systems were investigated and compared through time history analyses [22]. Results indicated that the seismic response of flag-shaped hysteretic systems was qualitatively similar to the elasto-plastic hysteretic systems. However, by adjusting values of α and β a flag-shaped hysteretic system can perform better than an elasto-plastic system in terms of displacement ductility. Specifically, after adjusting α and β values the flag-shaped hysteretic systems had higher absolute acceleration, less absorbed energy and no residual drifts as compared to the elasto-plastic systems. The elasto-plastic systems had lower values of absolute acceleration, more absorbed energy, and residual drifts in all systems. For elasto-plastic systems, residual drifts were the largest in systems with low strength and short periods; flag-shaped hysteretic systems had no residual drifts due to their self-centering capability.

2.3.1 Self-Centering Moment Frames

Post-tensioned (PT) moment connections have been developed for use in moment resisting frame (MRF) systems as an alternative to welded MRF connections. The development of PT connections is largely due to the unexpected premature connection fractures that occurred in welded MRF connections during the 1994 Northridge earthquake. Post-tensioned connections

have high strength posttensioned steel strands that run through the columns and are anchored outside the connection region. An example of the PT steel connection is shown in Figure 2-6 with a MRF welded connection for comparison. Research of PT connections has led to the development flag-shaped hysteretic behavior in steel systems and self-centering frames.

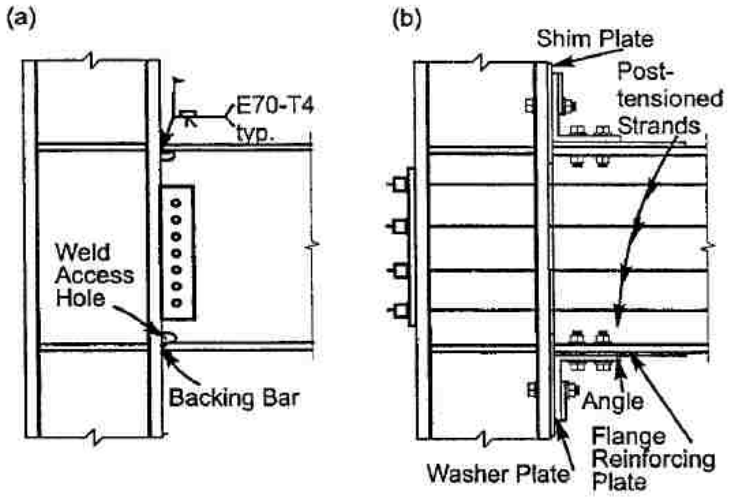

Figure 2-6. Moment connections: (a) pre-Northridge welded connection; (b) post-tensioned connection [23].

Ricles et al. [23] conducted experimental testing, analytical modeling, and time history analyses of the post-tensioned connections shown in Figure 2-6 and determined that these connections exceed the performance of MRF welded connections. The main advantages of post-tensioned connections are that field welding is not required, conventional materials and skills are used to make the connection, initial stiffness of PT connection are similar to that of welded connection, and that the connection is self-centering without residual deformation. This self-centering effect limits residual drifts from occurring at the base of columns and in the MRF's entirely. Other advantages include beam and columns remaining essentially elastic while connections provide energy dissipation through inelastic deformations, damage being confined to

angles of the connection, and the angles being easily replaced. The analyses showed that increases in the angle size or thickness and decreases in the angle length resulted in stronger and stiffer angles. Additionally, time history analyses showed adequate self-centering capability and stiffness, strength and ductility in MRFs with PT connections [23]. Clearly, research shows that PT connections are more advantageous than welded connections.

Garlock et al. [24] conducted experimental testing of post-tensioned connections subject to simulated earthquake loads. Specifically, six full-scale interior connections of PT wide flange beam-to-column moment connections were tested with earthquake loads. The set-up for experimental testing is shown in Figure 2-7.

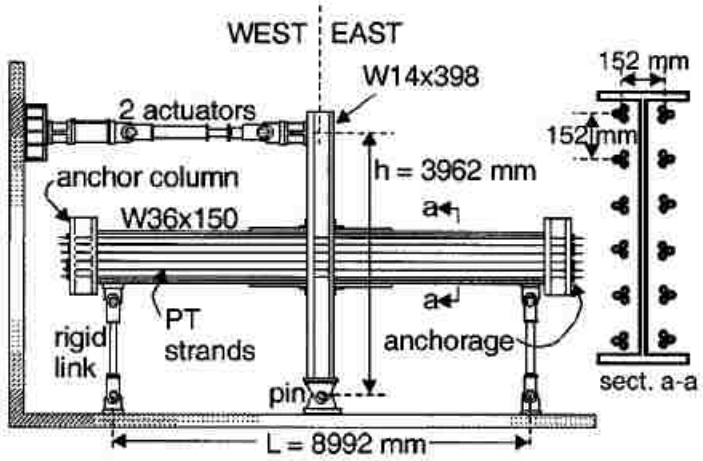

Figure 2-7. Test setup from Garlock et al. [24].

Garlock et al. [24] determined that frames with PT wide flange beam-to-column moment connections were able to self-center when the strands did not yield and the beams did not experience local buckling. Beam local buckling prevents the frames from self-centering. Connections were recommended to avoid this limit state. Also recommended was to add a larger number of post-tensioned strands in the connection prevented strand yielding. More strands give

greater ductility and a larger connection moment. This provides greater connection stiffness after decompression and angle yielding. Overall it was determined that PT steel connections can provide adequate strength, stiffness and drift capacity needed for MRFs under earthquake loading.

Chou et al. [25] further investigated post-tensioned beam-to column connects. Cyclic tests were conducted on systems which included two steel beams post-tensioned to a concrete filled tube column with high strength strands. For increased energy dissipation, reduced flange plates (RFPs) were welded to the column and bolted to the beam flange for two specimens. Results showed all PT connections experienced a flag-shaped hysteretic response and dissipated energy. Similar to Garlock et al. [24], Chou et al. [25] found that when the PT strands yielded or the beam experienced local buckling, the system had lots of strength, stiffness, and self-centering capacity.

Kim and Christopoulos [26] proposed a post-tensioned (PT) self-centering moment resisting frame. This PT self-centering friction damped (SCFR) moment resistant connection serves as an alternative to welded connection used in tradition moment resisting frames (MRFs). These two types of comparative frames were designed and tested with monotonic cyclic pushover and time history analyses. The SCFR frame test assembly is shown in Figure 2-8. Results showed that the maximum inter-story drifts and maximum floor accelerations of the SCFR frame were similar to those of the welded MRF. Both frames also displayed similar initial stiffness. The main difference observed was that the SCFR frame had almost zero residual drifts except for in the first story, whereas the welded MRF sustained significant inter-story drifts. The SCFR frame also displayed no structural damage.

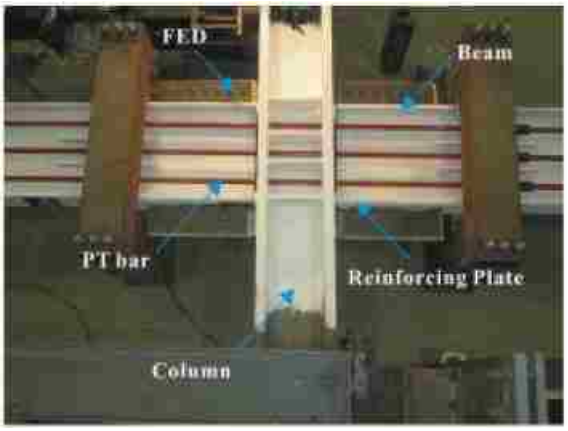

Figure 2-8.SCFR assembly test: interior SCFR beam- column assembly test [26].

2.3.2 Self-Centering Braced Frames

Fahnestock et al. [27] investigated the seismic response and performance of BRBFs with non-moment-resisting beam-column connections by conducting nonlinear dynamic analyses. The prototype building they designed and tested was a typical 4-story office building located on a stiff-soil site in Lost Angeles. Nonlinear dynamic analysis results showed fairly uniform story drifts (over the height of the frame) and maximum ductility demand. The residual story drifts that result after a large earthquake suggests that returning a building with BRBFs to service may require replacing the braces. The maximum ductility demands observed exceeds the prediction, suggesting that current methods are not conservative. Consequently, a prediction method was proposed to more rigorously predict maximum ductility demands in BRBFs.

Fahnestock et al. [28] also performed a large-scale experimental test to confirm seismic response of BRBFs with non-moment-resisting beam-column connections. The same prototype building used in the nonlinear dynamic analyses discussed above was used for this large-scale experimental testing. Results showed the beam-column-brace connections only sustained minor yielding at story drifts. Still, large residual drifts in frames were observed indicating possible

high repair costs of BRBFs. Overall, improved connection details in the BRBFs helped avoid undesirable failure modes and improved overall seismic resistance of BRBFs. Using BRBFs with new non-moment-resisting-beam-column connections helped lead to the development of self-centering energy dissipative braces.

Christopoulos et al. [29] proposed and validated a new lateral force resisting system as a viable alternative to current braced frame systems, called a self-centering energy dissipative (SCED) bracing system. This new SCED steel brace element is comprised of traditional steel bracing elements, a friction dissipative mechanism, and a pre-stress tensioning system. An embodiment of SCED system with the elements mentioned is shown in Figure 2-9.

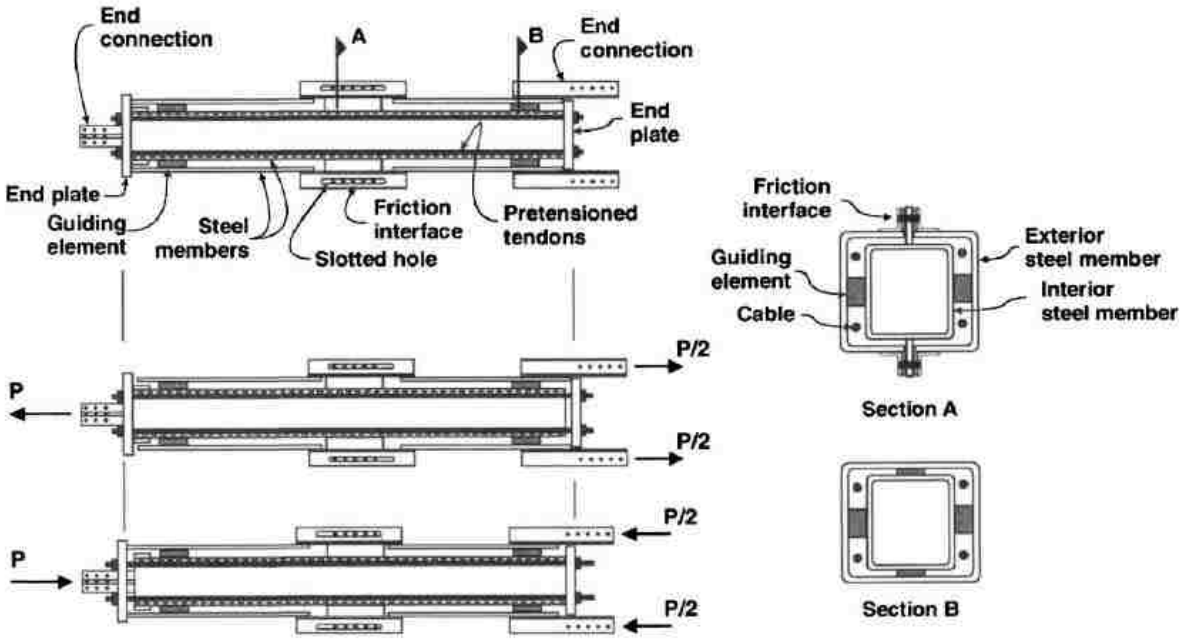

Figure 2-9. Embodiment of SCED system with steel tubes, tendons and dissipative mechanism [29].

This SCED steel brace system was designed to dissipate energy, provide a self-centering response within the target drift, and have no structural damage while undergoing large axial deformations. The response of the SCED brace system was calculated and then experimentally

determined. Results from experimental testing confirmed a self-centering hysteretic response under cyclic loading protocols. These results were also within the target design drift, as predicated with equations. Christopoulos et al. [29] proposed the SCED concept as a viable alternative to braced frame systems, especially with the attractive self-centering property.

Chou and Chen [30] researched and proposed a new steel dual-core self-centering brace (SCB) with a flag-shaped hysteretic response under cyclic loads. The proposed SCB applies post-tensioning technology in the brace and not in the beam to reduce the restraint from columns and slabs and residual drifts of structures. In comparison to the self-centering energy dissipative (SCED) bracing system proposed by Christopoulos et al. [29], the SCB has an additional core and tensioning element set in the brace as shown in Figure 2-10. These additional components make it possible to adopt tendons with low elastic strain capacity while preserving deformation capacity. Three dual-core SCBs were subject to cyclic testing and finite element analysis [30].

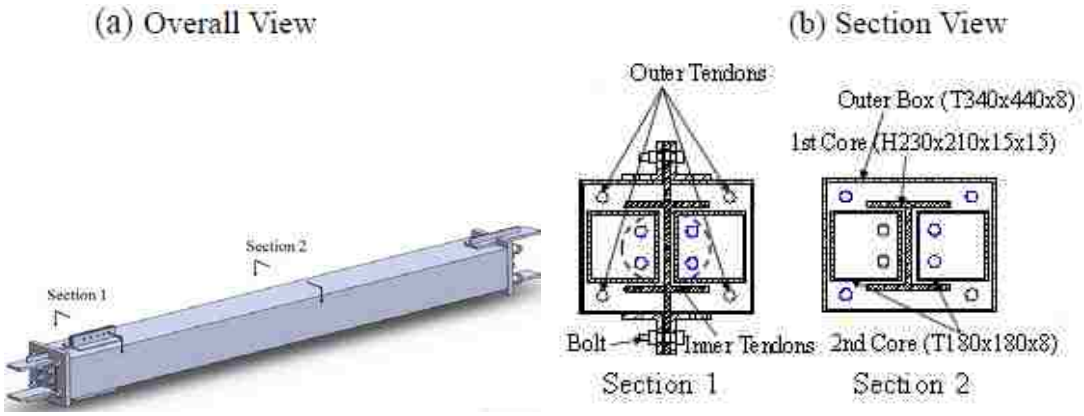

Figure 2-10. Proposed dual-core SCB by Chou and Chen [30]

Tests and finite element analyses confirmed that the dual-core SCB's elongation capacity is doubled, primarily due to the two tensioning element sets. Within a target drift of 2%, good energy dissipation and re-centering properties of the dual-core SCBs can be ensured. Also, at

1.5% drift, the dual-core SCBs under 15 low-cycle fatigue loading achieves repeatable flag-shaped responses. The finite element model confirmed the flag-shaped response of the dual-core SCB under the cyclic test [30].

2.4 **Dual Systems**

Dual systems, which combine two traditional systems together, have been found to be an effective way to reduce residual drifts. Dual systems are an alternative to self-centering frames, which were discussed in the previous section. Self-centering systems, yet to be implemented into practice, may take a long time to be implemented because they cannot be designed using conventional methods recognized by building codes.

Pettinga et al. [4] determined that adding a secondary system was successful in increasing stiffness and thus decreasing residual deformations in traditional framed and braced systems. This dual or secondary system approach introduces a secondary elastic frame to act in parallel with the primary system as shown in Figure 2-11. The secondary system approach was investigated through nonlinear time history and pushover analyses. Both the original primary frame and dual system were subjected to the far-field and near-field earthquake suites. Results of the near-field earthquake suites are shown in Figure 2-12. It is clear that drifts were reduced when a secondary frame was added.

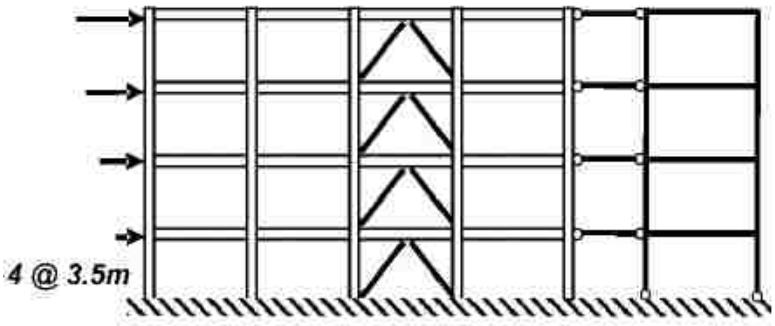

Figure 2-11. Schematic representation of dual system: primary BRBF rigidly connected to secondary internal elastic MRF [4].

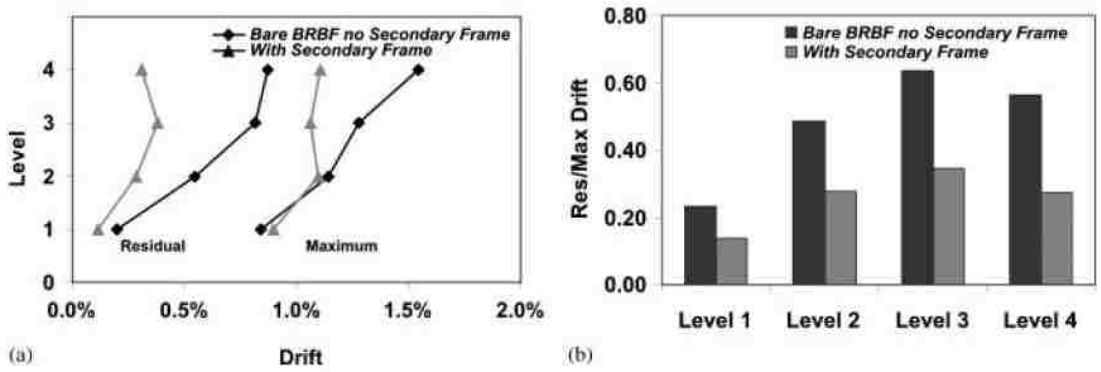

Figure 2-12. BRBF with and without secondary elastic steel moment-resisting frame subject to near-field earthquake set: (a) average maximum and residual drifts profiles and (b) average residual/maximum drifts profiles [4].

Pettinga et al. [4] determined that the introduction of an elastic secondary system was the most effective and consistent method in reducing residual deformations. Specifically, they found that residual drifts are reduced over the height of the structure, thus improving the performance level. Maximum drifts are slightly reduced, especially in the upper stories. This reduced drift in the upper story drifts implies that ductility is better distributed over the height of the building. Additionally, the favorable results with both residual and maximum drifts reduced as shown in Figure 2-12 are particularly important because structures tend to exhibit greater residual drifts

under near-field-type excitations. Overall, the authors recommend using secondary seismic-resisting systems (dual systems) to reduce residual drifts.

2.4.1 Dual Systems with Buckling-Restrained Braced Frames

Kiggins and Uang [5] proposed using special moment frames in combination with BRBFs to help minimize permanent deformations. The dual system tested consisted of a primary BRBF system with a secondary moment frame system as shown in Figure 2-13. The authors investigated both a 3-story and a 6-story dual system building and compared them to similar single braced framed systems. Nonlinear time history analyses resulted in reduced average residual and maximum drifts of about 10–12%. This is likely due to increased stiffness from the additional moment frames in the dual system. Results also showed the ductility demand of the brace was reduced only slightly. It is clear that increasing stiffness through dual systems helps to reduce drifts in steel buildings.

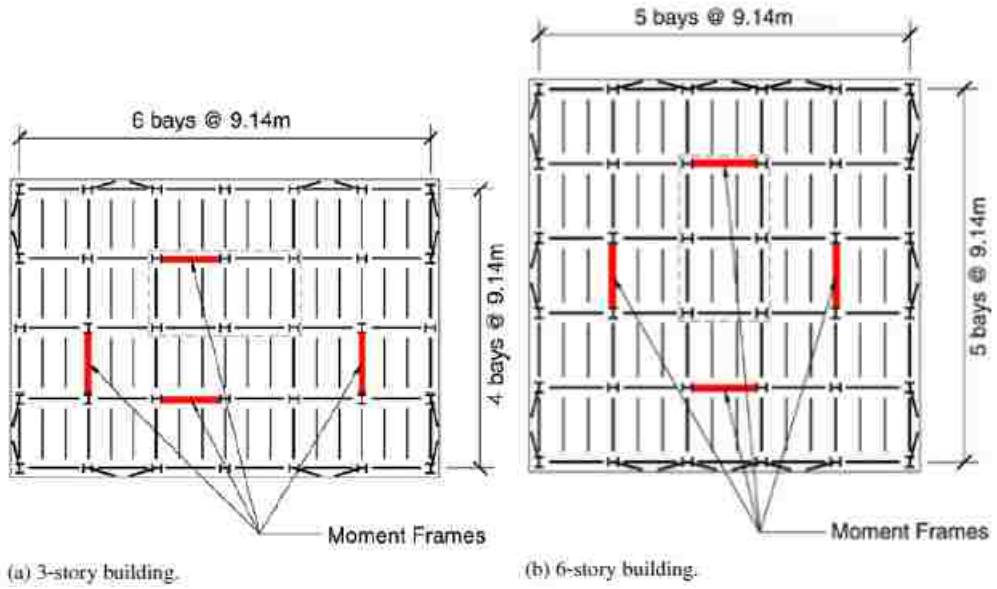

Figure 2-13. Dual system building plans [5].

Ariyaratana and Fahnestock [6] studied using BRBFs in parallel with SMRFs to increase reserve strength to reduce maximum and residual drifts after seismic loading. A nonlinear dynamic analysis was performed on a single prototype dual BRBF-SMRF building. This dual system configuration reduced residual story drift appreciably. The recommended configuration to reduce residual drift was to use a dual system with non-moment-resisting beam-column connections within the BRBF as opposed to using moment-resisting connections in the BRBF. Overall, when a BRBF with non-moment-resisting connections is used as part of a dual system, residual drifts are reduced significantly; the collapse prevention margin under the maximum considered earthquake is also increased by more than 25% in comparison to the isolated BRBF case.

2.4.2 BRBF's Coupled with Gravity Columns

Research has been conducted on buildings with BRBFs that operate with gravity columns functioning as a secondary system. Boston and Richards' [7] main goal was to determine the distribution of strength and stiffness between BRBFs and heavy columns that would give the most economical performance. Three variations of a 5-story building were analyzed in this research. First, a baseline model with fixed connection gravity columns was analyzed. Then, two variations were analyzed that added an extra heavy brace to either the top or middle story. This large brace did not yield (remained essentially elastic) under seismic impacts.

One of the conclusions of Boston and Richards [7] was that high stiffness yields low residual drift. As column stiffness's increased in higher stories, the residual drift at lower stories decreased. This was expected due to previous research. Additionally, adding a top heavy brace that was three times the size of the bottom brace resulted in lower residual drifts. As the column stiffness was increased, lower stories continued to see a decrease in residual drifts. Another test

showed that reducing brace areas of the lower four stories by 50% also decreases drift. Doubling the size of gravity columns caused residual drifts to decrease by half of the original building's drifts at the lower levels and even more at upper levels. Analysis was also conducted with a heavy brace in the third story. The drifts for this variation were lower than the original building's drifts; however they were higher than the previous variation, when a heavy top story was used. It was determined that drifts were best reduced when using a heavy brace in the top story of the building [7]. These results give potential for further research into finding the best ways to reduce drifts.

Boston [31] also performed an extended study with additional analyses to further determine ways to minimize drifts. In the study, the three variations, mentioned previously, were tested with four different column stiffnesses. The column sizes were increased to add stiffness and help reduce residual drifts of the building. Trends showed residual drifts decreased when column sizes were increased. However, the incremental benefit of drift reduction lessened as the column size was increased. Thus, increasing the column to two times the original size seems more favorable than further increases in the column size.

Boston's [31] study helped identify general trends; however, there were some limitations of the study. First, the study did not account for p-delta loads on the gravity columns. P-delta effects can have influence on the system and need to be accounted for to achieve more accurate results. The study assumed elastic-perfectly plastic braces. In buildings, braces do not behave perfectly elastic, however, this is a common assumption for initial analyses. Lastly, the study only included 5-story buildings, but analyses were not conducted on other taller or shorter buildings. The number of stories affects the drift levels and behavior.

3 RESEARCH METHODS

Numerical models were used to investigate residual and maximum drifts in BRBFs with and without elastic stories. The main focus of this research was to determine the optimal size and location of elastic stories that can best reduce drifts in steel buildings. The secondary focus was to determine how much additional reduction in drifts could be achieved by increasing the size of gravity columns. The following sub-sections outline the general procedure used to conduct this research. First, standard buildings were designed with differing elastic story sizes and locations. Then, gravity column sizes were increased. Next, the building frames were modeled for numerical analysis. Finally, the different buildings were analyzed using nonlinear response history analysis, with key outputs identified to be studied and presented as results.

3.1 **Frame Designs**

This section discusses the basic building layout used for design of all buildings, the differing parameters in the buildings, and the tools developed to assist these processes. In total, 389 buildings were designed. These buildings had the same basic building layout (floor plan). The variables were: number of stories, location of elastic stories, size of elastic story braces, and size of gravity columns.

3.1.1 Basic Building Layout and Design Parameters

Figure 3-1 below shows a plan view of the basic building layout used in this study. The basic design had 5 bay widths of 30 ft (9.1m) each. The height of each story, *h*, was 15 ft (4.6m) and a tributary seismic weight of 533.6 kip (2.37MN) per floor for each braced frame. The braces are located at the two middle bay locations on each side of the building. The dashed area shown in Figure 3-1 represents the respective tributary area of a floor in the building for one braced frame (for lateral loads in one direction). The tributary area is a symmetric section of the area of the building that is used for analysis in order to simplify the amount of analysis that needs to be completed. As shown in Figure 3-1, the tributary area is 25% of the original area of the building for one braced frame. The tributary area used in this study was 5929 ft^2. The spectra for the design basis earthquake (DBE) had S_{DS}=1.03g and S_{D1}=0.89g. An importance factor of 1.0 was used. The period of the building was also assumed to be equivalent to T_a. Detailed calculations are presented in Appendix A.

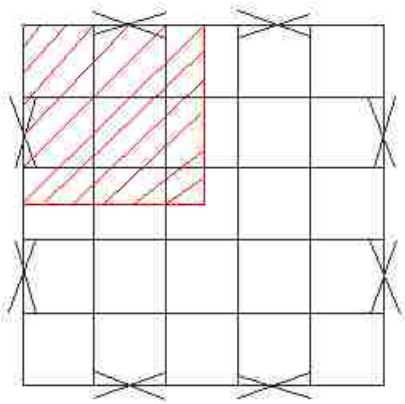

Figure 3-1. Basic design of building

A dual system with BRBFs paired with gravity columns as a secondary system was used for all building. Control buildings, as will be discussed in detail in the next section, are standard

BRBF buildings designed with no elastic stories. In these buildings, the gravity columns act passively under earthquake loads and do not contribute to lateral resistance. Elastic story buildings are designed by adding extra-large braces to chosen locations of the control buildings to create "elastic stories". These special stories engage the gravity columns and activate them as a secondary system to help in lateral resistance. The BRBF and gravity columns are assumed to be pinned at the base.

3.1.2 Control Building Designs

Standard BRBF buildings, referred to as control design buildings, were designed based on the basic building layout discussed above and developed into 4-, 6-, 8-, 12-, and 16-story buildings. First, BRBFs were designed. The process for designing these braces consisted of: determining the base shear of the entire building using ASCE 7 equations [32], computing the equivalent lateral force at each level, determining the lateral forces on each BRBF, computing the brace axial loads, and finally determining the core area for braces at each level. Second, columns supporting the BRBFs were designed. Column design required determining the tension and compression values developed in the braces and corresponding values transferred to each column. The BRBF beams were chosen to be W16X57 for all stories of all buildings. Also, gravity column design was performed by finding the factored demand based on the weight of the floors and reduced live load. Appendix A shows sample calculations for an 8-story control building. The visual basic code (VBA) and Excel tables developed to automate these design processes are contained in Appendix B. The frame designs for the 4-, 6-, 8-, 12-, and 16-story control buildings can be found in Table 3-1 through Table 3-5, respectively. Figure 3-2 shows the frame layout and serves as a key for the frame design tables.

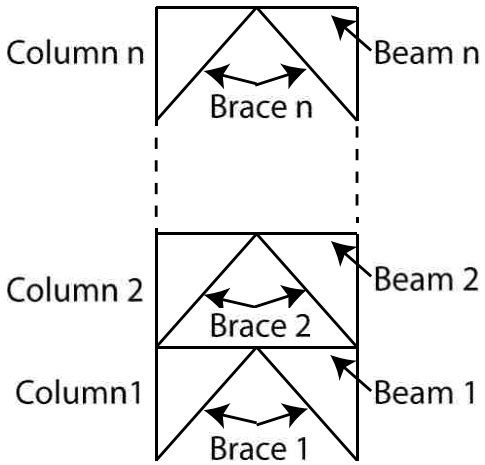

Figure 3-2. Frame layout for control buildings.

Table 3-1. Frame Sizes for 4-Story Control Building

Story	BRBF			P-Delta Column
	Brace Area [in^2]	Column Shape	Beam Shape	Effective Moment of Inertia [in^4]
4	2.5	W12X40	W16X57	1229
3	4.5	W12X40	W16X57	1229
2	5.5	W12X65	W16X57	1823
1	6.0	W12X65	W16X57	1823

Table 3-2. Frame Sizes for 6-Story Control Building

Story	BRBF			P-Delta Column
	Brace Area [in^2]	Column Shape	Beam Shape	Effective Moment of Inertia [in^4]
6	3.0	W12X40	W16X57	1229
5	5.0	W12X40	W16X57	1229
4	6.5	W12X72	W16X57	1823
3	7.5	W12X72	W16X57	1823
2	8.5	W12X152	W16X57	2475
1	8.5	W12X152	W16X57	2475

Table 3-3. Frame Sizes for 8-Story Control Building

Story	BRBF			P-Delta
	Brace Area [in^2]	Column Shape	Beam Shape	Effective Moment of Inertia [in^4]
8	2.50	W12X40	W16X57	1229
7	4.50	W12X40	W16X57	1229
6	6.00	W12X65	W16X57	1823
5	7.00	W12X65	W16X57	1823
4	8.00	W12X136	W16X57	2475
3	8.50	W12X136	W16X57	2475
2	9.00	W12X210	W16X57	3073
1	9.50	W12X210	W16X57	3073

Table 3-4. Frame Sizes for 12-Story Control Building

Story	BRBF			P-Delta
	Brace Area [in^2]	Column Shape	Beam Shape	Effective Moment of Inertia [in^4]
12	2.0	W14X48	W16X57	1874
11	4.0	W14X48	W16X57	1874
10	5.0	W14X61	W16X57	2615
9	6.5	W14X61	W16X57	2615
8	7.5	W14X120	W16X57	2951
7	8.5	W14X120	W16X57	2951
6	9.0	W14X193	W16X57	4764
5	9.5	W14X193	W16X57	4764
4	10.0	W14X283	W16X57	4764
3	10.0	W14X283	W16X57	4764
2	10.0	W14X370	W16X57	5905
1	10.0	W14X370	W16X57	5905

Table 3-5. Frame Sizes for 16-Story Control Building

Story	BRBF			P-Delta
	Brace Area [in^2]	Column Shape	Beam Shape	Effective Moment of Inertia [in^4]
16	2.0	W14X48	W16X57	1874
15	3.5	W14X48	W16X57	1874
14	4.5	W14X61	W16X57	2615
13	6.0	W14X61	W16X57	2615
12	7.0	W14X109	W16X57	2951
11	8.0	W14X109	W16X57	2951
10	8.5	W14X176	W16X57	4764
9	9.0	W14X176	W16X57	4764
8	9.5	W14X257	W16X57	4764
7	10.0	W14X257	W16X57	4764
6	10.5	W14X342	W16X57	5905
5	10.5	W14X342	W16X57	5905
4	11.0	W14X426	W16X57	6563
3	11.0	W14X426	W16X57	6563
2	11.0	W14X550	W16X57	8320
1	11.0	W14X550	W16X57	8320

3.1.3 Elastic Story Locations and Sizes

Control buildings were modified to have elastic stories at different locations and of various sizes. Figure 3-3 shows the 4-story control building and two 4-story buildings with elastic stories (indicated by bolded lines) at different locations. These elastic story buildings were analyzed with elastic story brace sizes varying 2, 3, 4, and 10 times the original brace size.

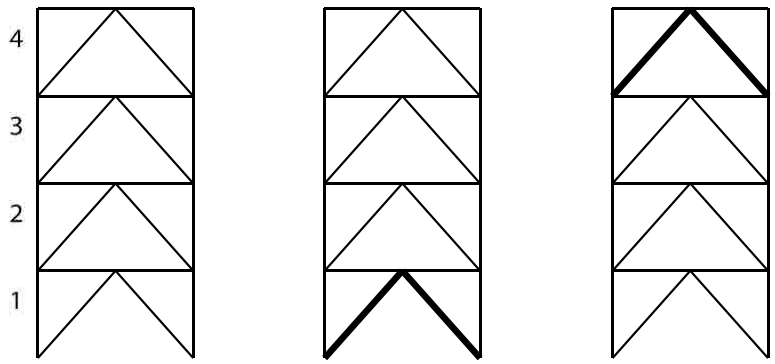

Figure 3-3. Elastic story locations for 4-story building.

The 6-story buildings were analyzed with an elastic story at every level to determine the optimal location of elastic stories to produce low residual and maximum drifts. Figure 3-4 gives a visual representation of the 6-story buildings analyzed with varying elastic stories. Previous research determined that elastic stories are most effective when located at the top story [31]. The same trend was anticipated to appear from the 6-story analysis. Again, for every design building shown the elastic story brace size was increased 2, 3, 4, and 10 times the original (control) brace size at that location. When multiple elastic stories were used, they were placed at least four levels apart in order to prevent the columns from yielding.

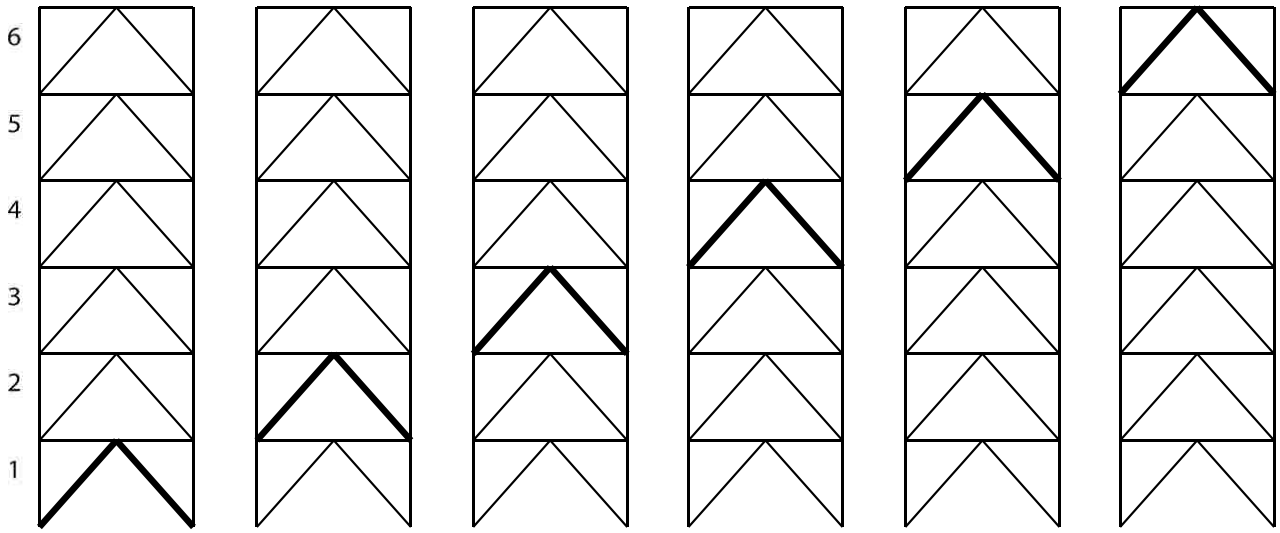

Figure 3-4. Elastic story locations for 6-story buildings.

Analyses on the 6-story buildings were also conducted with two possible locations for elastic stories: 1 & 5 and 2 & 6 stories. Figure 3-5 shows these buildings along with the 6-story control building. Again, the elastic story brace sizes were increased as stated previously.

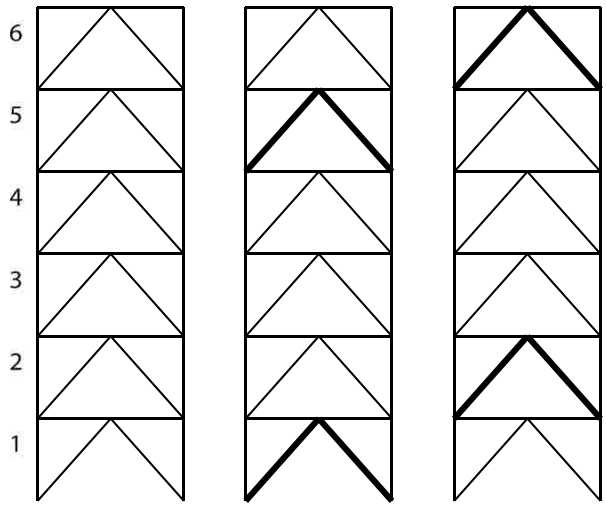

Figure 3-5. Elastic story combination locations for 6-story buildings.

Locations for elastic stories in the 8-, 12-, and 16-story buildings are shown in Figure 3-6, Figure 3-7, and Figure 3-8, respectively. The pattern used is the same as that in the second set of 6-story buildings. The BRBF size at these elastic stories was increased by 2, 3, 4, and 10 times the original (control) brace size in different analyses.

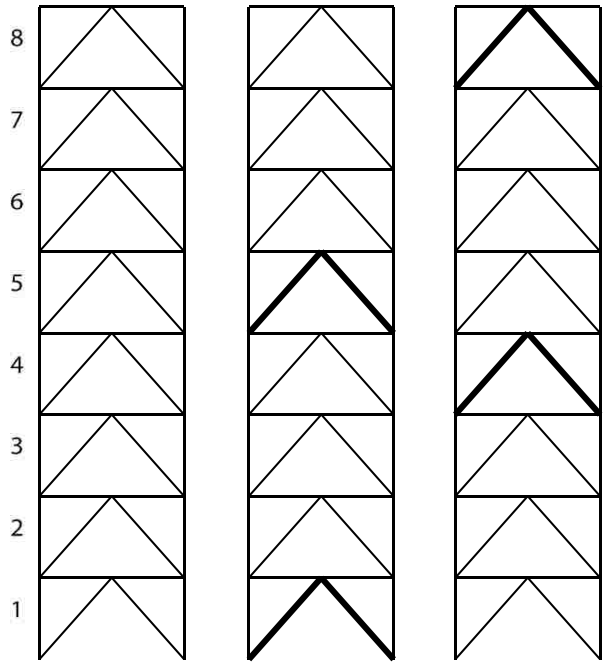

Figure 3-6. Elastic story combination locations for 8-story buildings.

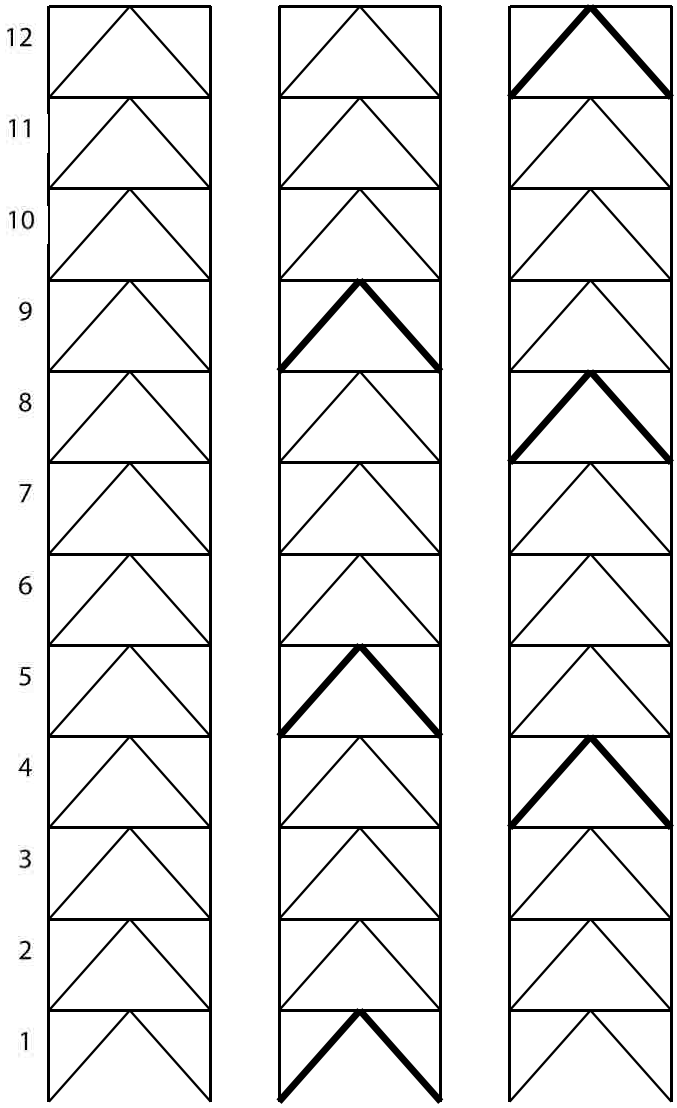

Figure 3-7. Elastic story combination locations for 12-story buildings.

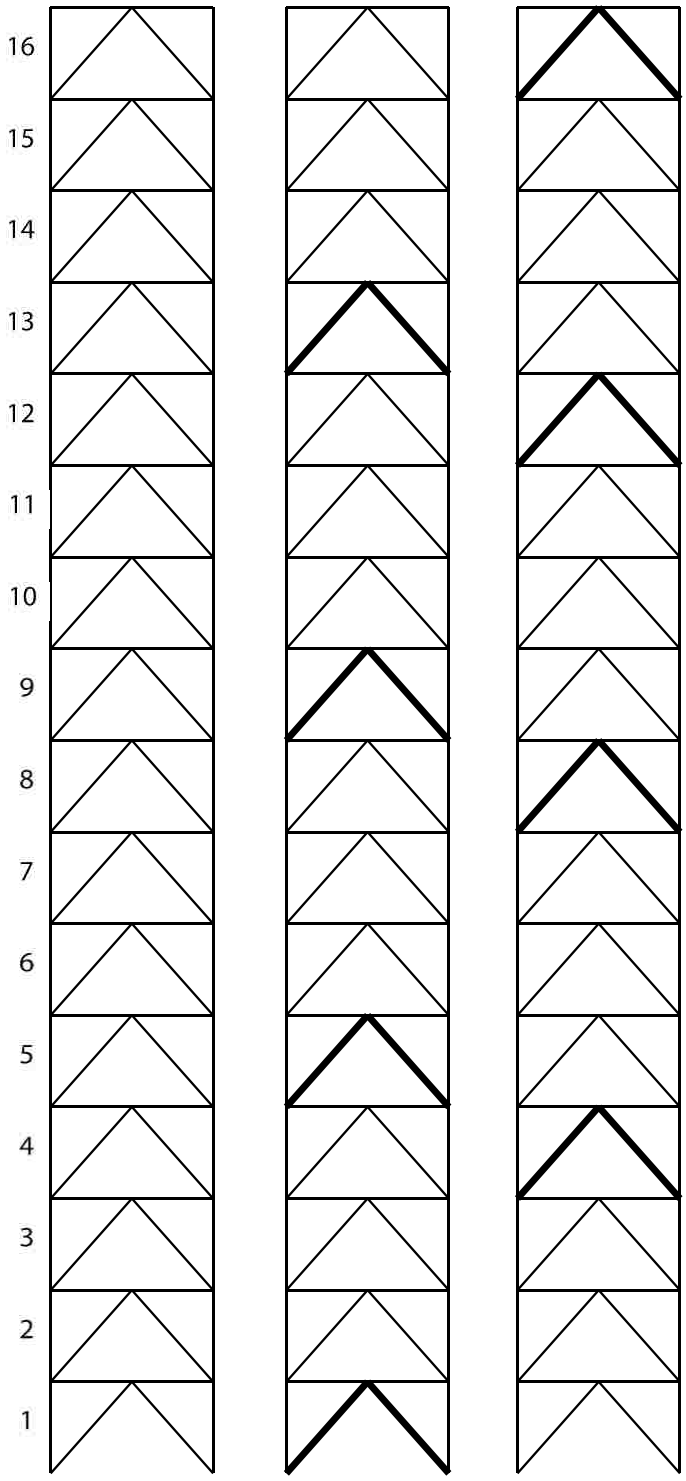

Figure 3-8. Elastic story combination locations for 16-story buildings.

3.1.4 Gravity Column Sizes

Control buildings were modified to include varied gravity columns sizes. After the control buildings were designed, locations were chosen for elastic stories with brace sizes increased by 2, 3, 4, and 10 times. For each of these cases, the gravity columns sizes were modified by 0.5, 2, 3, 4, and 10 times the standard (control) size. Then analyses were performed on the buildings. This process was repeated for each control buildings. A summary of the 4-, 6-, 8-, 12-, and 16-story design buildings are shown in Figure 3-9, Figure 3-10, Figure 3-11, Figure 3-12, and Figure 3-13, respectively. In total, there were 389 different buildings analyzed.

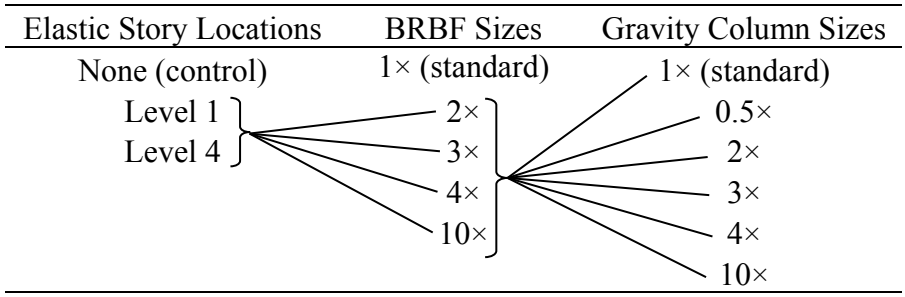

Note: Total 4-story combinations = 1 control + (2 locations × 4 ES sizes × 6 GC sizes) = 49 buildings

Figure 3-9. Four-story design buildings.

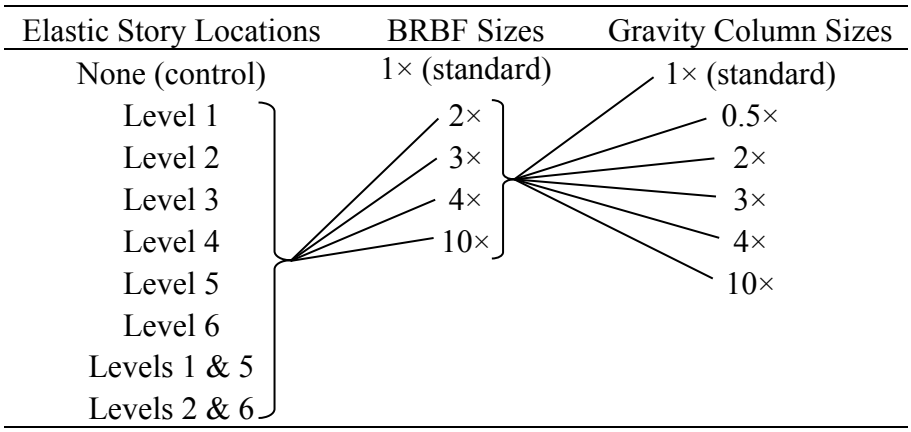

Note: Total 4-story combinations = 1 control + (8 locations × 4 ES sizes × 6 GC sizes) = 193 buildings

Figure 3-10. Six-story design buildings.

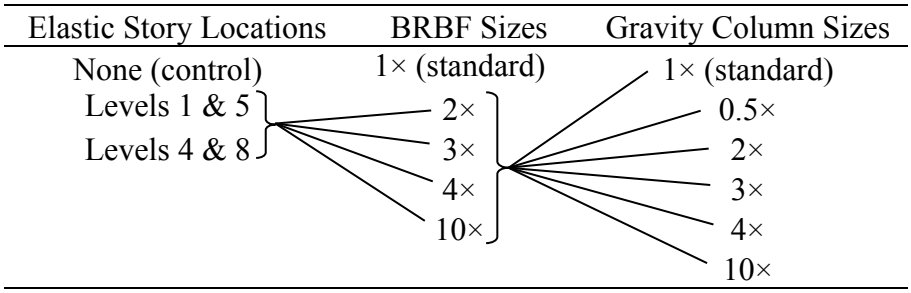

Note: Total 4-story combinations = 1 control + (2 locations × 4 ES sizes × 6 GC sizes) = 49 buildings

Figure 3-11. Eight-story design buildings.

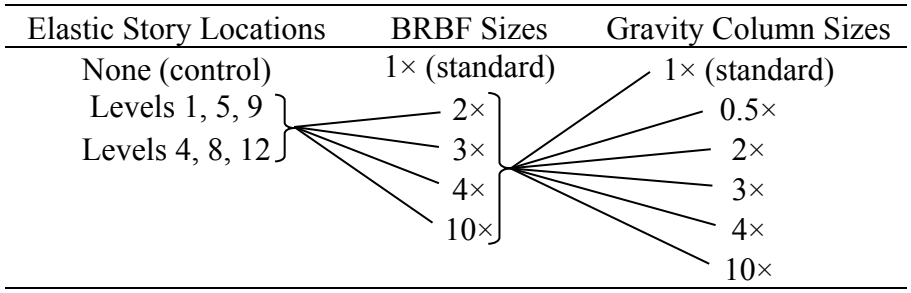

Note: Total 4-story combinations = 1 control + (2 locations × 4 ES sizes × 6 GC sizes) = 49 buildings

Figure 3-12. Twelve-story design buildings.

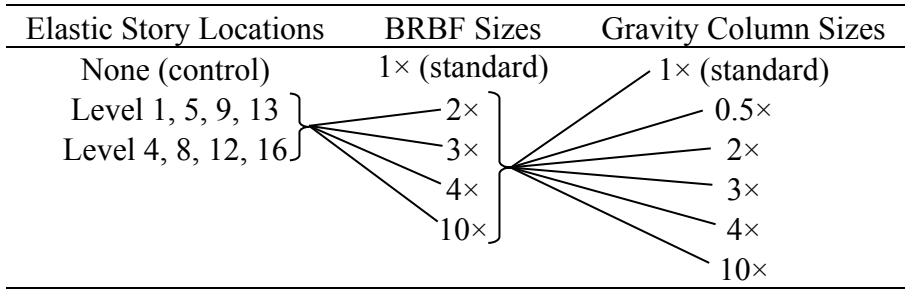

Note: Total 4-story combinations = 1 control + (2 locations × 4 ES sizes × 6 GC sizes) = 49 buildings

Figure 3-13. Sixteen-story design buildings.

3.1.5 Spreadsheet

A spreadsheet was developed to assist in the design, storage, and graphical development of outputs. Appendix B contains pictures of the main tabs of the spreadsheet. The spreadsheet contains automated design processes for both brace and column design.

3.2 Frame Modeling

Frames were modeled and analyzed using OpenSees (Open System for Earthquake Engineering Simulation) [33]. OpenSees is an open-source program developed at the University of California-Berkeley that can be used to simulate the response of structural and geotechnical systems subject to earthquakes. In order to utilize OpenSees, the brace frames had to be defined using TCL programming language and files. This section discusses how the frames were modeled and the different templates created and used for analyses.

3.2.1 Element Braces

Models for BRBF and gravity column dual systems were generated in OpenSees [33]. Specifically, two-dimensional models for the systems described were created. Geometry for the model was based on beam, column and brace centerline dimensions. A leaning column was added to the dual system representing the gravity columns. The properties for the leaning column, based on the gravity column designs for the prototype buildings, are summarized in the last column of Table 3-1 through Table 3-5.

Beams and columns were modeled using elastic beam-column elements with inelastic spring elements at the non-pinned ends to simulate yielding. The modulus of elasticity for the beams was 200,000 MPa (29,000 ksi). The inelastic spring properties were based on nominal cross-sectional dimensions, a yield strength of 345 MPa (50 ksi), and 5 percent kinematic

hardening. The BRBF columns were assumed to be fixed, whereas the gravity columns were assumed to be pinned at the base. Beam-column connections were considered pinned.

Buckling-restrained braces were modeled using truss elements with calibrated material properties. An effective material modulus of 1.6E (1.6×29,000 ksi) was used, where the scaling factor of 1.6 is based on brace design tables [34] and accounts for non-uniform cross-sectional area along the length of the braces and axially rigid end zones. Yielding and hardening was simulated using the Steel02 material model in OpenSees which incorporates the Giuffre-Menegotto-Pinto Model with both kinematic and isotropic hardening. The yield stress was specified as 248 MPa (36 ksi). The factors to define the hardening were calibrated from brace tests [35] with the following values used: b = 0.003, RO = 20, CR1 = 0.925, CR2 = 0.15, a1 = 0.065, a2 = 1, a3 = 0.045, a4 = 1; see [33] for definitions of each parameter. Figure 3-14 shows the response of a 65cm^2 (10 in^2) brace during one of the dynamic analyses, typical of the braces in the models.

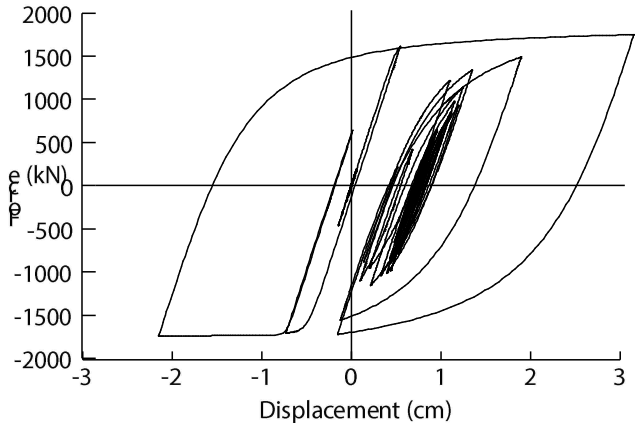

Figure 3-14. Typical brace hysteretic behavior from response history analysis.

3.2.2 Templates

Several templates were developed to generate the building models and complete appropriate analyses. These templates are listed and described in Appendix B.

3.3 Analysis

3.3.1 Ground Motions

Nonlinear response time history analysis was performed under two suites of earthquakes scaled to represent the design basis earthquake (DBE). The 4-, 6-, and 8- story buildings were analyzed under a suite of 11 different earthquakes. The earthquake records in this suite are all from California events except for two from the Duzce, Turkey event. This suite of earthquakes is summarized in Table 3-6. The 12- and 16-story buildings were analyzed under a second suite of earthquakes with 12 different earthquakes. These earthquake records are from various locations including California, the California-Mexico border, Turkey, and Taiwan. This second suite of earthquakes is summarized in Table 3-7.

The ground motion acceleration records were each scaled up to match particular design spectra. The scaled factors for the 4-, 6-, and 8-story control buildings are shown in Table 3-8. The scaled factors for 12- and 16-story control buildings are shown in Table 3-9. Figure 3-15 show spectra from each suite scaled for two particular systems.

Table 3-6. Suite1 Ground Motion Information used for 4-, 6-, and 8-Story Analyses

Earthquake[d]	Station	Component	M_w[a]	R (km)[b]	PGA (g)[c]
Loma Prieta	1028 Hollister city hall	HCH180	6.9	28.2	0.215
Loma Prieta	57382 Gilroy array #4	G04000	6.9	16.1	0.417
Loma Prieta	57382 Gilroy array #4	G04090	6.9	16.1	0.212
Loma Prieta	1695 Sunnyvale Colton Ave.	SVL360	6.9	28.8	0.209
Northridge	90053 Canoga Park – Topanga Canyon	CNP106	6.7	15.8	0.356
Northridge	90053 Canoga Park – Topanga Canyon	CNP 196	6.7	15.8	0.42
Northridge	90091 LA – Saturn St.	STN020	6.7	30	0.474
Northridge	90091 LA – Saturn St.	STN110	6.7	30	0.439
Whittier Narrows	90078 Compton – Castlegate St.	CAS000	6	16.9	0.332
Duzce	Bolu	BOL000	7.1	17.6	0.728
Duzce	Bolu	BOL090	7.1	17.6	0.822

a. Moment magnitude

b. Distance to epicenter

c. Peak ground acceleration

d. This suite of time history is a subset of the suite used by Ariyaratana and Fahnestock [6].

Table 3-7. Suite2 Ground Motion Information used for 12- and 16-Story Analyses

Earthquake[d]	Station	Component	M_w[a]	R (km)[b]	PGA (g)[c]
Imperial Valley 1979	Delta	H-DLT262	6.5	22.0	0.242
Imperial Valley 1979	Delta	H-DLT352	6.5	22.0	0.321
Imperial Valley 1979	Westmore	WSM180	6.5	15.2	0.098
Loma Prieta	Hollister- South and Pine	HSP090	6.9	27.9	0.271
Kocaeli, Turkey 1999	Duzce	DZC180	7.5	15.4	0.282
Chi-Chi Taiwan 1999	TCU061	TCU061-E	7.6	17.2	0.141
Chi-Chi Taiwan 1999	TCU061	TCU061-N	7.6	17.2	0.143
Chi-Chi Taiwan 1999	TCU067	TCU067-E	7.6	0.60	0.558
Chi-Chi Taiwan 1999	TCU067	TCU067-N	7.6	0.60	0.312
Chi-Chi Taiwan 1999	TCU071	TCU071-E	7.6	5.30	0.565
Chi-Chi Taiwan 1999	TCU120	TCU120-N	7.6	7.40	0.192
Chi-Chi Taiwan -03	CHY104	CHY104-W	6.2	35.0	0.081

a. Moment magnitude

b. Distance to epicenter

c. Peak ground acceleration

Table 3-8. Scale Factors for Suite1 Earthquake Time Histories

Earthquake Record	Scale Factor		
	4-story[a]	6-story[b]	8-story[c]
Loma Prieta, HCH180	1.62	1.13	1.29
Loma Prieta, G04000	2.46	2.94	2.11
Loma Prieta, G04090	2.66	1.78	1.91
Loma Prieta, SVL360	4.23	3.05	3.23
Northridge, CNP106	2.00	3.29	3.07
Northridge, CNP 196	1.44	2.00	1.45
Northridge, STN020	2.15	4.70	3.61
Northridge, STN110	1.87	2.47	2.63
Whittier Narrows, CAS000	1.89	2.79	6.06
Duzce, BOL000	1.28	1.70	1.85
Duzce, BOL090	0.75	0.93	1.91

a. 4-story building natural period = 0.86s

b. 6-story building natural period = 1.15s

c. 8-story building natural period = 1.57s

Table 3-9. Scale Factors for Suite2 Earthquake Time Histories

Earthquake Record	Scale Factor	
	12-story[a]	16-story[b]
Imperial Valley 1979, H-DLT262	2.66	2.46
Imperial Valley 1979, H-DLT352	2.09	2.52
Imperial Valley 1979, WSM180	4.49	5.15
Loma Prieta, HSP090	2.93	2.95
Kocaeli, Turkey 1999, DZC180	1.78	1.08
Chi-Chi Taiwan 1999, TCU061-E	2.25	2.41
Chi-Chi Taiwan 1999, TCU061-N	1.93	1.21
Chi-Chi Taiwan 1999, TCU067-E	0.91	1.75
Chi-Chi Taiwan 1999, TCU067-N	1.74	1.56
Chi-Chi Taiwan 1999, TCU071-E	1.72	1.80
Chi-Chi Taiwan 1999, TCU120-N	2.38	1.99
Chi-Chi Taiwan -03, CHY104-W	1.71	2.12

a. 12-story building natural period = 2.47s

b. 16-story building natural period = 3.48s

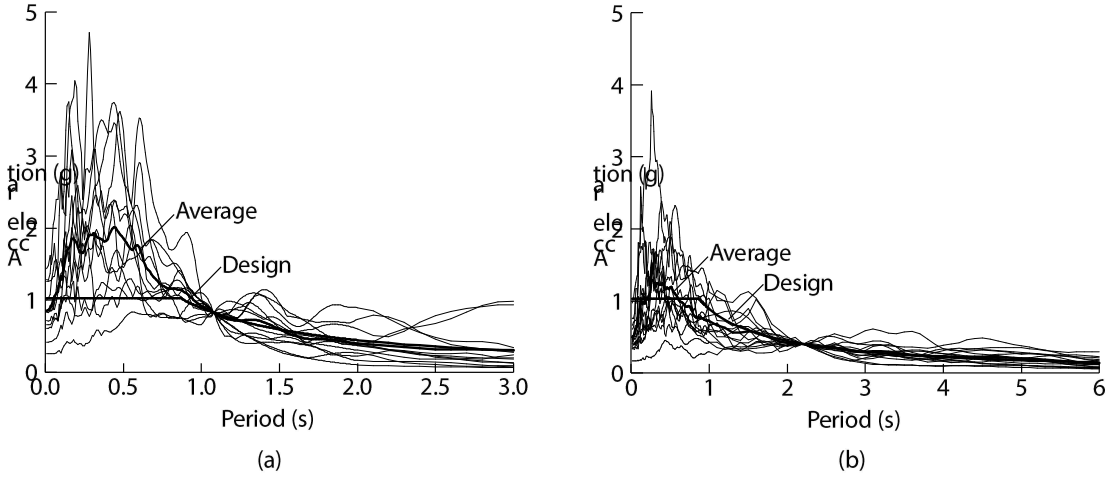

Figure 3-15. Scaled spectra from time histories : (a) Suite1 shown scaled for a 6-story building; (b) Suite2 shown scaled for a 12-story building.

3.3.2 Procedure

After designing the buildings, the analysis was conducted through a step-by-step process. First, the input file was updated correctly to match the building design that was being analyzed. Then, "source dynamic.tcl" was written in the OpenSees execute file to trigger analysis to start running. After the program was completed, the outputs were recorded in designated tables. This analysis process was repeated for each of the 389 buildings designed.

3.4 Outputs

The outputs from analyses were inter-story residual and maximum drift values. Specifically the program outputs average maximum drift, average residual drift, 85th percentile maximum drift and 85th percentile residual drift per story. For residual and maximum drifts, a drift value is compiled for each story from each earthquake. Thus, for the 4-, 6-, and 8-story buildings every story has 11 drift values corresponding with the 11 earthquakes in Suite1. These 11 drift values for each story are then averaged together to determine one drift value per story.

These single drift values per story are then divided by the story height to normalize drifts relative to their story heights using Equation 3-1. These values are simply referred to as "average residual drift" or "average maximum drift" and are given for every story in the building analyzed. The 85th percentile drift is computed using a normal distribution.

$$Average\ (story)\ drift = \left(\frac{\Sigma earthquake\ story\ drift}{number\ of\ earthquakes}\right) \Big/ Storyheight \tag{3-1}$$

In order to quantify the drift outputs, drift plots were generated and comparison criteria identified. Two main criteria were observed to effectively quantify results. The first criterion is to identify the maximum story drift occurring in the elastic story building (with standard gravity columns) and compare that value to the corresponding story drift in the control building. The purpose of this comparison is to quantify the amount of drift reduction elastic story buildings can provide. A similar comparison can be made between any drift values on the same story level in both the elastic story building and control building. The second criterion is to find the average story drift for the entire building. This involves summing the outputted drift values at every story and dividing the sum by the number of stories in the building. This process can be repeated for elastic story buildings, gravity column buildings, and control buildings. Then appropriate comparisons can be made. This process helps highlight the overall reduction of drifts that results from adding elastic stories and increasing gravity columns.

4 RESULTS

This section summarizes results from the nonlinear response history analyses for the various frames that were investigated.

4.1 4-Story Building

Results from the nonlinear response history analysis are summarized in figures similar to Figure 4-1. The figures highlight either residual drift or maximum story drift resulting from seismic activity. The solid black line with circular markers represents the control building with no elastic stories and standard gravity (p-delta) columns. The grey line with circular markers represents the building with at least one elastic story and standard gravity columns.

The title of each figure ("Average residual drifts for 3× ES at level 1, 4S") identifies the type of drift being presented and the size and location of the elastic story. First, the type of drift is described. Figure 4-1 shows average residual drift, Figure 4-2 shows 85th percentile (85%tile) residual drift, Figure 4-3 shows average maximum drift, and Figure 4-4 shows 85th percentile maximum drift. Second, the increase in brace size is identified. The "3× ES" in Figure 4-1's title indicates that the elastic story has a brace that is three times larger than the original (control) brace. Third, the title explicitly specifies the level of the elastic story. Figure 4-1 has an elastic story "at level 1". Finally, the "4S" at the end of the title represents the total number of stories in the building. Figure 4-1 highlights a 4-story (4S) building.

Figure 4-1 shows a reduction of residual drifts at every story after adding an elastic story to the bottom level (1st story). As the black control line is compared to the grey elastic story line with circular markers (p-delta stiffness = 1×), it becomes clear that adding an elastic story to the bottom level helps reduce residual drifts, especially at the first story. Numerically comparing the control and standard elastic story buildings shows a 33.8% decrease in the average residual drift over the entire building as shown in Table 4-2.

The 4-story elastic story building results in a significant reduction in overall residual drift; however, not every story experiences favorable decreases in drift. Figure 4-1 shows almost no residual drift at the 1st story, as expected, because this is the location of the elastic story. At this level, the residual drift fell from 0.0137 to 0.0004 after adding an elastic story, a 97.1% decrease. This is a favorable decrease especially because the 1st story drift is the largest in the 4-story control building. Looking at level 3 and 4 and comparing the control line to the grey line with circular markers, it is clear the residual drift actually increases at the 3rd and 4th story. Specifically, the control drift at level 4 is 0.00326 and increases to 0.00874 when an elastic story is added to level 1. This increase in drift is unfavorable; however, the significant decrease of residual drift at level 1 may be worth the trade-off. Overall, Figure 4-1 shows a general trend of greatest residual drift reduction at the bottom story with lessening residual drift reduction at every story after continuing to the top story. The greatest reduction of residual drift occurs at the elastic story and the least amount of residual drift reduction occurs in levels farthest from the elastic story.

Increasing the gravity (p-delta) column stiffness helps decrease residual drift, but may be expensive to implement. The varying grey lines shown in Figure 4-1 represent the various gravity column stiffnesses. The lines with '×' markers would not be economical for use, but are

included to help demonstrate the range of drift reduction possible by increasing the gravity column stiffnesses. Increasing gravity column stiffness 4× reduces average residual drifts in the building by 63.5% as compared to a decrease of 33.8% when standard stiffnesses are used, as shown in Table 4-1. Maximum drifts are also improved from an increase of 0.4% to a decrease of 8.2% when increasing gravity column stiffness 4×. This reduction in drifts is impactful, but causes a significant increase in the amount of steel required in the building. For example, in a 4-story building adding a 3× elastic story increases the amount of steel required by ~3,500 lbs, whereas increasing the gravity column stiffnesses by 4× adds ~48,300 lbs of steel. Clearly, adding elastic stories is considerably more economical than increasing the stiffnesses of gravity columns in elastic story buildings.

The 85th percentile residual drift plots have very similar reductions in drift as compared to the average residual drift plots in Figure 4-1. In 85th percentile case shown in Figure 4-2, the overall average residual drift in building is decreased by 46.8% after adding an elastic story at level 1. This reduction in 85th percentile residual drifts is significant because it shows that in extreme cases, elastic stories are beneficial to reducing residual drifts. Reductions in 85th percentile residual drifts are also seen by increasing gravity column sizes; however, these reductions are less significant than those reductions from adding elastic stories. For example, increasing gravity column stiffness 4× reduces overall average 85th percentile residual drifts 48.9% as compared to a decrease of 46.8% when only adding an elastic story to a 4-story building as shown in Table 4-1.

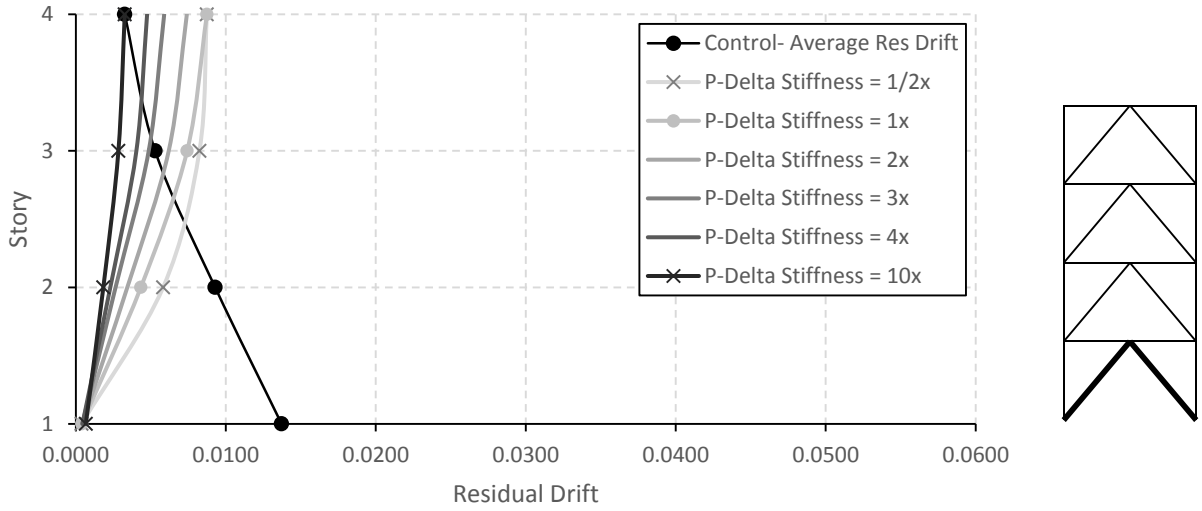

Figure 4-1. Average residual drifts for 3× ES at level 1, 4S.

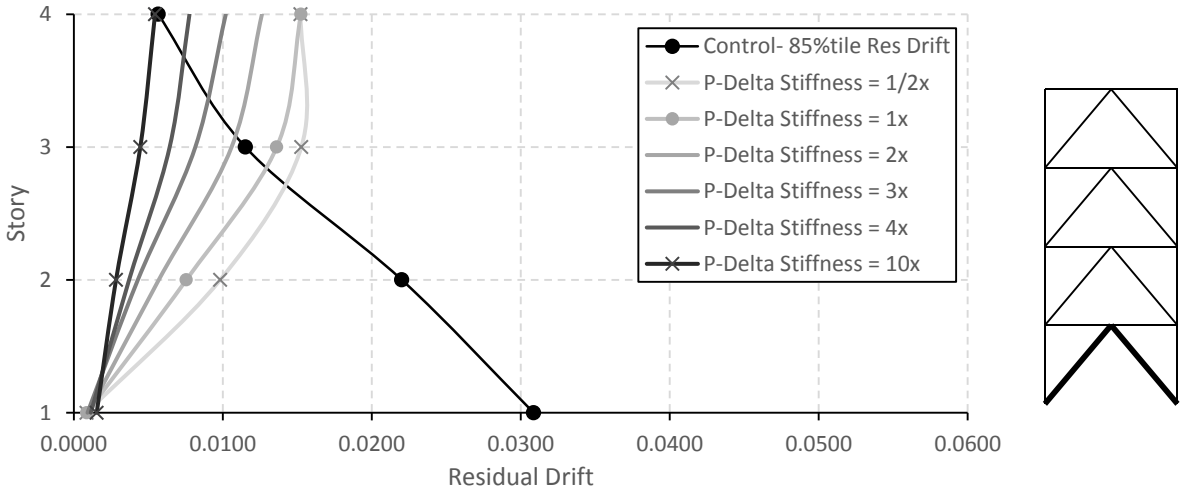

Figure 4-2. 85%tile residual drifts for 3× ES at level 1, 4S.

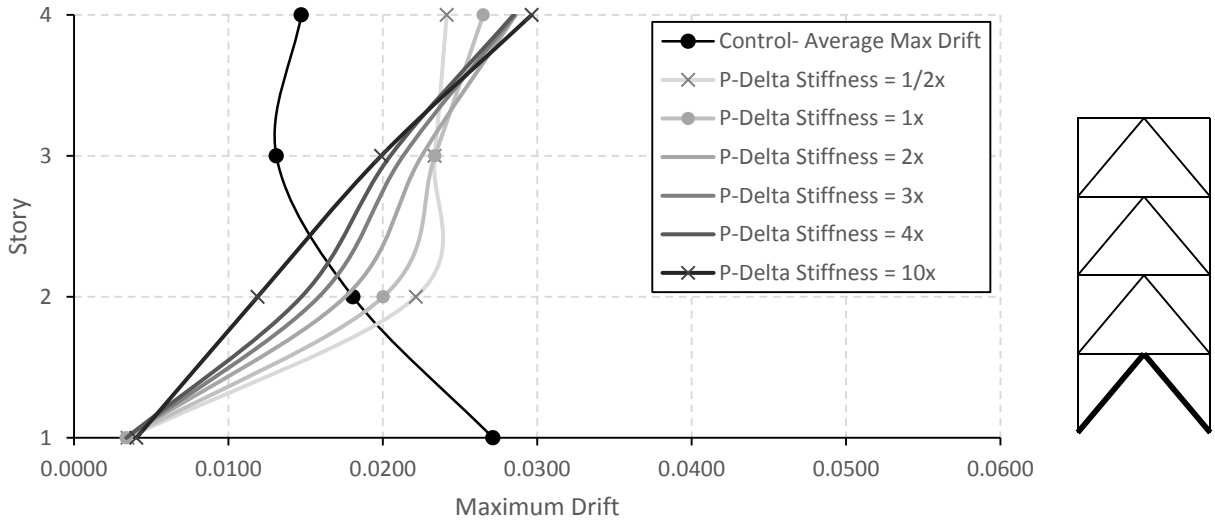

Figure 4-3. Average maximum drifts for 3× ES at level 1, 4S.

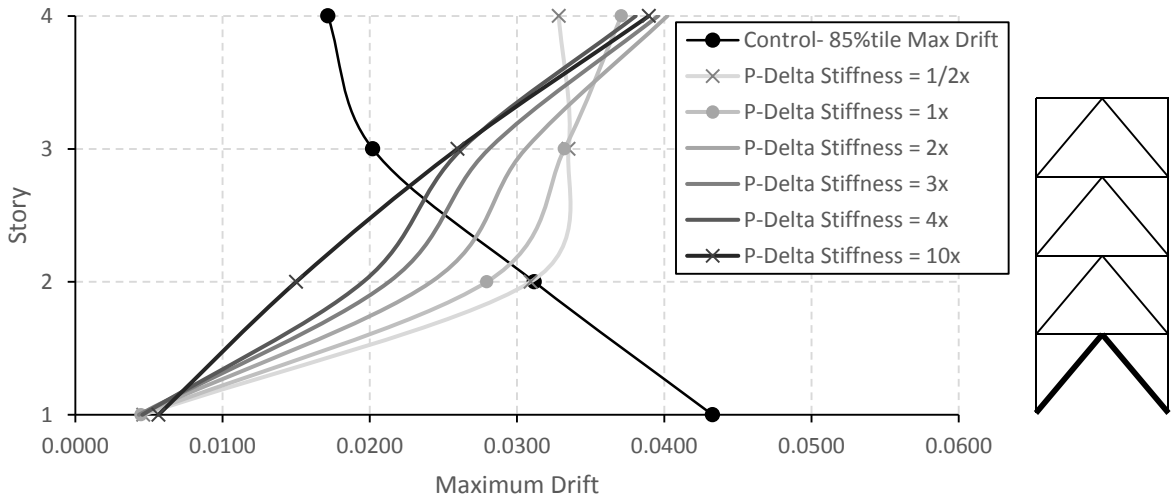

Figure 4-4. 85%tile maximum drifts for 3× ES at level 1, 4S.

Table 4-1. Comparison of Gravity Column Stiffnesses in 4-Story 3× ES Building

Stiffness Amount	% decrease in avg. residual drift	% decrease in avg. maximum drift
0.5× p-delta stiffness	26.5%	-0.1%
1× p-delta stiffness	33.8%	-0.4%
2× p-delta stiffness	44.8%	1.4%
3× p-delta stiffness	56.1%	5.3%
4× p-delta stiffness	63.5%	8.2%
10× p-delta stiffness	72.8%	10.4%

Increasing the elastic story brace to 3× the original (control) brace may be the most reasonable brace size because drifts are decreased significantly and the effects are still economical. For 4-story buildings, this trend is evident by comparing drift reductions between 2, 3, 4, and 10 times elastic stories as shown in Figure 4-6. The legend corresponding to Figure 4-6 is found in Figure 4-5. By comparing the black control lines with circular markers to the grey elastic story lines with circular markers, it is clear that using a 3× elastic story brace size reduces drifts more than when the brace is only increased 2×. When comparing 3× to and 10× elastic stories, a decrease in drift is evident by using the 10×, however, it does not seem worth the added cost for small improvement compared to the 6× difference in size. A trend of diminishing returns is also evident when using the 4× elastic story size. Similar results were found for the 6-, 8-, 12-, and 16-story buildings; thus, 3× elastic stories plots will be shown throughout the remainder of this chapter. All plots can be found in corresponding Appendices.

Table 4-2 shows the percentage of decrease in residual drifts throughout the entire building for various elastic story locations and sizes. For these 4-story buildings, the 3× elastic story building decreases overall residual drifts by 33.8%, which is the greatest reduction shown. The quantified results in Table 4-2 match those trends observed from the plots. Again, the 3× elastic story size may be the most optimal elastic story brace size to use.

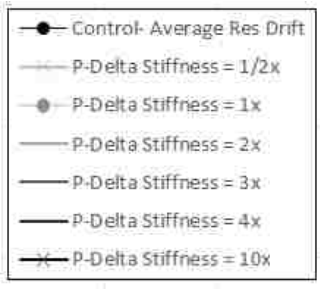

Figure 4-5. Legend for previous comparison plots.

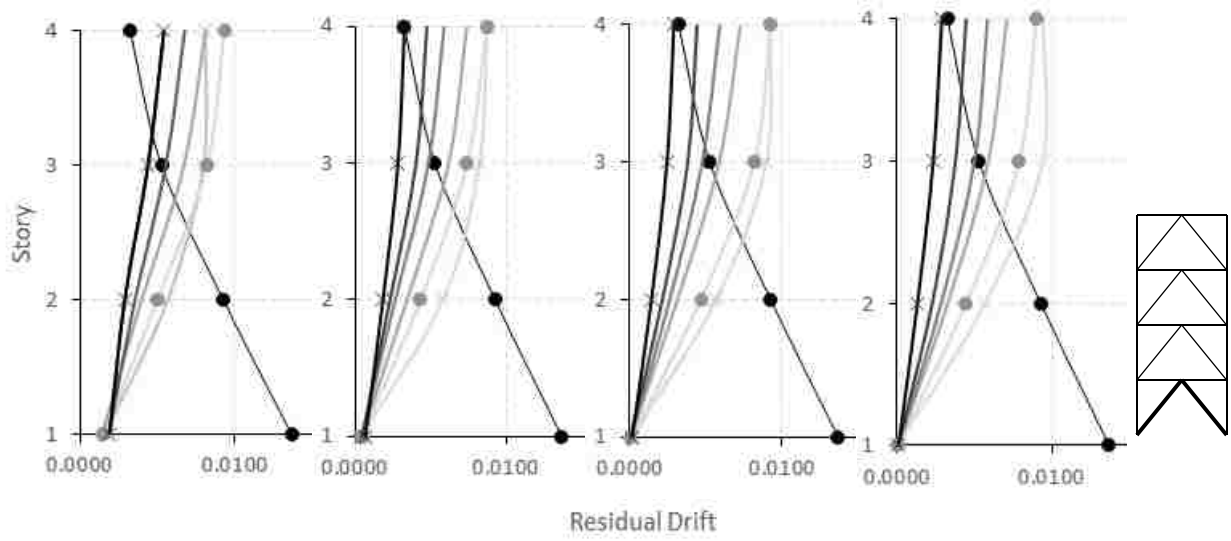

Figure 4-6. Comparison of average residual drifts for 2×, 3×, 4×, and 10× ES at level 1, 4S.

Table 4-2. Quantifiable Comparison of 4-Story Buildings with Various Elastic Stories

Building	Elastic story at Level 1 % decrease in avg. residual drift	Elastic story at Level 4 % decrease in avg. residual drift
2× elastic story	23.5%	-13.5%
3× elastic story	33.8%	-13.0%
4× elastic story	29.1%	-2.5%
10× elastic story	32.2%	-1.0%

Figure 4-3 and Figure 4-4 show a significant reduction in maximum drifts at the bottom (1st) story of the 4-story building after an elastic story is added there; however, an increase in maximum drifts is apparent at the upper stories. The 1st story has an 87.6% reduction in maximum drift; whereas the 2nd, 3rd, and 4th stories have a 10.6%, 78.4%, and 80.1% increase in drift, respectively. The addition of an elastic story at level 1 results in a 0.4% increase in maximum drifts over the entire building. The decrease in maximum drift at level 1 is essentially cancelled out by the increases in drift at the upper stories. A trade-off in the location of maximum drifts occurs. Increasing the stiffness of gravity columns help decrease maximum drifts some, but not significantly. The 85th percentile maximum drift plot follows similar trends.

Compared to residual drifts, maximum drifts have significantly less improvements (reductions) in drift values after adding elastic stories and increasing gravity column stiffness.

In 4-story buildings, adding an elastic story to the 1st level reduces residual drifts more than an elastic story at the 4th level. This is clear by comparing the values in Table 4-2. The far right column shows that adding an elastic story at the 4th level results in an overall increase in residual drifts. , which negatively affect the building. The building with an elastic story located at level 1 has an overall average story drift of 33.8% as compared to the an increase of 13.0% average story drift in the building with an elastic story at level 4. One of the main reasons for this significant decrease in residual drift is that the 1st story has the largest drifts in the control building and are thus, most affected by the addition of an elastic story at that level. The 4-story building with an elastic story at level 4 is shown in Figure 4-7 and can be compared to Figure 4-1.

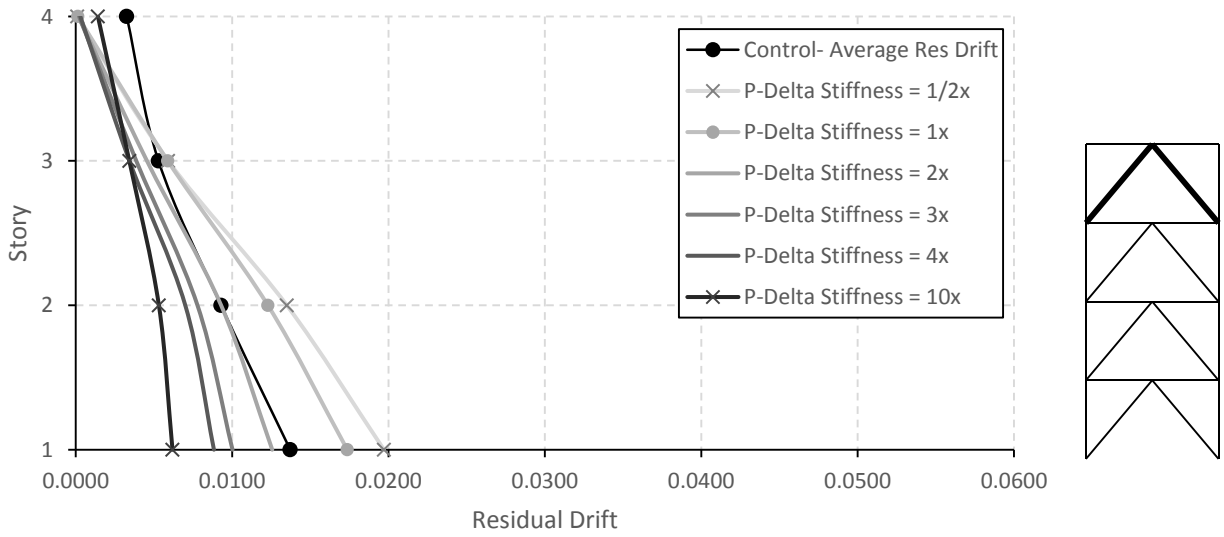

Figure 4-7. Average residual drifts for 3× ES at level 4, 4S.

All results for the 4-story buildings with an elastic story in the 4th story are presented in Appendix C. These results show a reduction in drifts at level 4, but only a slight reduction in drifts at level 1 if gravity column stiffnesses are also increased after the elastic story is added.

4.2 **6-Story Building**

Results for all the various locations of elastic stories 6-story buildings are summarized in Table 4-3. For 6-story buildings with elastic stories at one level, placing an elastic story at level 2 reduces residual drifts the most with a 35.5% decrease. Placing an elastic story at level 1 reduces the overall residual drifts in the building by 26.4%. Combination elastic stories (elastic stories at more than one location) were also analyzed. The building with elastic stories at levels 1 and 5 has a 52.8% reduction in residual drifts as compared to the building with elastic stories at levels 2 and 6 with a 60.2% reduction. Combination elastic stories are significantly more effective at reducing drifts than single elastic stories as shown in Table 4-3.

Figure 4-8 and Figure 4-9 show the two combination elastic story buildings with elastic stories at level 1 and 5, followed by 2 and 6, respectively. Comparing these plots, the building with elastic stories at levels 1 and 5 increases residual drifts at levels 3 and 4, whereas the building with elastic stories at levels 2 and 6 only increases drifts at level 4. Table 4-3 also shows the 2 and 6 elastic story building has the largest decrease in both residual and maximum drifts. This indicates that the 2 and 6 elastic story locations may be most beneficial to reducing drifts.

Table 4-3. Quantifiable Comparison of 6-Story Buildings with 3× ES

Location of ES	% decrease in avg. residual drift	% decrease in avg. maximum drift
Story 1	26.4%	5.9%
Story 2	35.5%	2.8%
Story 3	11.0%	5.2%
Story 4	-1.5%	2.6%
Story 5	9.6%	5.9%
Story 6	10.2%	9.0%
Stories 1 & 5	52.8%	15.8%
Stories 2 & 6	60.2%	18.5%

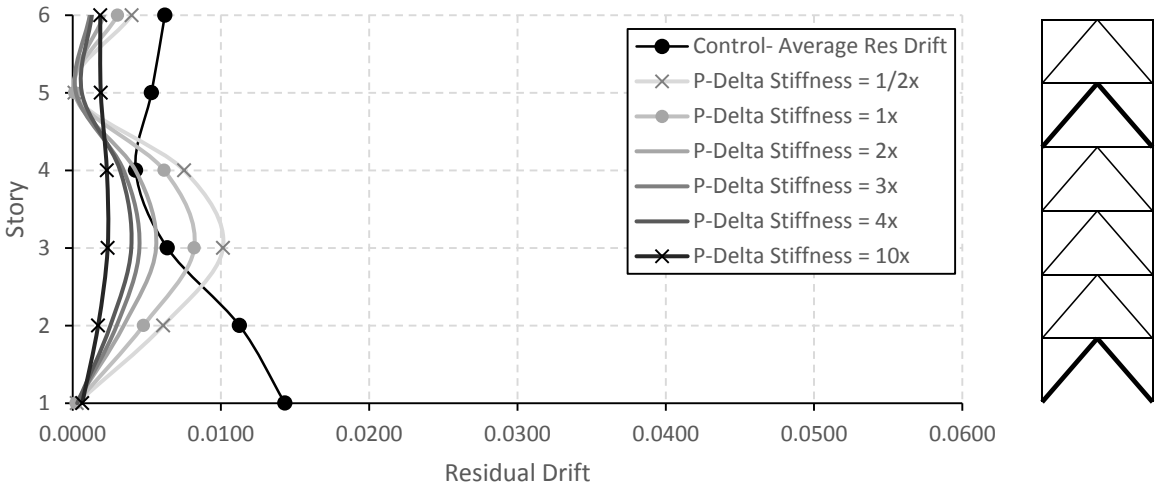

Figure 4-8. Average residual drifts for 3× ES at level 1&5, 6S.

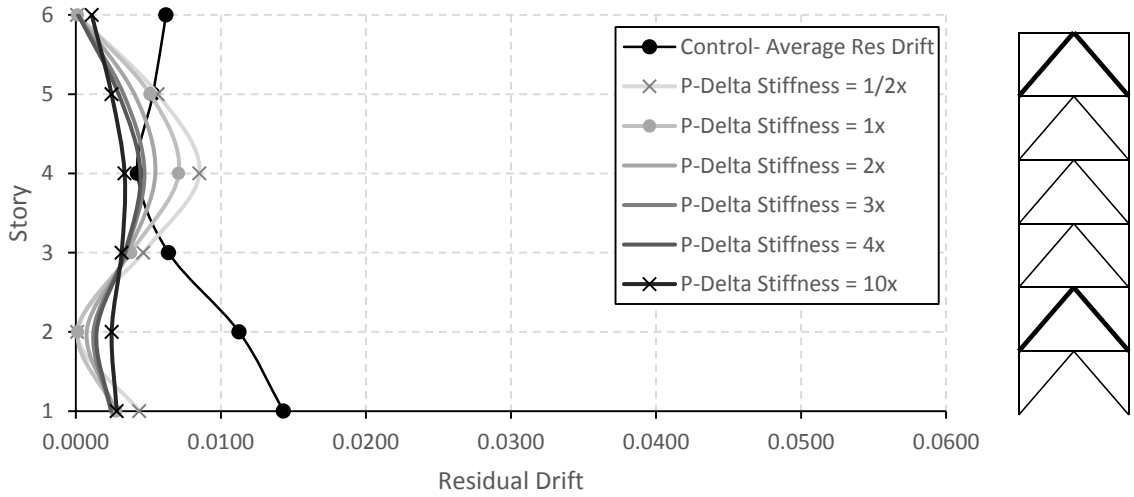

Figure 4-9. Average residual drifts for 3× ES at level 2&6, 6S.

From Table 4-3 it is clear that maximum drifts are reduced significantly less than residual drifts by the addition of elastic stories. Only the combination building with elastic stories at levels of 1 and 5 had greater than 10% decrease in maximum drifts, whereas, all 8 buildings with varying elastic story locations except 2 had greater than 10% decrease in residual drift. Additionally, both combination stories have a decrease greater than 50% in residual drifts, but less than 20% decrease in maximum drifts. Overall, maximum drifts seem to experience a "trade-off" effect when elastic stories are used. This effect includes some stories experiencing a decrease in maximum drifts, whereas other stories experience an increase in maximum drift due to the same change size and location of elastic stories. This trade-off at different levels results in little to no overall decrease in maximum drifts as shown in Figure 4-10. This is one of the main reasons the average maximum building drifts have low reduction percentages. All 6-story plots are presented in Appendix D.

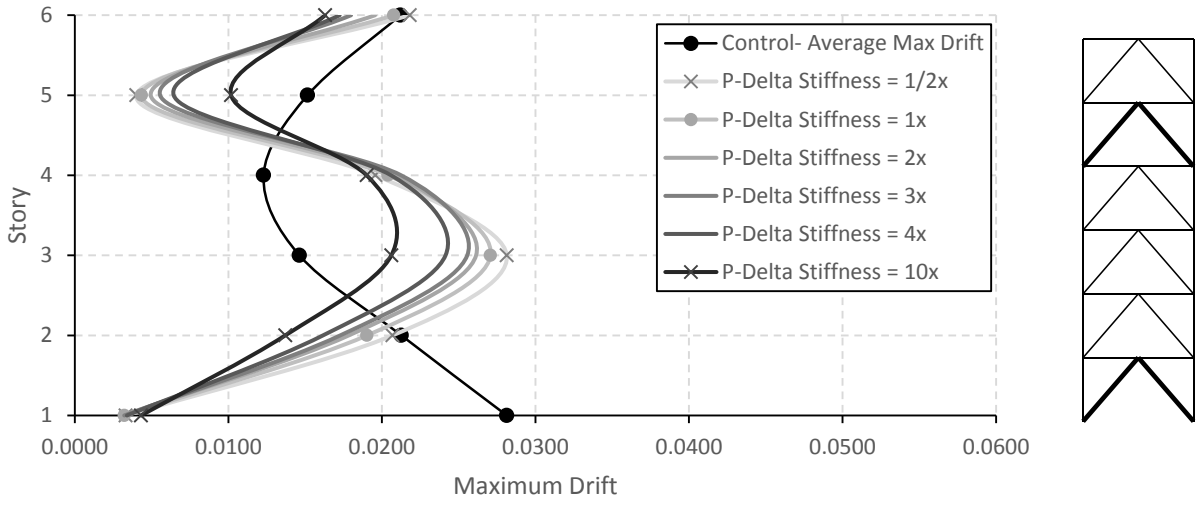

Figure 4-10. Average maximum drifts for 3× ES at level 1&5, 6S.

4.3 **8-Story Building**

8-story building's residual drifts decreased most when elastic stories were added on both the 1st and 5th floor. This is evident by first comparing the overall residual drift values of both the standard gravity column 1 and 5 elastic story building and the standard gravity column 4 and 8 elastic story building as shown in Table 4-4. The 1 and 5 elastic story building has a 1.5× greater reduction in residual drifts than the 4 and 8 elastic story building. Additionally, comparing the 1 and 5 elastic stories building in Figure 4-11 to the 4 and 8 elastic stories building in Figure 4-12, confirms that having an elastic story close to the bottom level helps reduce residual drifts significantly because the greatest residual drift in the control building is at the 1st story. Perhaps further research could determine if elastic stories at levels 2 and 6 have greater reductions in residual drifts than elastic stories at levels 1 and 5. The large residual drifts at the top level in Figure 4-11 imply that an elastic story closer to the top may be beneficial. Overall, placing elastic stories at the bottom level and continuing every 4-stories above reduce drifts more than starting an elastic story at the top level; still, further research is recommended to determine if elastic stories at more intermediate locations perform more favorably.

Increasing gravity column sizes continue to decrease drifts, although the economic advantage is uncertain, as discussed with the 4-story results. It is clear from the Figure 4-11 that the elastic stories help reduce residual drifts significantly more than increasing gravity column stiffness. This is similar to the trends discussed with the 4- and 6-story buildings.

Table 4-4.Quantified Comparison of 8-Story Buildings with 4× ES

Location of ES	% decrease in avg. residual drift	% decrease in avg. maximum drift
Stories 1 & 5	44.4%	14.2%
Stories 4 & 8	27.6%	19.3%

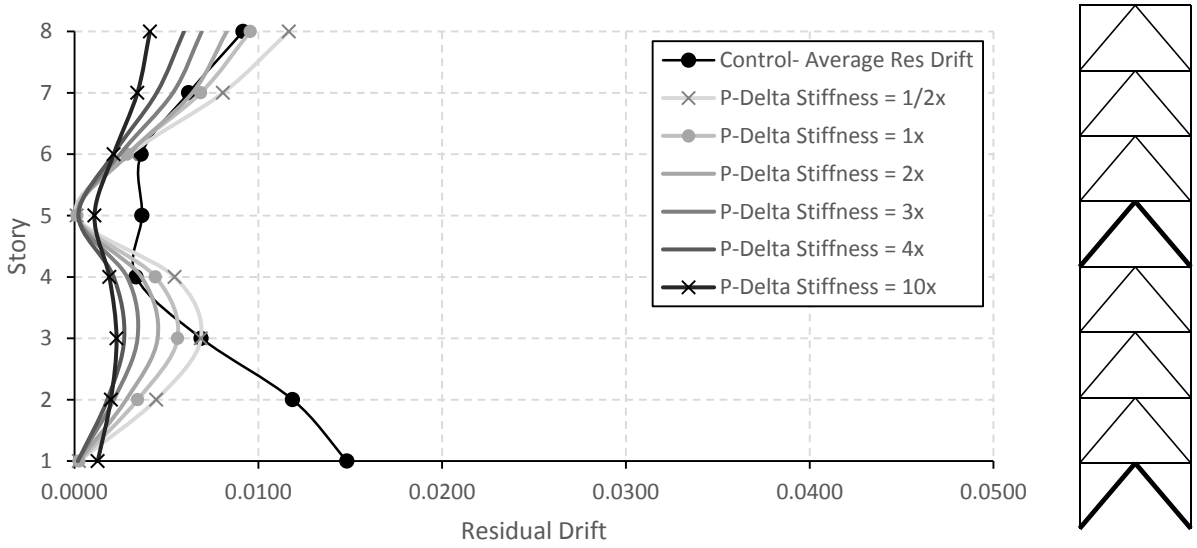

Figure 4-11. Average residual drifts for 3× ES at level 1&5, 8S.

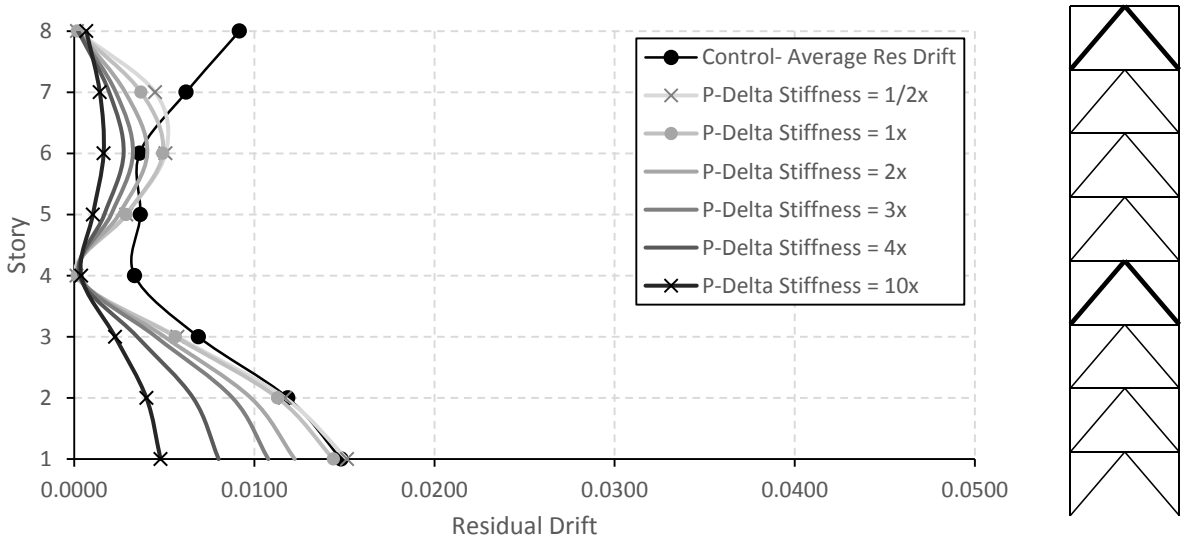

Figure 4-12. Average residual drifts for 3× ES at level 4&8, 8S.

Maximum drifts, again, show no significant decrease in drifts as indicated in Table 4-4. Some levels in the buildings continue to have higher maximum drifts, while others have lower drifts after elastic stories are added. This trade-off effect continues as shown in Figure 4-13. Graphs of all 8-story analyses performed are presented in Appendix E.

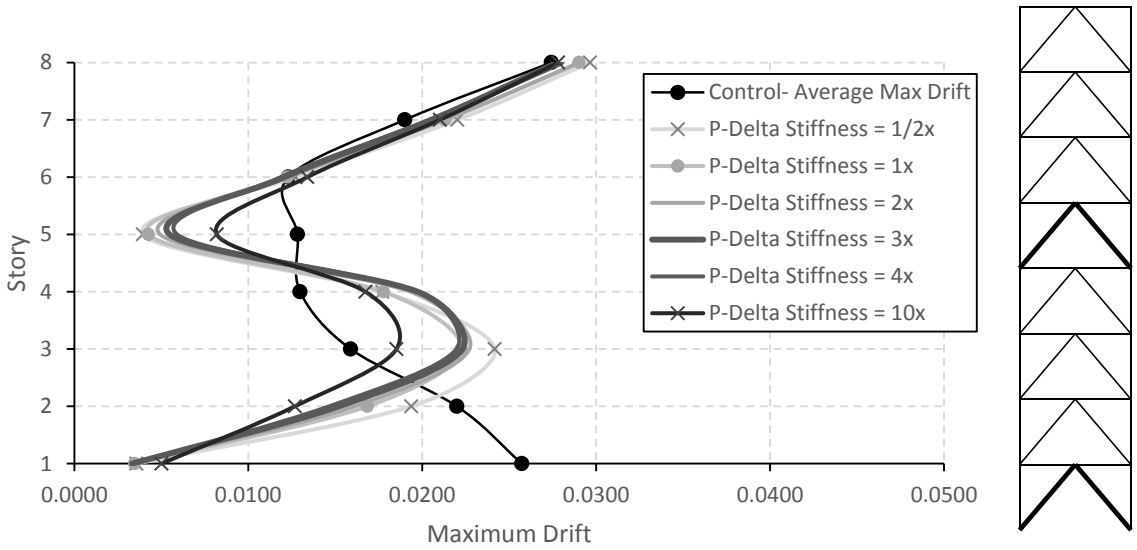

Figure 4-13. Average maximum drifts for 3× ES at level 1&5, 8S.

4.4 **12-Story Building**

The 12-story (12S) 1, 5, & 9 elastic story (ES) building has the greater overall decrease in residual and maximum drifts as compared to the 4, 8, & 12 elastic story building as shown in Table 4-5. The 12-story building with elastic stories at levels 1, 5, & 9 has a 64.8% decrease in residual drift, whereas the 4, 8, & 12 ES building has a 31.3% decrease. The 12-story building with an elastic story starting at the bottom level and continuing every 4 stories above has twice the decrease in residual drifts. For the elastic story locations researched here in, it is clear that having an elastic story at the bottom level helps decrease drifts most because control drifts are the highest at level 1.

Further research is recommended to study the effects of elastic stories at intermediate locations. The 1, 5, & 9 ES building shown in Figure 4-14 has the largest drifts at the top level. The 4, 8, & 12 ES building shown in Figure 4-15 has the largest drifts at the bottom level. This implies that perhaps using elastic stories at more intermediate locations, such as starting elastic stories at levels 2 or 3, could further reduce drifts.

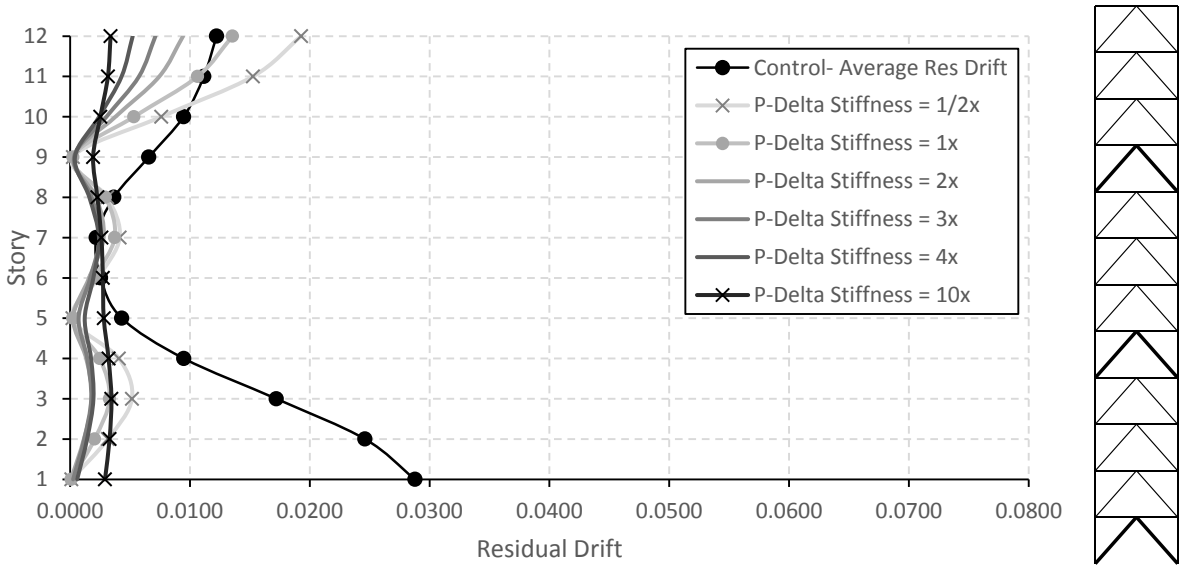

Figure 4-14. Average residual drifts for 3× ES at level 1, 5, & 9, 12S.

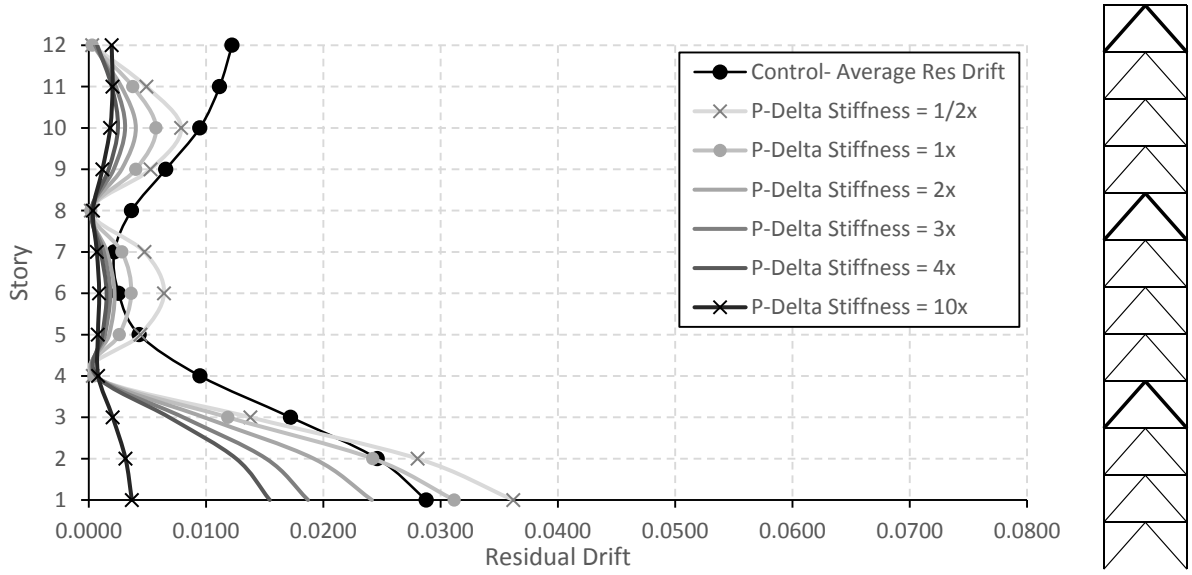

Figure 4-15. Average residual drifts for 3× ES at level 4, 8, & 12, 12S.

Table 4-5. Quantified Comparison of 12-Story Buildings with 3× ES

Location of ES	% decrease in avg. residual drift	% decrease in avg. maximum drift
Stories 1, 5, & 9	64.8%	15.6%
Stories 4, 8, & 12	31.3%	14.4%

Maximum drifts did not improve with the addition of elastic stories as observed with previous buildings. A similar trade-off effect as noted in previous buildings is shown in Figure 4-16. Graphs of all 12-story analyses performed are presented in Appendix F.

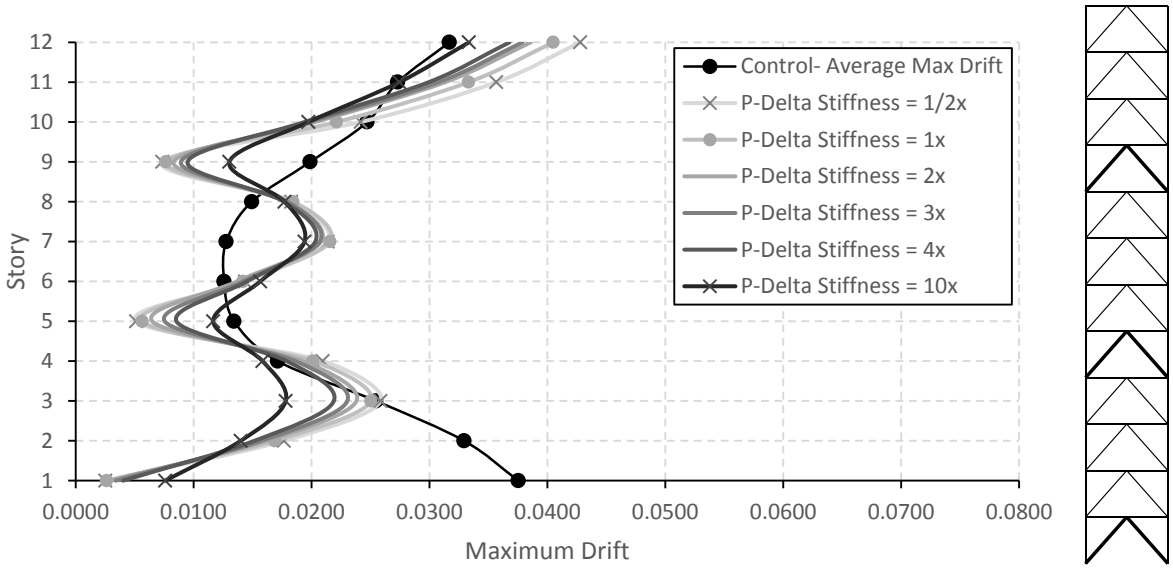

Figure 4-16. Average maximum drifts for 3× ES at level 1, 5, & 9, 12S.

4.5 **16-Story Building**

The 16-story buildings had similar reductions in drifts to those in previous buildings, with the 1, 5, 9, & 13 ES buildings having greater residual drift reductions than the 4, 8, 12, &16 ES building. This is shown by comparing Figure 4-17 and Figure 4-18. Specific reduction values corresponding to the 16-story plots are shown in Table 4-6.

Further research is recommended to confirm optimal elastic story locations. A pattern of significantly reduced residual drifts in between two elastic stories is shown in Figure 4-17. This implies that for a 17-story building with elastic stories at levels 1, 5, 9, 13, & 17, the drifts would be significantly reduced, likely even more than is observed in the 16-story buildings. To further

reduce drifts in the 16-story buildings, intermediate elastic story locations are recommended to be studied. Perhaps elastic stories at levels 2, 6, 10, & 14 or levels 3, 7, 11 & 15 would reduce drifts further. Also, additional testing justifying the need for 4 story increments between elastic stories is recommended.

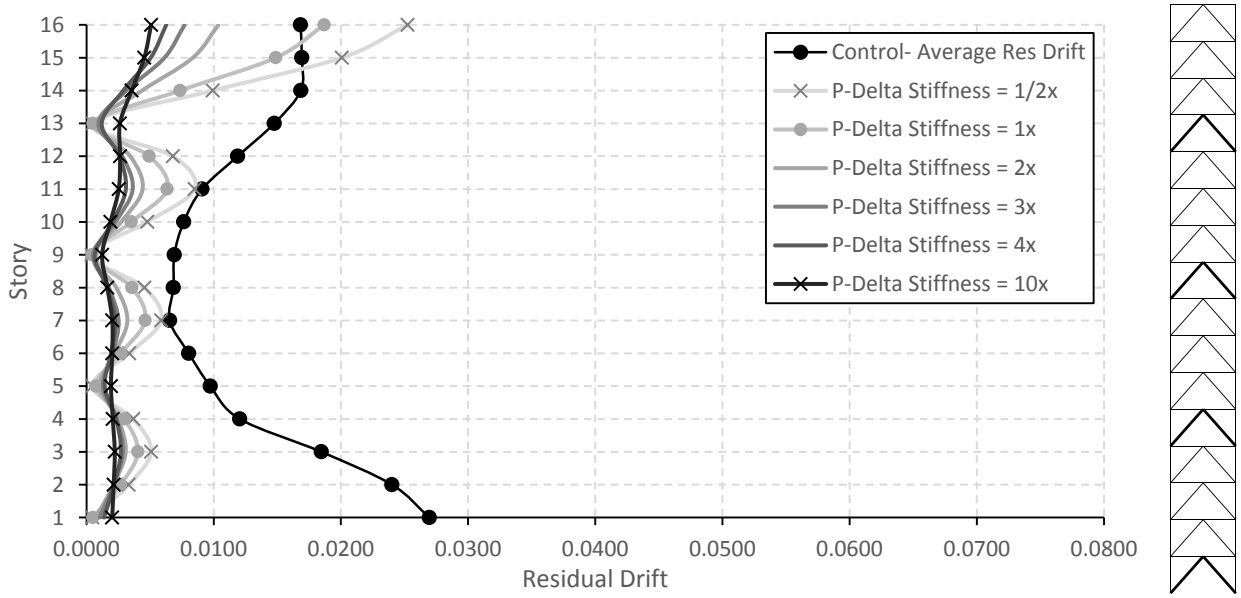

Figure 4-17. Average residual drifts for 3× ES at level 1, 5, 9, & 13, 16S.

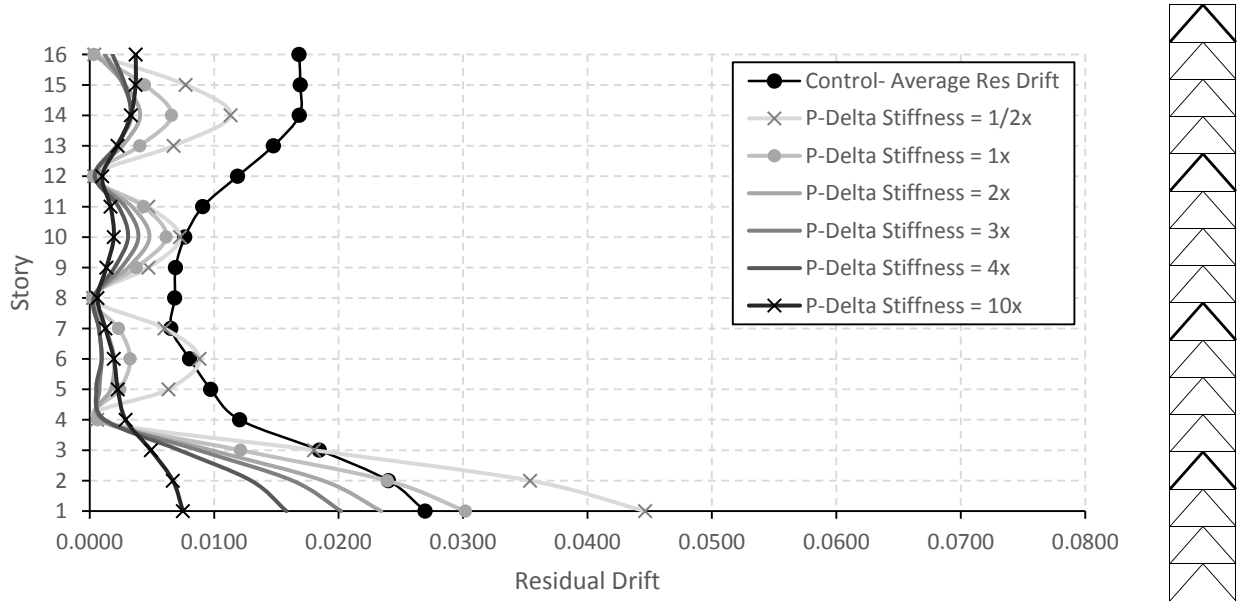

Figure 4-18. Average residual drifts for 3× ES at level 4, 8, 12, &16, 16S.

Table 4-6. Quantified Comparison of 16-Story Buildings with 3× ES

Location of ES	% decrease in avg. residual drift	% decrease in avg. maximum drift
Stories 1, 5, 9, & 13	63.2%	19.5%
Stories 4, 8, 12 & 16	50.8%	18.5%

Maximum drifts did not significantly improve (decrease) with the addition of elastic stories as observed with previous buildings. The trade-off effect continues in the 16-story buildings as shown in Figure 4-19. Graphs of all 16-story analyses performed are presented in Appendix G.

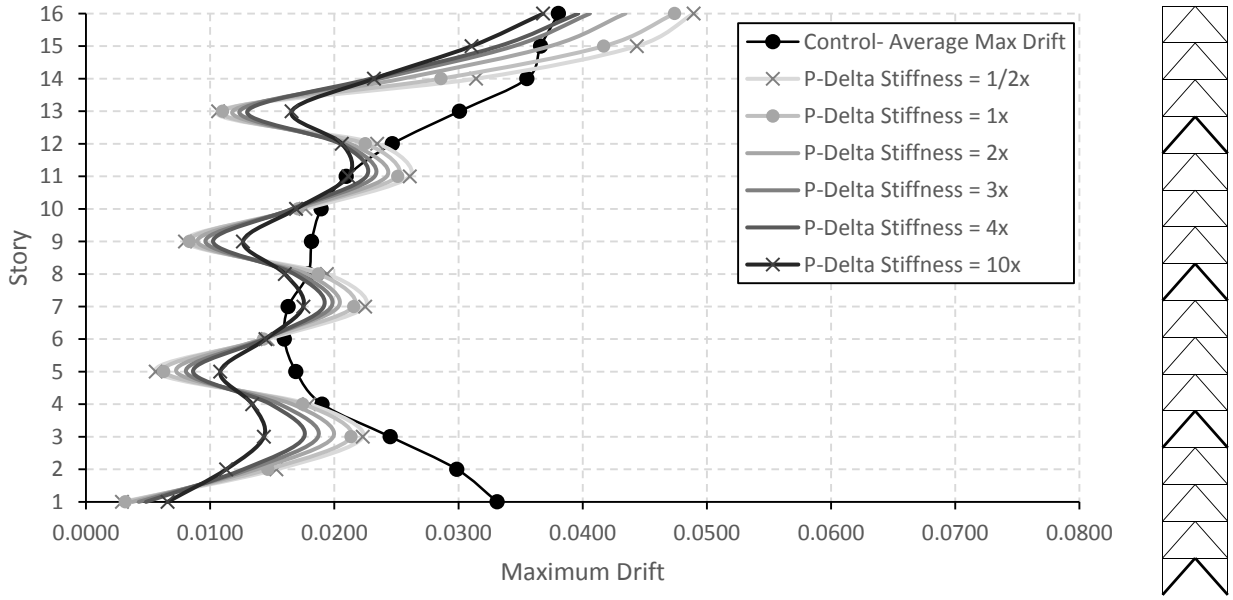

Figure 4-19. Average maximum drifts for 3× ES at level 1, 5, 9, & 13, 16S.

5 SUMMARY AND CONCLUSION

From the research presented here, adding elastic stories helps reduce residual drifts. The main conclusions found include:

1. Residual drifts are reduced by an average of 34–65% when elastic stories are added in buildings ranging from 4–16 stories.
2. Maximum drifts are minimally affected by the addition of elastic stories. Some levels show decrease in drifts, while others are increased.
3. Increasing gravity column stiffness decreases residual drifts; however, this procedure may not be economical. The addition of elastic stories has a greater impact on decreasing residual drifts than the combination of adding elastic stories and increasing gravity column stiffness in steel BRBF buildings.
4. The optimal location of elastic stories was observed to be at the 1st floor and every 4th story thereafter (e.g., elastic stories would be at levels 1, 5, and 9 for a 12-story building). It can be inferred that this pattern would work especially well for 5-, 9-, 13-, and 17-story buildings because an elastic story would be located at the top and bottom level, causing significant drift reduction at these locations. The optimal size of elastic stories braces was observed to be 3× the size of the control brace.
5. The reduction in residual drifts is greater in taller buildings than shorter buildings. As the number of stories increases, the residual drift reduction also increases.

Overall, adding elastic stories reduces residual drifts. It was observed that adding elastic stories to the bottom stories provides the most significant decrease in drift. Specifically, adding elastic stories starting at the bottom level decreases drifts more than starting at the top level. Interestingly, the 6-story results showed a greater decrease in drifts when elastic stories were added at levels 2 and 6 versus levels 1 and 5. This implies that having an elastic story close to the bottom and at the top could be an optimal configuration. Additional research is recommended to investigate arrangements of elastic stories starting at level 2 or 3 and continuing every four stories, especially in buildings with six or more stories. Further research is also recommended to confirm the optimal brace size for an elastic story.

REFERENCES

[1] Erochko, J., Christopoulos, C., Tremblay, R., & Choi, H. (2011). "Residual drift response of SMRFs and BRB frames in steel buildings designed according to ASCE 7-05." *Journal of Structural Engineering*, 137(5), 589-599.

[2] AISC. (2011). *Manual of Steel Construction*, Fourteenth Edition. American Institute of Steel Construction, Chicago, IL.

[3] StarSeismic (2014). "StarSeismic buckling restrained braced frame system." StarSeismic, Park City, UT.

[4] Pettinga, D., Christopoulos, C., Pampanin, S., & Priestley, N. (2007). "Effectiveness of simple approaches in mitigating residual deformations in buildings." *Earthquake Engineering & Structural Dynamics*, 36(12), 1763-1783.

[5] Kiggins, S., & Uang, C. M. (2006). "Reducing residual drift of buckling-restrained braced frames as a dual system." *Engineering Structures*, 28(11), 1525-1532.

[6] Ariyaratana, C., & Fahnestock, L. A. (2011). "Evaluation of buckling-restrained braced frame seismic performance considering reserve strength." *Engineering Structures*, 33(1), 77-89.

[7] Boston, M. & Richards, P. W. (2012) "Seismic response of BRBFs coupled with heavy gravity columns." In *Proceedings of the 15th World Conference on Earthquake Engineering*, Lisbon, Portugal.

[8] McCormick, J., Aburano, H., Ikenaga, M., & Nakashima, M. (2008, October). "Permissible residual deformation levels for building structures considering both safety and human elements." In *Proceedings of the 14th World Conference on Earthquake Engineering* (pp. 12-17).

[9] Christopoulos, C., & Pampanin, S. (2004). "Towards performance-based design of MDOF structures with explicit consideration of residual deformations." *ISET Journal of Earthquake Technology*, 41(1), 53-57.

[10] MacRae, G. A., & Kawashima, K. (1997). "Post-earthquake residual displacements of bilinear oscillators". *Earthquake engineering & structural dynamics*, 26(7), 701-716.

[11] Hatzigeorgiou, G. D., Papagiannopoulos, G. A., & Beskos, D. E. (2011). "Evaluation of maximum seismic displacements of SDOF systems from their residual deformation." *Engineering structures*, 33(12), 3422-3431.

[12] Borzi, B., Calvi, G. M., Elnashai, A. S., Faccioli, E., & Bommer, J. J. (2001). "Inelastic spectra for displacement-based seismic design." *Soil Dynamics and Earthquake Engineering*, 21(1), 47-61.

[13] Yazgan, U., & Dazio, A. (2012). "Post-earthquake damage assessment using residual displacements." *Earthquake Engineering & Structural Dynamics*, 41(8), 1257-1276.

[14] Lestuzzi, P., Wenk T., & Backmann H. (1999). "Dynamische versuche an stahlbetontragwänden auf dem ETH-Erdbebensimulator (Dynamic tests of reinforced concrete structural walls on the ETH earthquake simulator)." *Nr.240, Institute of Structural Engineering (IBK)*, ETH Zurich, http://e-collection.ethbib.ethz.ch/view/eth:23297

[15] Christopoulos, C., Pampanin, S., & Nigel Priestley, M. J. (2003). "Performance-based seismic response of frame structures including residual deformations." Part I: Single-degree of freedom systems. *Journal of Earthquake Engineering*, 7(1), 97-118.

[16] Pampanin, S., Christopoulos, C., & Nigel Priestley, M. J. (2003). "Performance-based seismic response of frame structures including residual deformations. Part II: Multi-degree of freedom systems." *Journal of Earthquake Engineering*, 7(1), 119-147.

[17] Ruiz-García, J., & Miranda, E. (2006). "Residual displacement ratios for assessment of existing structures." *Earthquake engineering & structural dynamics*, 35(3), 315-336.

[18] Clark, P. W., Aiken, I. D., Kasai, K., & Kimura, I. (2000, May). "Large-scale testing of steel unbonded braces for energy dissipation." In *Proceedings of the Structural Congress*.

[19] Sabelli, R., Mahin, S., & Chang, C. (2003). "Seismic demands on steel braced frame buildings with buckling-restrained braces." *Engineering Structures*, 25(5), 655-666.

[20] Tremblay, R., Lacerte, M., & Christopoulos, C. (2008). "Seismic response of multistory buildings with self-centering energy dissipative steel braces." *Journal of structural engineering*, 134(1), 108-120.

[21] Choi, H., Erochko, J., Christopoulos, C., & Tremblay, R. (2008). "Comparison of the seismic response of steel buildings incorporating self-centering energy dissipative braces, buckling restrained braced and moment resisting frames." In *Proceedings of the 14th World Conference on Earthquake Engineering*, (No. 05).

[22] Christopoulos, C., Filiatrault, A., & Folz, B. (2002). "Seismic response of self-centring hysteretic SDOF systems." *Earthquake engineering & structural dynamics*, 31(5), 1131-1150.

[23] Ricles, J. M., Sause, R., Garlock, M. M., & Zhao, C. (2001). "Posttensioned seismic-resistant connections for steel frames." *Journal of Structural Engineering*, 127(2), 113-121.

[24] Garlock, M. M., Ricles, J. M., & Sause, R. (2005). "Experimental studies of full-scale posttensioned steel connections." *Journal of Structural Engineering*, 131(3), 438-448.

[25] Chou, C. C., Chen, J. H., Chen, Y. C., & Tsai, K. C. (2006). "Evaluating performance of post-tensioned steel connections with strands and reduced flange plates." *Earthquake engineering & structural dynamics*, 35(9), 1167-1185.

[26] Kim, H. J., & Christopoulos, C. (2009). "Seismic design procedure and seismic response of post-tensioned self-centering steel frames." *Earthquake Engineering & Structural Dynamics*, 38(3), 355-376.

[27] Fahnestock, L. A., Sause, R., & Ricles, J. M. (2007). "Seismic response and performance of buckling-restrained braced frames." *Journal of Structural Engineering*, 133(9), 1195-1204.

[28] Fahnestock, L. A., Ricles, J. M., & Sause, R. (2007). "Experimental evaluation of a large-scale buckling-restrained braced frame." *Journal of structural engineering*, 133(9), 1205-1214.

[29] Christopoulos, C., Tremblay, R., Kim, H. J., & Lacerte, M. (2008). "Self-centering energy dissipative bracing system for the seismic resistance of structures: Development and validation." *Journal of structural engineering*, 134(1), 96-107.

[30] Chou, C. C., & Chen, Y. C. (2012, September). "Development and seismic performance of steel dual-core self-centering braces." In *15th World Conference on Earthquake Engineering* (pp. 24-28).

[31] Boston, M. (2012). "Reducing residual drift in buckling-restrained braced frames by using gravity columns as part of a dual system." Master's thesis, Brigham Young University, Provo, UT.

[32] ASCE (2005). *Minimum Design Loads for Buildings and Other Structures*. ASCE/SEI 7-05, American Society of Civil Engineers, Reston, VA.

[33] Mazzoni S, McKenna F, Scott M, Fenves G. (2006). "OpenSees command language manual." *Pacific Earthquake Engineering Research Center (PEER)*, Berkeley, CA.

[34] CoreBrace (2013). "Bolted lub corebrace BRB tables." CoreBrace, West Jordan, UT.

[35] Newell J, Uang C-M, & Benzoni G (2001). "Subassemblage testing of corebrace buckling-restrained braces (G series)." University of California, San Diego, La Jolla, CA.\

APPENDIX A. BRACE AND COLUMN DESIGN CALCULATIONS

The following section shows detailed calculations of the brace and column design.

A.1 Brace Design Calculations

Sample calculations for 8-story BRBF buildings are shown below. To determine the base shear of the building, an assumed seismic mass of 90 psf was used.

8-Story Building Brace Design

The steps to design building BRBF braces:
A) Determine the design base shear of the entire building
B) Compute the equivalent lateral force at each level
C) Determine the lateral forces at each level of BRBF
D) Compute the brace axial loads at each level of BRBF
E) Determined the core area for the braces at each level
Note: Round up to the nearest 0.5 in^2 for braces under 10 in^2, and round up to nearest 1 in^2 for bigger braces. Assume $F_{ysc\ min}$=38 ksi for the brace core material.

Input Variables:

$Story_{height} := 180in = 15 \cdot ft$ $N_{stories} := 8$

$Bay_{width} := 360in = 30 \cdot ft$ $N_{bays} := 2$

$S_{height} := 15$

$Area_{trib} := \left(Bay_{width} \cdot 2 + 0.5 \cdot Bay_{width} + 2ft\right)^2 = 5929 \cdot ft^2$

$Perimeter := \frac{\left(Bay_{width} \cdot 5 + 4ft\right) \cdot 4}{4} = 154 \cdot ft$

$Dead_{roof} := 80psf$ $Partition := 20psf$

Assumptions

$I_e := 1.0$ $R_a := 8$ Ra from ASCE 7, section 14.1, Table 12.2-1

$S_{DS} := 1.03$

$S_{D1} := 0.89$

$C_u := 1.4$

$C_t := 0.03$ Cu from ASCE 7, Table 12.8-1; Ct and x from Table 12.8-2

$x_{value} := 0.75$

$SeismicMass_{assumed} := 90psf$

Assume Base Fixity is Pinned

A) Determine the base shear of the entire building

$Height_{building} := S_{height} \cdot N_{stories} = 120$

$T_a := C_t \cdot \left(Height_{building}\right)^{x_{value}} = 1.088$

Assume $T_1 := T_a = 1.088$

$Dead_{floor} := 80psf$ $Live_{load} := 50psf$

$Dead_{extwall} := 375plf$

$C_{s1} := \dfrac{S_{DS}}{\left(\dfrac{R_a}{I_e}\right)} = 0.129$

- Calculate Cs values- use the minimum between Cs1 and Cs2
- Check Cs3 and make sure it is the minimum of all. If not, then Cs3 governs.

$C_{s2} := \dfrac{S_{D1}}{T_1 \cdot \left(\dfrac{R_a}{I_e}\right)} = 0.1023$

Cs2 < Cs1 so Cs2 governs

$C_{s3} := 0.044 \cdot S_{DS} \cdot I_e = 0$

Cs3 < Cs2 therefore Cs2 governs

$SeismicWeight_{floor} := \left(Dead_{extwall} \cdot Perimeter\right) + Partition \cdot Area_{trib} + Dead_{floor} \cdot Area_{trib} = 650.7 \cdot kip$

$Weight_{roof} := \left(Dead_{extwall} \cdot Perimeter\right) \cdot 0.5 + Dead_{roof} \cdot Area_{trib} = 503.2 \cdot kip$

$Weight_{total} := \left(N_{stories} - 1\right) \cdot SeismicWeight_{floor} + Weight_{roof} = 5057.7 \cdot kip$

$AssumedWeight_{total} := N_{stories} \cdot SeismicMass_{assumed} \cdot Area_{trib} = 4268.9 \cdot kip$

Use assumed value for weight

$V_{base} := C_{s2} \cdot AssumedWeight_{total} = 436.6 \cdot kip$ <---------- Design case shear of the entire building

B) Compute the equivalent lateral force at each level

$slope_1 := \dfrac{2 - 1}{2.5 - .5} = 0.5$

$y := slope_1 \cdot \left(T_1 - .5\right) + 1 \rightarrow 1.29384757152421825$

$k := 1.294$

w = weight, h = cumulative height of building at level

$C_{vx} = w_{hk}/sum(w_{hk})$

$Fx = V_b * C_{vx}$

Table A-1. Brace Design: Equivalent Lateral Forces at Each Level

Levels	w (kips)	h (ft)	h^k (ft)	wh^k	C_{vx}	F_x (kips)
1	533.61	15	33.24167	17738	0.017	7.41
2	533.61	30	81.50228	43490	0.042	18.17
3	533.61	45	137.7225	73490	0.070	30.70
4	533.61	60	199.8282	106630	0.102	44.54
5	533.61	75	266.7126	142320	0.136	59.45
6	533.61	90	337.6696	180184	0.172	75.26
7	533.61	105	412.2027	219955	0.210	91.88
8	533.61	120	489.9408	261437	0.250	109.20
Totals	4268.88			1045246	1.00	436.60

C) Determine the lateral forces at each level of BRBF
-from top story (bottom of table) sum F_x values

D) Compute the brace axial loads at each level of BRBF
$Pu_{brace} = (1/2)*((Baywidth/2)^2+StoryHeight^2)^{0.5}*LateralForces$

E) Determined the core area for the braces at each level
$Area_{brace} = Pu_{brace}/(fi*Fy) = Pu_{brace}/(0.9*38)$

Note: Round up to the nearest 0.5 in^2 for braces.
Assume $Fy_{sc,min}$=38 ksi for the brace core material.

Table A-2. Brace Design: Core Area Required at Each Level

Level	F_x (kip)	Sum lat forces	Axial Force of BRBF Brace	Core Area Required (in^2)	Rounded Area (in^2)
1	7.41	436.60	308.72	9.03	9.5
2	18.17	429.19	303.48	8.87	9.0
3	30.70	411.02	290.64	8.50	8.5
4	44.54	380.33	268.93	7.86	8.0
5	59.45	335.79	237.44	6.94	7.0
6	75.26	276.34	195.40	5.71	6.0
7	91.88	201.08	142.18	4.16	4.5
8	109.20	109.20	77.22	2.26	2.5
		Step C	Step D	Step E	

The text above outlines the process followed throughout this research. A spreadsheet was developed to automate this process for buildings with varying number of stories.

A.2 Column Design Calculations

This section shows sample calculations for column design in an 8-story building. Excel formulas are also shown that were used to automate the column design process for various buildings. The BRBF beams were not calculated but assumed to be W16X57 for all buildings.

8-Story Building Column Design

Information about building and brace design:

$Area_{scL8} := 2.5in^2$ $Area_{scL5} := 7.0in^2$ $Area_{scL2} := 9.0in^2$

$Area_{scL7} := 4.5in^2$ $Area_{scL4} := 8.0in^2$ $Area_{scL1} := 9.5in^2$ $N_{braces} := 2$

$Area_{scL6} := 6.0in^2$ $Area_{scL3} := 8.5in^2$ $Story_{height} = 15 \cdot ft$ $Bay_{width} = 30 \cdot ft$

Assumptions:

$F_{ymax} := 46ksi$

$\omega := 1.36$

$\beta := 1.1$

A) Calculate maximum tension and compression forces

$Max_{TenL8} := F_{ymax} \cdot Area_{scL8} \cdot \omega = 156.4 \cdot kip$ $Max_{CompL8} := F_{ymax} \cdot Area_{scL8} \cdot \omega \cdot \beta = 172 \cdot kip$

B) Calculate vertical tension and compression forces

$$Ver_{TenL8} := \left[\frac{Story_{height}}{\sqrt{Story_{height}^2 + \left(\frac{Bay_{width}}{N_{braces}} \right)^2}} \right] \cdot Max_{TenL8} = 110.6 \cdot kip$$

$$Ver_{CompL8} := \left[\frac{Story_{height}}{\sqrt{Story_{height}^2 + \left(\frac{Bay_{width}}{N_{braces}} \right)^2}} \right] \cdot Max_{CompL8} = 121.7 \cdot kip$$

C) Add loads to get largest possible demand placed on each column.

Table A-3. Automated Column Design Table

Level	Height (ft)	Width (ft)	Asc (in2)	Max Ten (k)	Max Comp (k)	Max Ty (k)	Max Cy (k)	Vert Column (k)	Col Size
8	15	30	2.5	156.4	172.04	110.6	121.7	0.0	W12X40
7	15	30	4.5	281.52	309.672	199.1	219.0	121.7	W12X40
6	15	30	6.0	375.36	412.896	265.4	292.0	340.6	W12X65
5	15	30	7.0	437.92	481.712	309.7	340.6	632.6	W12X65
4	15	30	8.0	500.48	550.528	353.9	389.3	973.2	W12X136
3	15	30	8.5	531.76	584.936	376.0	413.6	1362.5	W12X136
2	15	30	9.0	563.04	619.344	398.1	437.9	1776.1	W12X210
1	15	30	9.5	594.32	653.752	420.2	462.3	2214.0	W12X210

The vertical column values were calculated by summing the vertical compression values (Max C_y) from the above stories because compression members are always larger than tension members and thus, govern.

Gravity columns were designed by finding the demand in the column and then selecting a shape with a greater capacity than the calculated demand. The process is detailed below. Table A-4 shows a summary of this process using Excel formulas.

Gravity Column Design

Live Load Reduction

$$A_t := L_{bay} \cdot L_{bay} = 900 \cdot ft^2$$

$$LL_{red1} := w_{live} \cdot \left(0.25 + \frac{15}{\sqrt{4 \cdot \frac{A_t}{ft^2}}} \right) = 25 \cdot psf \qquad LL_{red2} := 0.4 \cdot w_{live} = 20 \cdot psf$$

If LLred1 is less than LLred2, use LLred2. Going to assume all maxed out.

$$w_{redlive} := LL_{red2} = 20 \cdot psf \qquad w_{floor} := 80psf$$

Typical Gravity Column Design

$$P_{gcol} := \left(1.2 w_{floor} + 0.5 \cdot w_{redlive} \right) \cdot A_t = 95.4 \cdot kip$$

Table A-4. Gravity Column Design

Level	Height (ft)	Width (ft)	Pgcol (kip)	Pg for col n (kip)	Governing Demand (kip)	ΦPn, Capacity (kip)	Size
8	15	30	95.4	95.4	190.8	281	W12X40
7	15	30	95.4	190.8	190.8	281	W12X40
6	15	30	95.4	286.2	381.6	478	W12X53
5	15	30	95.4	381.6	381.6	478	W12X53
4	15	30	95.4	477	572.4	663	W12X65
3	15	30	95.4	572.4	572.4	663	W12X65
2	15	30	95.4	667.8	763.2	809	W12X79
1	15	30	95.4	763.2	763.2	809	W12X79

APPENDIX B. DESIGN AND ANALYSIS TOOLS

The following sections discuss tools used for the design and analysis process. The first section contains the VBA code written to automate BRBF design. This code links to an automated spreadsheet that calculates these values for buildings with varying number of stories. The second section shows the main spreadsheet used throughout the research process. The last section summarizes the OpenSees templates used for analysis.

B.1 VBA Code for Brace Design

```
For i = 1 To numStories

Ta = (Ctvalue * ((StoryHeight / 12) * numStories) ^ (xvalue))
    T1 = Ta * Cuvalue
    ActiveSheet.Cells(5 + i, 14) = T1

    Cs1 = (SDS / (Rfactor / ImportanceFac))
    Cs2 = (SD1 / (T1 * (Rfactor / ImportanceFac)))
    Cs3 = 0.044 * SDS * ImportanceFac

    WeightFloor = ((WallDead * Perimeter) + Partition * TribArea + FloorDead * TribArea) / 1000
    WeightRoof = ((WallDead * Perimeter) * (1 / 2) + RoofDead * TribArea) / 1000
    WeightTotal = (numStories - 1) * WeightFloor + WeightRoof
    AssumedWeightTotal = (numStories) * (AssumedSeismicMass * TribArea) / 1000

    If Cs1 < Cs2 Then
        If Cs1 > Cs3 Then
            ActiveSheet.Cells(5 + i, 15) = Cs1
            Vb = Cs1 * AssumedWeightTotal
        Else
            ActiveSheet.Cells(5 + i, 15) = Cs3
            Vb = Cs3 * AssumedWeightTotal
        End If
    Else
        If Cs2 > Cs3 Then
            ActiveSheet.Cells(5 + i, 15) = Cs2
            Vb = Cs2 * AssumedWeightTotal
        Else
            ActiveSheet.Cells(5 + i, 15) = Cs3
            Vb = Cs3 * AssumedWeightTotal
        End If
    End If
```

```
    ActiveSheet.Cells(5 + i, 16) = Vb

    k = ((2 - 1) / (2.5 - 0.5)) * (T1 - 0.5) + 1
    ActiveSheet.Cells(3, 20) = k


    If i = numStories Then
        ActiveSheet.Cells(5 + i, 17) = (AssumedSeismicMass * TribArea) / 1000
    Else
        ActiveSheet.Cells(5 + i, 17) = (AssumedSeismicMass * TribArea) / 1000
    End If

    ActiveSheet.Cells(5 + i, 18) = i * (StoryHeight / 12)
    ActiveSheet.Cells(5 + i, 19) = (i * (StoryHeight / 12)) ^ (k)

    If i = numStories Then
        whk = WeightRoof * (i * (StoryHeight / 12)) ^ k
        ActiveSheet.Cells(5 + i, 20) = whk
    Else
        whk = WeightFloor * (i * (StoryHeight / 12)) ^ k
        ActiveSheet.Cells(5 + i, 20) = whk
    End If

Next i

whkSum = Range("T6").Value + Range("T7").Value + Range("T8").Value + Range("T9").Value + Range("T10"
         + Range("T11").Value + Range("T12").Value + Range("T13").Value + Range("T14").Value + Range
         + Range("T16").Value + Range("T17").Value + Range("T18").Value + Range("T19").Value + Range
         + Range("T21").Value + Range("T22").Value + Range("T23").Value + Range("T24").Value + Range

ActiveSheet.Cells(26, 20) = whkSum

For j = 1 To numStories

    whk = ActiveSheet.Cells(5 + j, 20).Value
    ActiveSheet.Cells(5 + j, 21) = whk / whkSum

Next j

For k = 1 To numStories

    Vbase = ActiveSheet.Cells(5 + k, 16).Value
    Cvx = ActiveSheet.Cells(5 + k, 21).Value
    ActiveSheet.Cells(5 + k, 22) = Vbase * Cvx

Next k
CvxSum = Range("U6").Value + Range("U7").Value + Range("U8").Value + Range("U9").Value + Range("U10
         + Range("U11").Value + Range("U12").Value + Range("U13").Value + Range("U14").Value + Rang
         + Range("U16").Value + Range("U17").Value + Range("U18").Value + Range("U19").Value + Rang
         + Range("U21").Value + Range("U22").Value + Range("U23").Value + Range("U24").Value + Rang

ActiveSheet.Cells(26, 21) = CvxSum

Fsum = Range("V6").Value + Range("V7").Value + Range("V8").Value + Range("V9").Value + Range("V10")
         + Range("V11").Value + Range("V12").Value + Range("V13").Value + Range("V14").Value + Rang
         + Range("V16").Value + Range("V17").Value + Range("V18").Value + Range("V19").Value + Rang
         + Range("V21").Value + Range("V22").Value + Range("V23").Value + Range("V24").Value + Rang

ActiveSheet.Cells(26, 22) = Fsum

j = numStories
FxSum = 0

Do While j <> 0
    FxSum = FxSum + ActiveSheet.Cells(5 + j, 22).Value
    ActiveSheet.Cells(5 + j, 23) = FxSum
    j = j - 1
Loop
```

```
For i = 1 To numStories

    FxSum = ActiveSheet.Cells(5 + i, 23).Value
    Fbr = (FxSum / 2) * (((Baywidth / 2) ^ 2 + (StoryHeight) ^ 2) ^ (1 / 2)) / (Baywidth / 2)
    ActiveSheet.Cells(5 + i, 24) = Fbr

    Acore = Fbr / (0.9 * 38)
    ActiveSheet.Cells(5 + i, 25) = Acore

    Around = (WorksheetFunction.RoundUp(Acore * 2, 0)) / 2
    ActiveSheet.Cells(5 + i, 26) = Around

Next

End Sub
```

B.2 Main Spreadsheet

The main spreadsheet was primarily used for design and output storage. The first part of the spreadsheet contained tabs for output data collection and then corresponding tabs that contained graphs of that data. Figure B-1 and Figure B-2 show the tables and corresponding graphs for 4-story drifts. The second part of the spreadsheet had tabs used for design as mentioned in Chapter 3 of paper. Figure B-3 shows an example of design in the spreadsheet by highlighting gravity column design and corresponding p-delta parameters.

Comparison of the effects of P-delta Stiffnesses on Residual Drifts

BRBF Pattern	Chevron	
Number of Stories	8	
Story Height	15	[ft]
Number of Bay Widths	5	
Bay Width	30	[ft]
Location of Elastic Stories	6	[level]
Stiffness of Control Design		[k/in]

Average Drift Improvement by adding 4x Elastic Stories
0.00341757 45.87307856
0.00403249 54.12692144

Average Drift Improvement by adding 4x ES and 2x PD
0.00399592 53.63600141

Average Drift Improvement by adding 4x ES and 4x PD
0.00500090 67.12557325

Location of Elastic Stories			1 & 5	[level]

Control Design- Brace Amplification = 1 (no elastic story)

P-Delta Stiffness = 1/2x

	Residual Drift [in]		Maximum Drift [in]	
Story	Average	85th percentile	Average	85th percentile
1	0.01926716	0.00302061	0.00226968	0.00232279
2	0.01542231	0.00625391	0.00393158	0.00359615
3	0.00895964	0.00742993	0.00533383	0.00459832
4	0.00435213	0.00802411	0.00623852	0.00552886
5	0.00524213	0.00891411	0.00712852	0.00641886
6	0.00613213	0.00980411	0.00801852	0.00730886
7	0.00702213	0.01069411	0.00890852	0.00819886
8	0.00791213	0.01158411	0.00979852	0.00908886

P-Delta Stiffness = 1 (Base Stiffness)

	Residual Drift [in]		Maximum Drift [in]	
Story	Average	85th percentile	Average	85th percentile
1	0.014820895	0.02819743	0.025724182	0.038053888
2	0.011863319	0.022240591	0.021991234	0.031995463
3	0.006892032	0.012636924	0.015883561	0.023054779
4	0.003347789	0.00653152	0.012978257	0.020408939
5	0.003670189	0.007602217	0.012829627	0.021199919
6	0.003622399	0.00654322	0.012299246	0.016037509
7	0.006212567	0.010226186	0.018998345	0.023145925
8	0.009171343	0.013712089	0.027422636	0.032405089
Average drift	0.00745007	0.01346127	0.01851589	

Figure B-1. Main spreadsheet screenshot: Tables of 8-story output drifts.

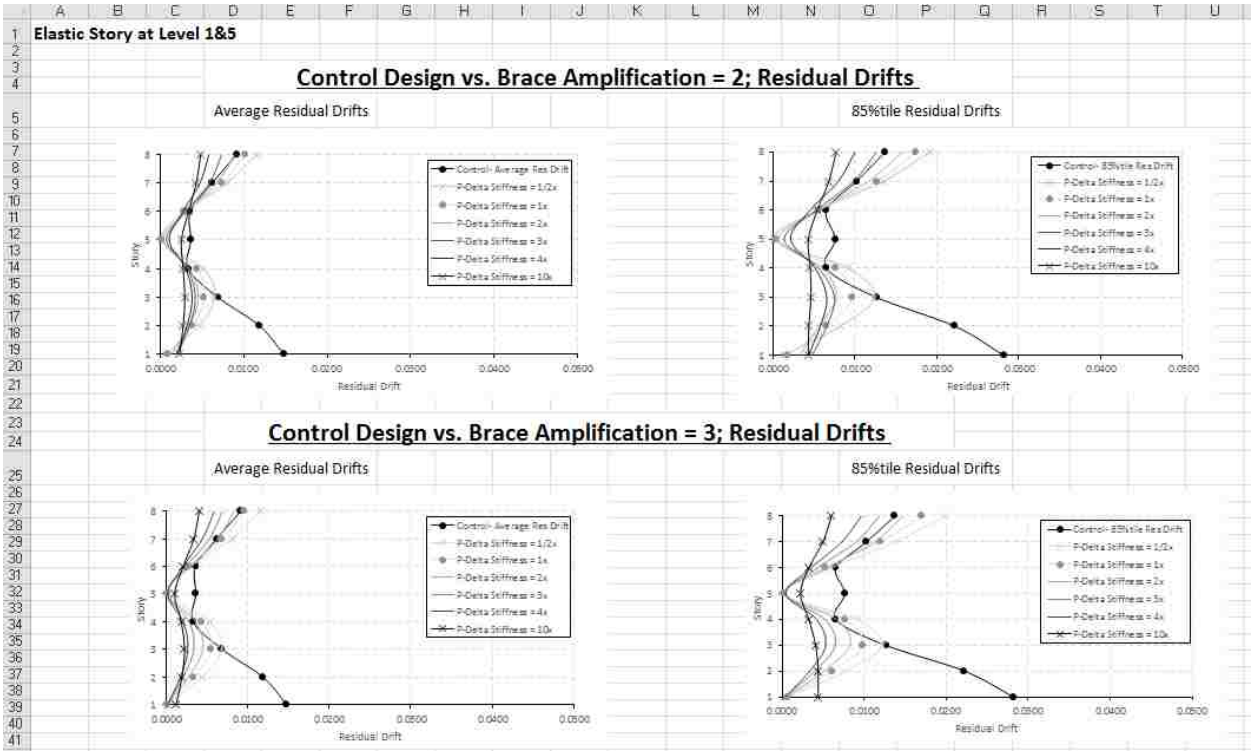

Figure B-2. Main spreadsheet: Graphs of 8-story drifts.

Gravity Column Design **Pdelta parameters**

Pgcol: 95.4 kip calculated on MathCAD sheet- for every n stories

8 Story Building

Level	Height (ft)	Width (ft)	Pgcol (kip)	Pg for col n (kip)	Governing Demand (kip)	ΦPn, Capacity (kip)	Size
8	15	30	95.4	95.4	190.8	281	W12X40
7	15	30	95.4	190.8	190.8	281	W12X40
6	15	30	95.4	286.2	381.6	478	W12X53
5	15	30	95.4	381.6	381.6	478	W12X53
4	15	30	95.4	477	572.4	663	W12X65
3	15	30	95.4	572.4	572.4	663	W12X65
2	15	30	95.4	667.8	763.2	809	W12X79
1	15	30	95.4	763.2	763.2	809	W12X79

Level	# of columns	Ix	Iy	Is	Zx	Area
8	7	307	44.1	1229	399	81.9
7	7	307	44.1	1229	399	81.9
6	7	425	95.8	1823	545.3	109.2
5	7	425	95.8	1823	545.3	109.2
4	7	533	174	2474.5	677.6	133.7
3	7	533	174	2474.5	677.6	133.7
2	7	662	216	3073	833	162.4
1	7	662	216	3073	833	162.4

Figure B-3. Main spreadsheet: Gravity column design (p-delta parameters).

B.4 OpenSees Templates

Table B-1 contains names and corresponding descriptions of template files used in OpenSees analyses.

Table B-1. Templates used in OpenSees

TCL file	Description
Input file (input8s@control.tcl)	Contains information about basic design of the building including braces, columns and beams sizes and corresponding properties.
template42.tcl	Creates frame configuration (chevron braces) by defining nodes, elements and springs.
procedures32.tcl	Determines the coordinates for all the nodes and for the 32 template. Constrains overlapping column and beam nodes for all DOFs. May be used to generate multiple 32 frames.
generalProcedures.tcl	Contains various common procedures to be used during analyses.
dynamic521.tcl	This script will create models based on templates and analyze the models under combined gravity and earthquake loading.
dynamicAnalysisProcedures.tcl	Contains procedures used for dynamic analysis.
dynamicAnalysisSettings.tcl	Contains various settings used for dynamic analysis.
pushover521.tcl	This script will create a model based on templates and perform a pushover analysis of the model.
postProcessing.tcl	Identifies maximum value from list and first value from list; returns values requested.
LookupShapeProp.tcl	Reads in requested steel shape, looks up corresponding properties, and returns specific properties of requested shape.
eqSuites.tcl	Define earthquake suites that could be used for analysis. Also, define procedures for accessing the suites..
combinedTemplates.tcl	This procedure adds a constraint so that all of the frames from different templates are tied together at the left column nodes at each floor.

APPENDIX C. GRAPHS OF 4-STORY BUILDINGS

The following graphs show all results of residual and maximum drifts for 4-story (4S) buildings with elastic stories (ES) at different levels.

C.1 Elastic Story at Level 1

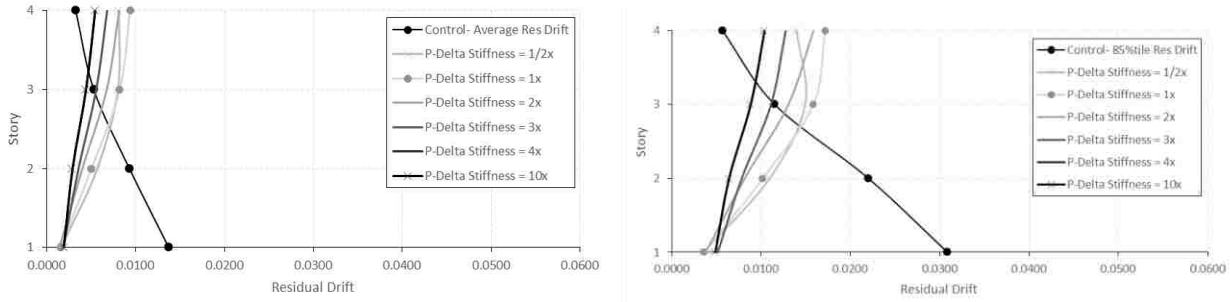

Figure C-1. Average & 85%tile residual drifts for 2× ES at level 1, 4S.

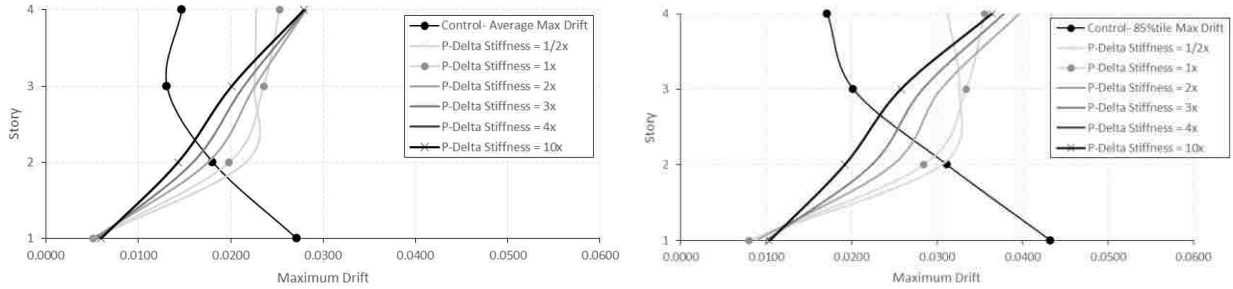

Figure C-2. Average & 85%tile maximum drifts for 2× ES at level 1, 4S.

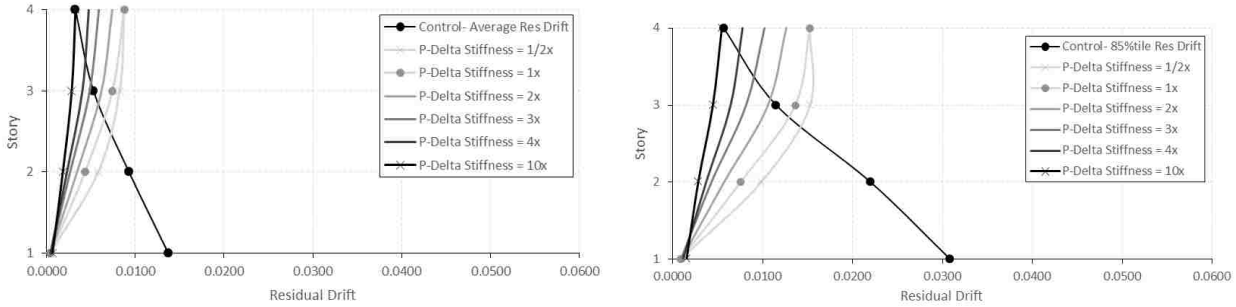

Figure C-3. Average & 85%tile residual drifts for 3× ES at level 1, 4S.

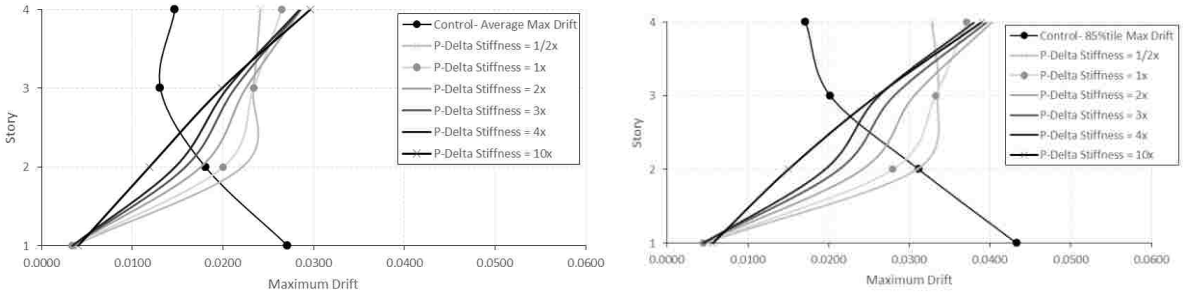

Figure C-4. Average & 85%tile maximum drifts for 3× ES at level 1, 4S.

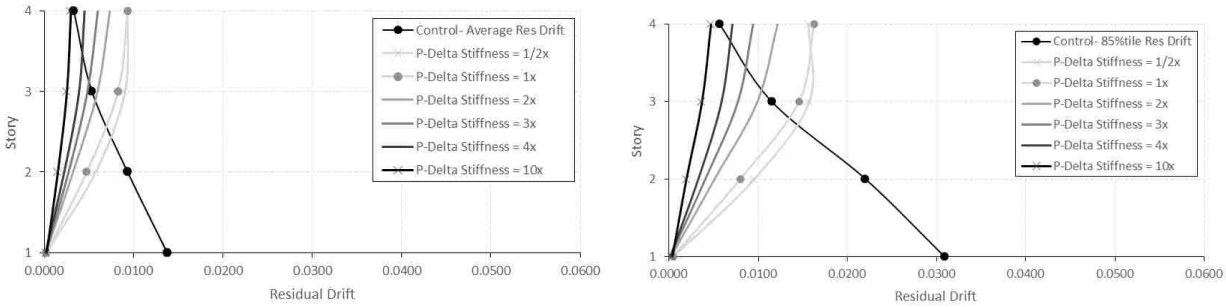

Figure C-5. Average & 85%tile residual drifts for 4× ES at level 1, 4S.

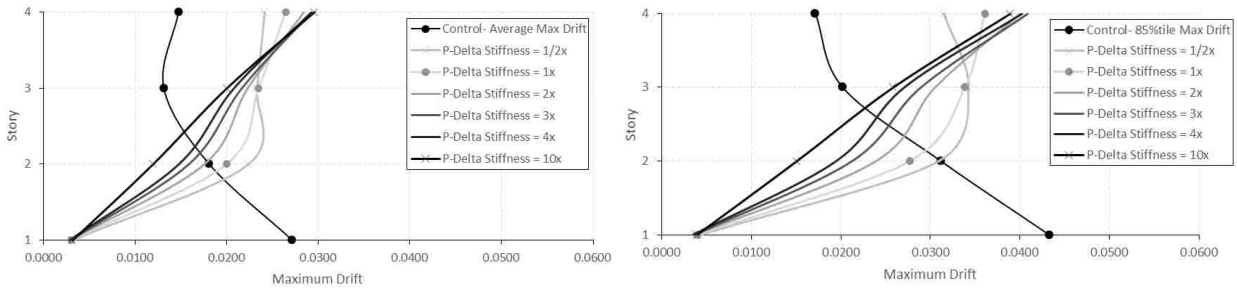

Figure C-6. Average & 85%tile maximum drifts for 4× ES at level 1, 4S

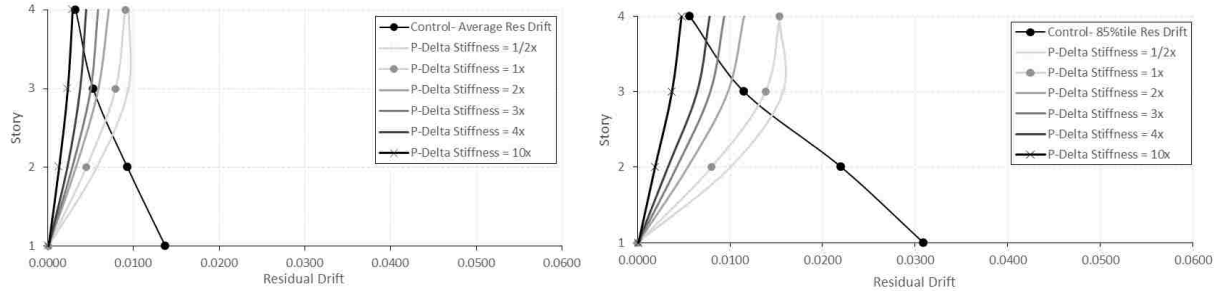

Figure C-7. Average & 85%tile residual drifts for 10× ES at level 1, 4S.

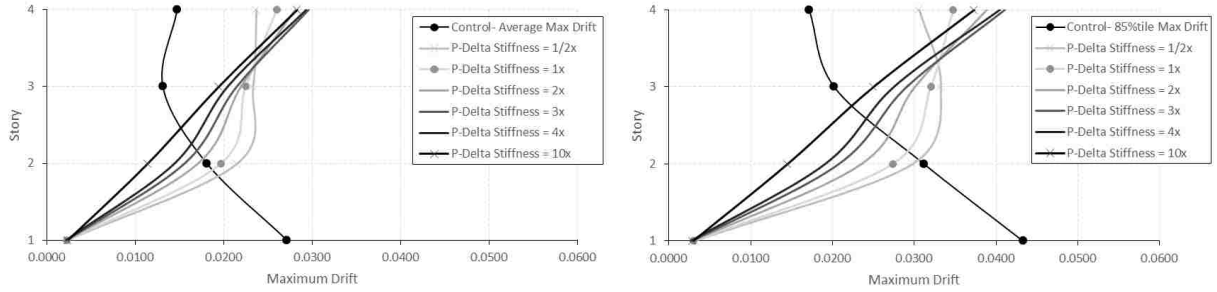

Figure C-8. Average & 85%tile maximum drifts for 10× ES at level 1, 4S.

C.2 Elastic Story at Level 4

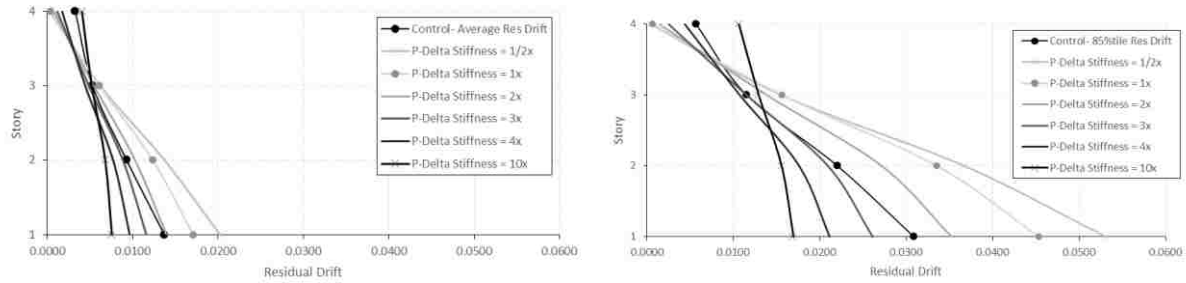

Figure C-9. Average & 85%tile residual drifts for 2× ES at level 4, 4S.

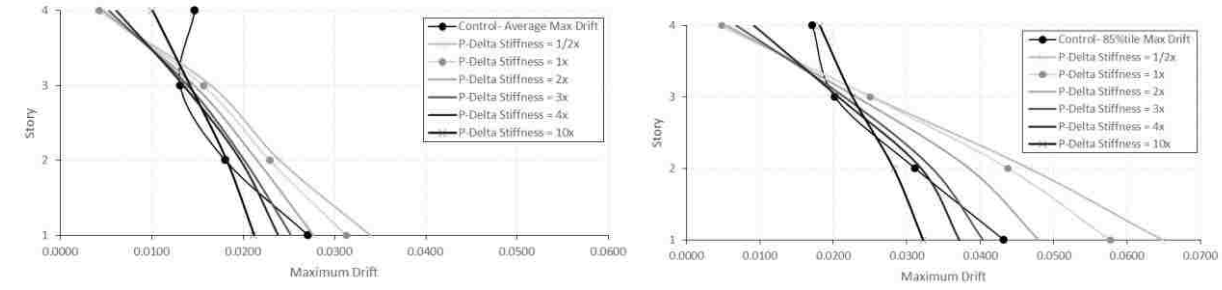

Figure C-10. Average & 85%tile maximum drifts for 2× ES at level 4, 4S.

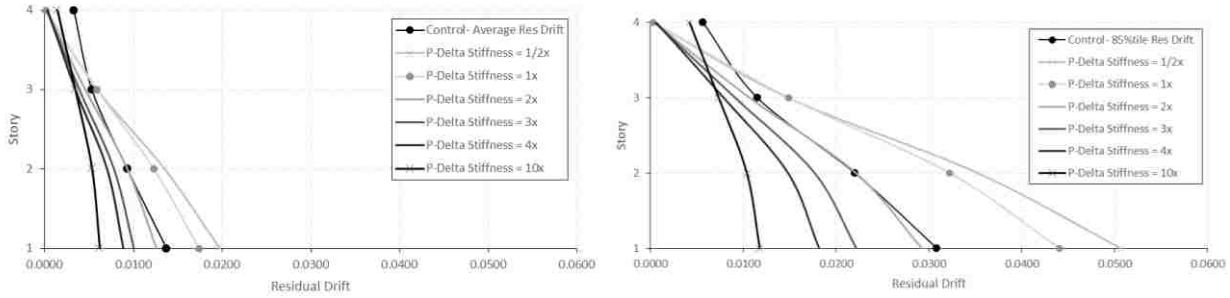

Figure C-11. Average & 85%tile residual drifts for 3× ES at level 4, 4S.

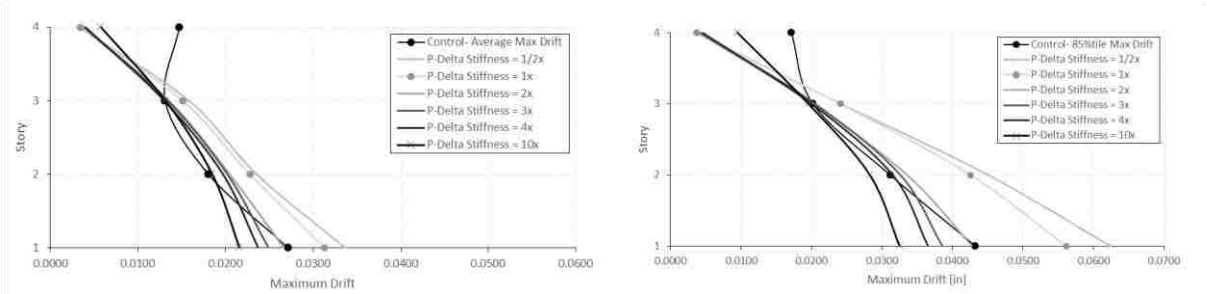

Figure C-12. Average & 85%tile maximum drifts for 3× ES at level 4, 4S.

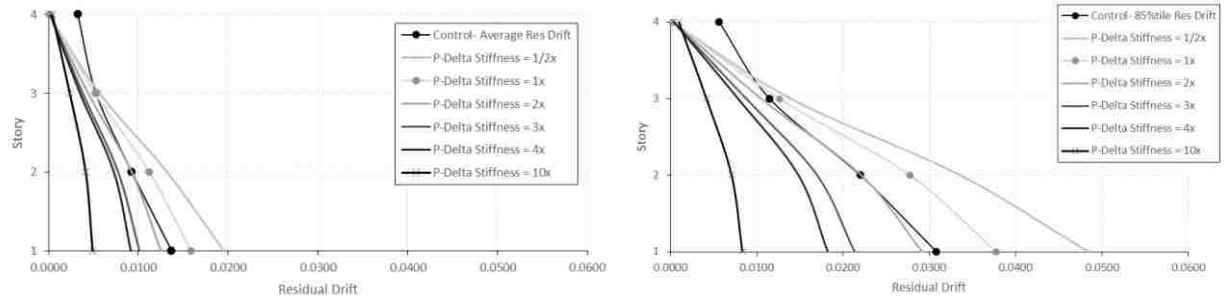

Figure C-13. Average & 85%tile residual drifts for 4× ES at level 4, 4S.

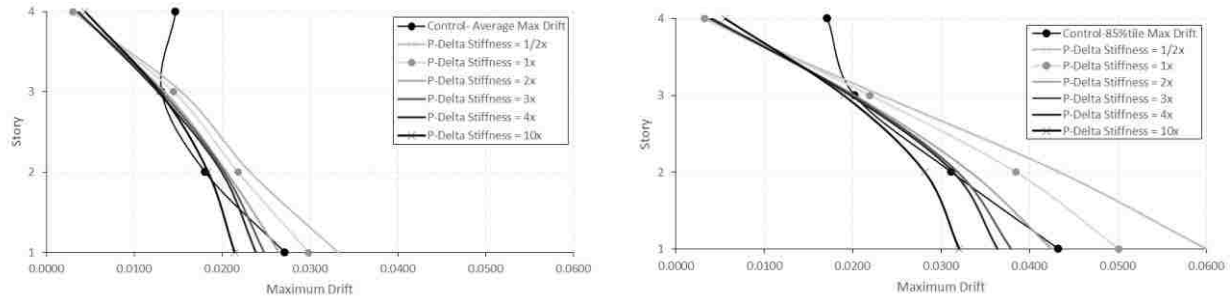

Figure C-14. Average & 85%tile maximum drifts for 4× ES at level 4, 4S.

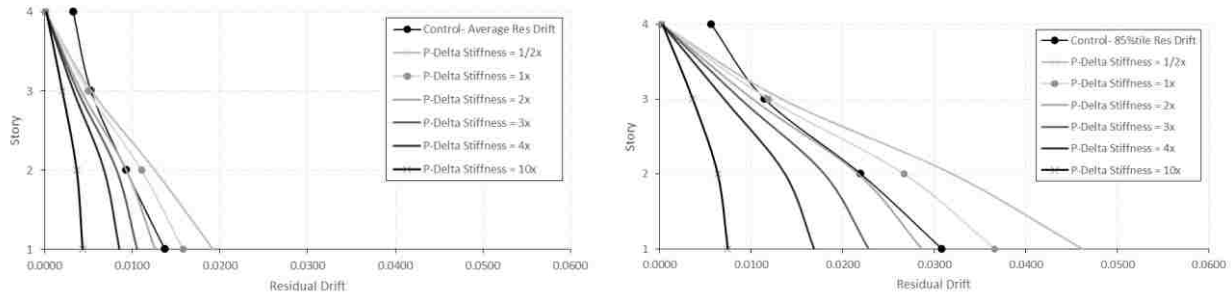

Figure C-15. Average & 85%tile residual drifts for 10× ES at level 4, 4S.

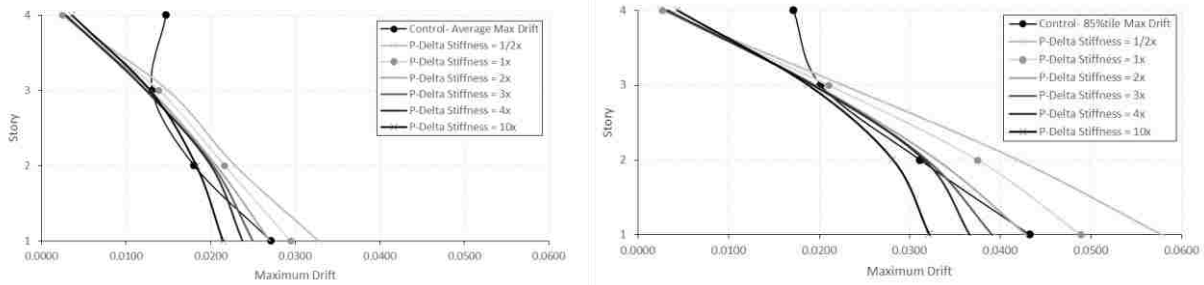

Figure C-16. Average & 85%tile maximum drifts for 10× ES at level 4, 4S.

APPENDIX D. GRAPHS OF 6-STORY BUILDINGS

The following graphs show all results of residual and maximum drifts for 6-story (6S) buildings with elastic stories at different levels. First, combination elastic stories results are presented followed by single elastic story results.

D.1 Elastic Story at Level 1&5

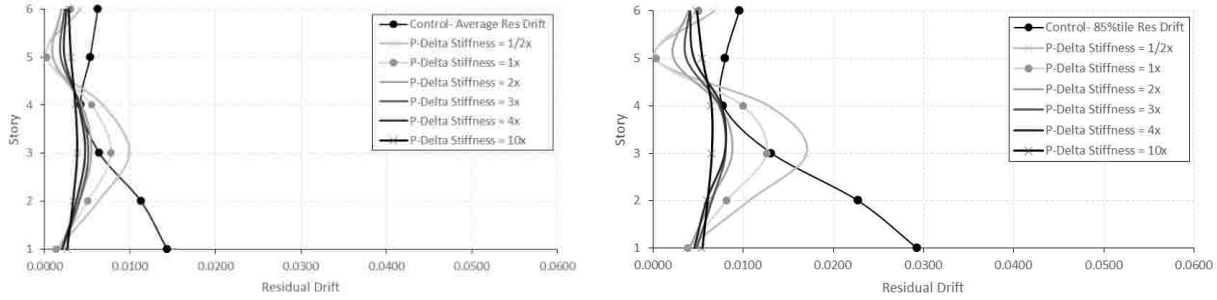

Figure D-1. Average & 85%tile residual drifts for 2× ES at level 1&5, 6S.

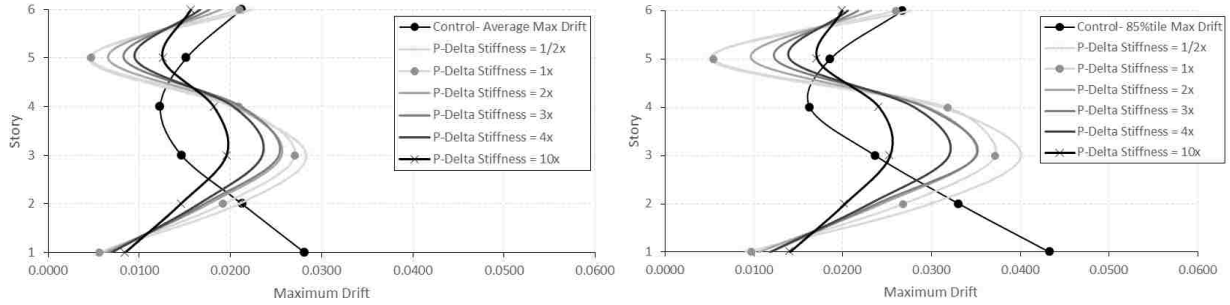

Figure D-2. Average & 85%tile maximum drifts for 2× ES at level 1&5, 6S.

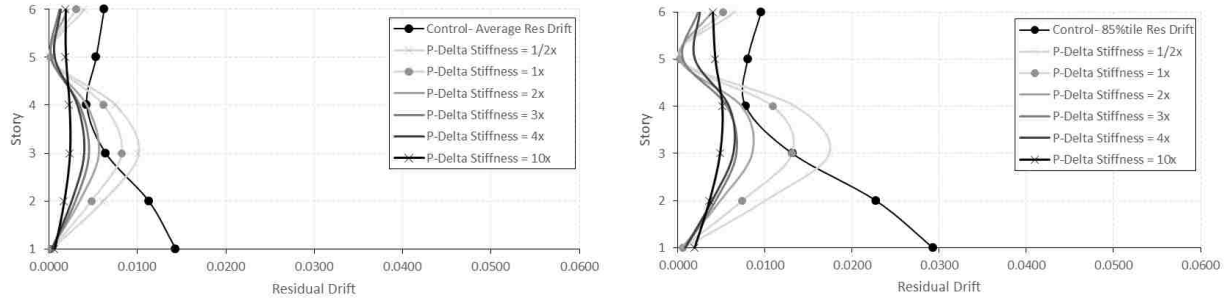

Figure D-3. Average & 85%tile residual drifts for 3× ES at level 1&5, 6S.

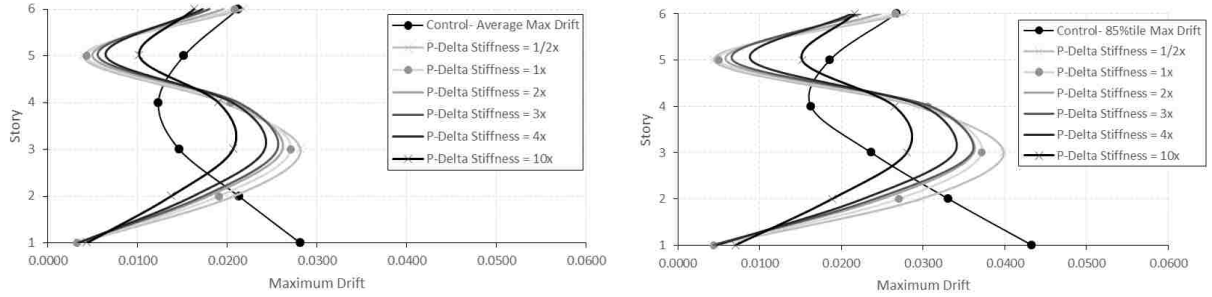

Figure D-4. Average & 85%tile maximum drifts for 3× ES at level 1&5, 6S.

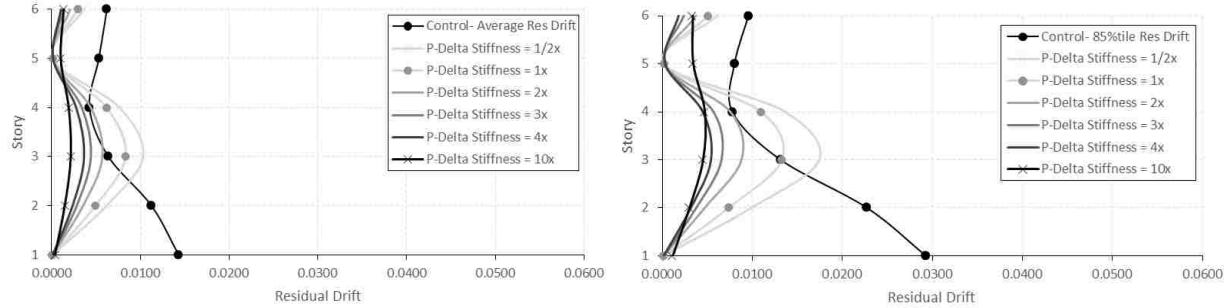

Figure D-5. Average & 85%tile residual drifts for 4× ES at level 1&5, 6S.

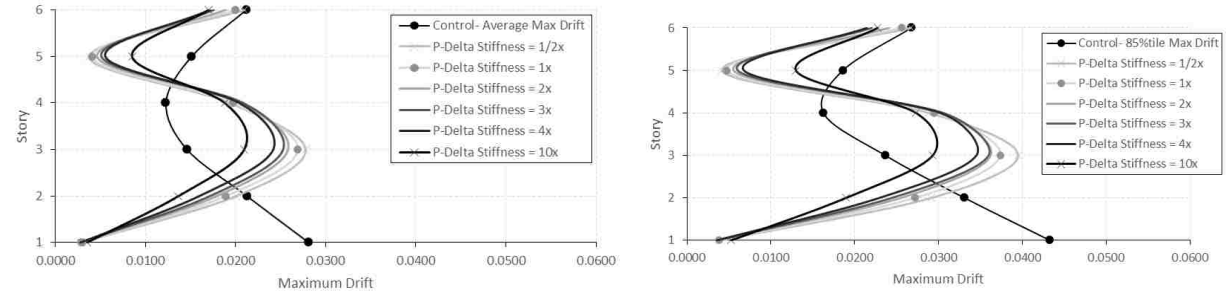

Figure D-6. Average & 85%tile maximum drifts for 4× ES at level 1&5, 6S.

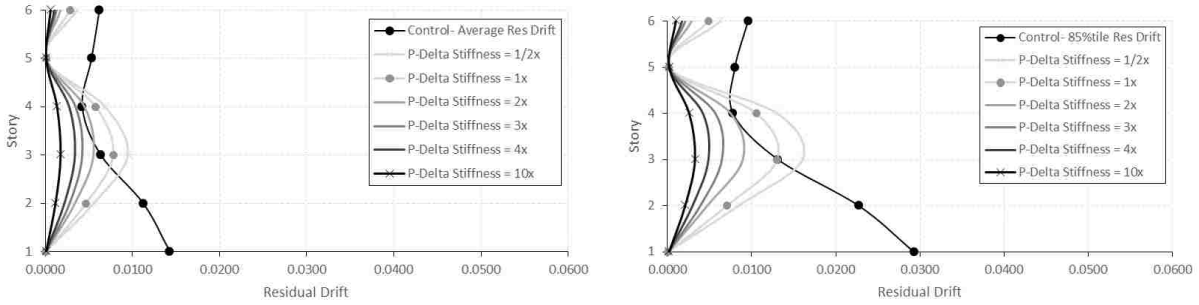

Figure D-7. Average & 85%tile residual drifts for 10× ES at level 1&5, 6S.

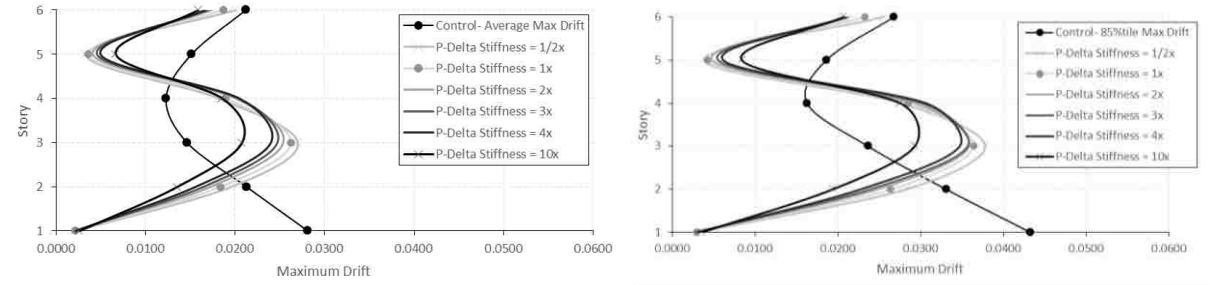

Figure D-8. Average & 85%tile maximum drifts for 10× ES at level 1&5, 6S.

D.2 Elastic Story at Level 2&6

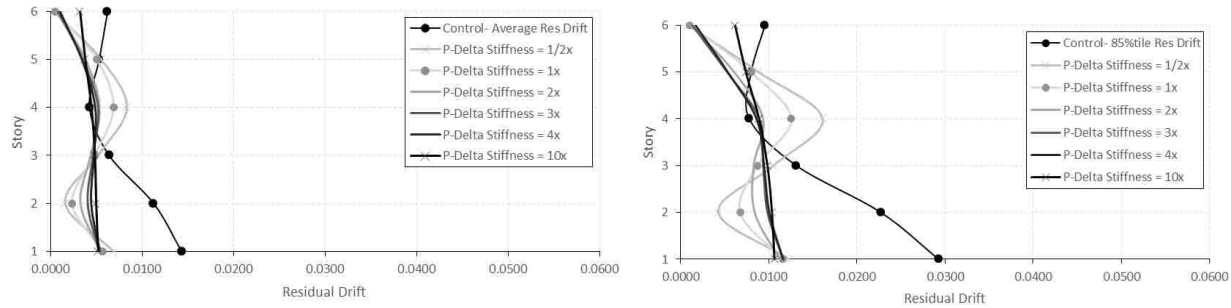

Figure D-9. Average & 85%tile residual drifts for 2× ES at level 2&6, 6S.

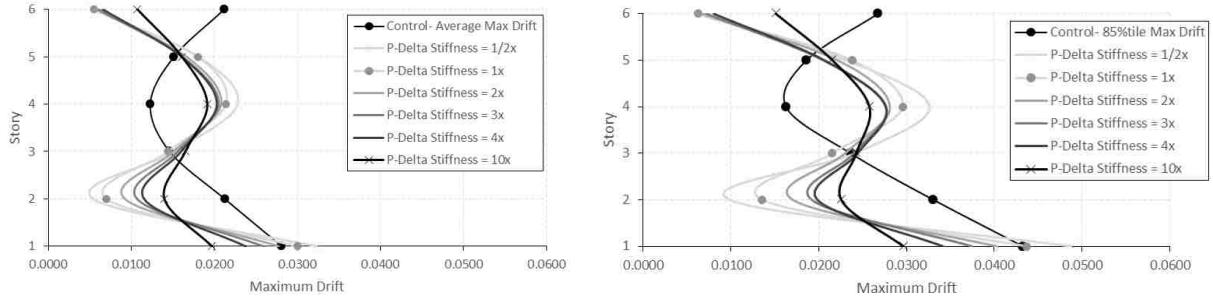

Figure D-10. Average & 85%tile maximum drifts for 2× ES at level 2&6, 6S.

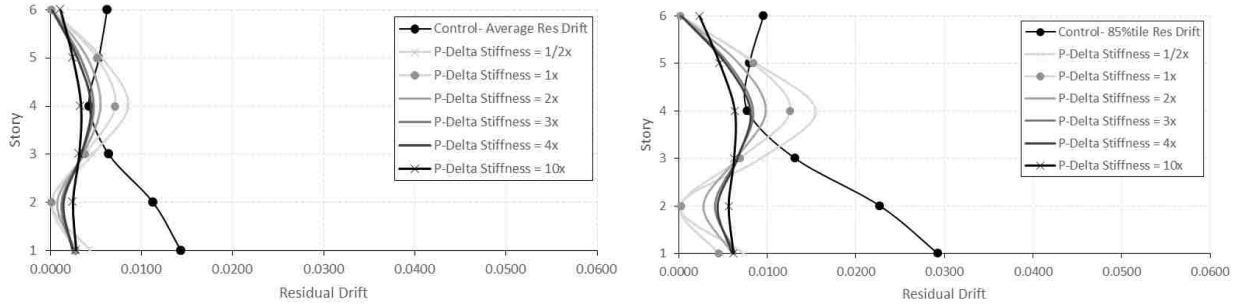

Figure D-11. Average & 85%tile residual drifts for 3× ES at level 2&6, 6S.

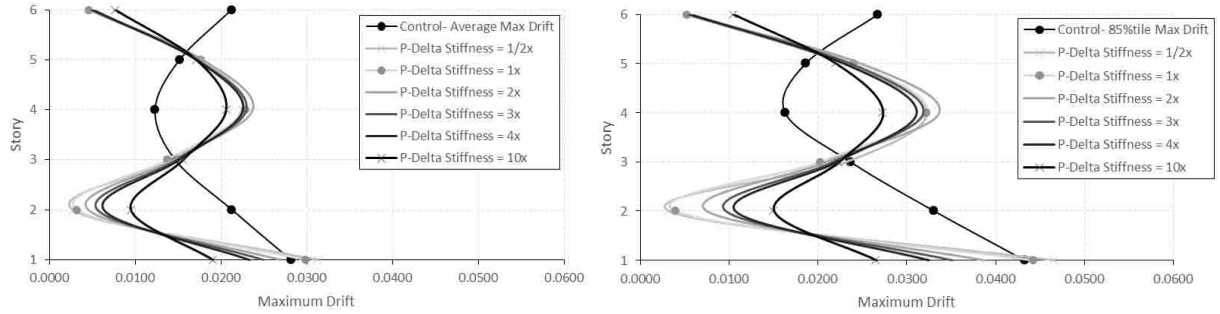

Figure D-12. Average & 85%tile maximum drifts for 3× ES at level 2&6, 6S.

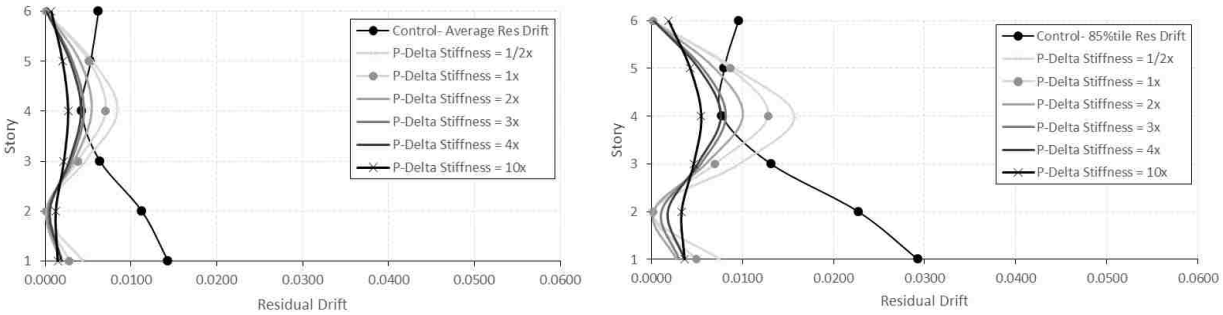

Figure D-13. Average & 85%tile residual drifts for 4× ES at level 2&6, 6S.

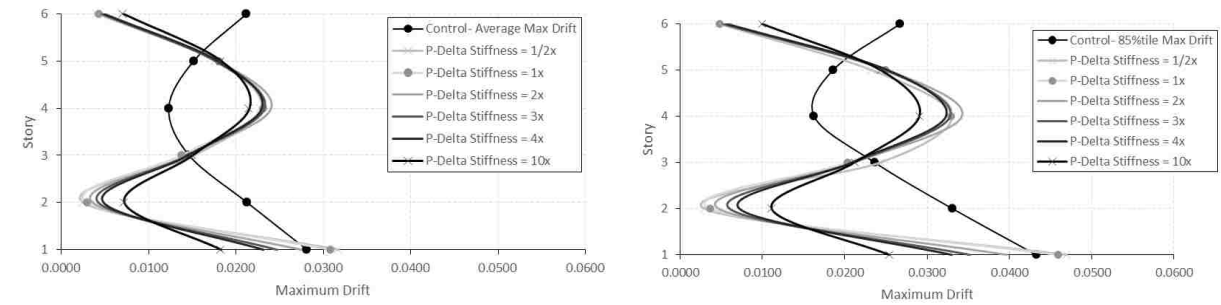

Figure D-14. Average & 85%tile maximum drifts for 4× ES at level 2&6, 6S.

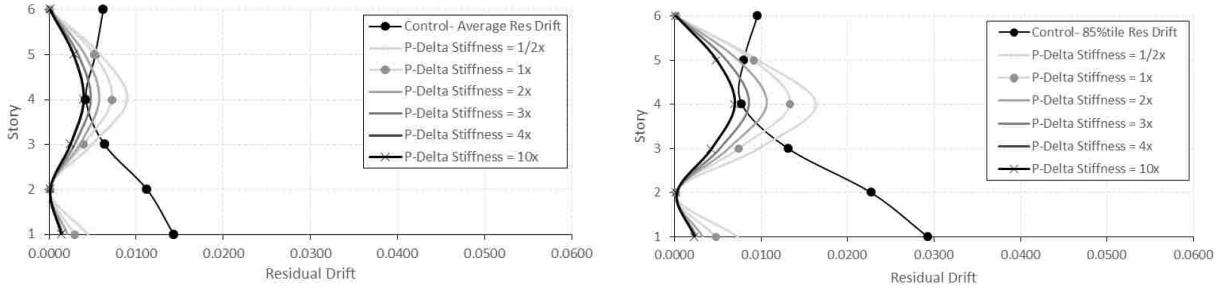

Figure D-15. Average & 85%tile residual drifts for 10× ES at level 2&6, 6S.

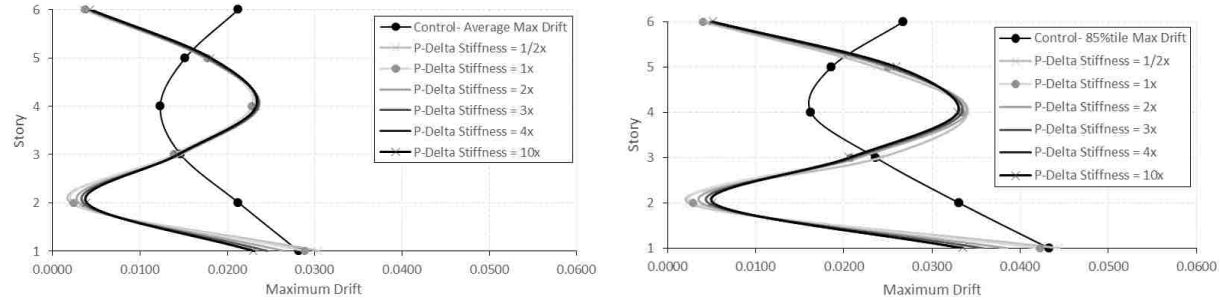

Figure D-16. Average & 85%tile maximum drifts for 10× ES at level 2&6, 6S.

D.3 Elastic Story at Level 1

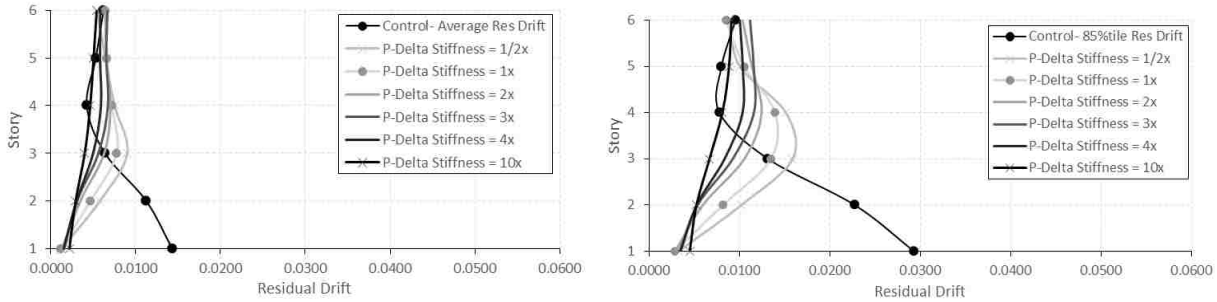

Figure D-17. Average & 85%tile residual drifts for 2× ES at level 1, 6S.

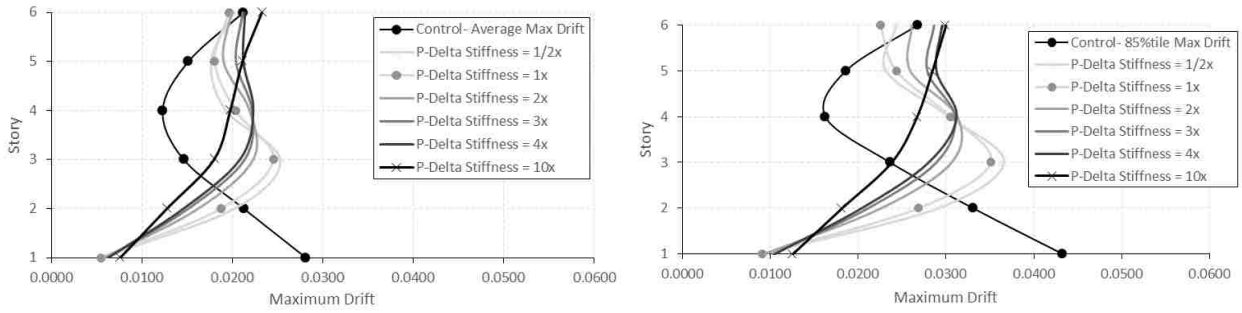

Figure D-18. Average & 85%tile maximum drifts for 2× ES at level 1, 6S.

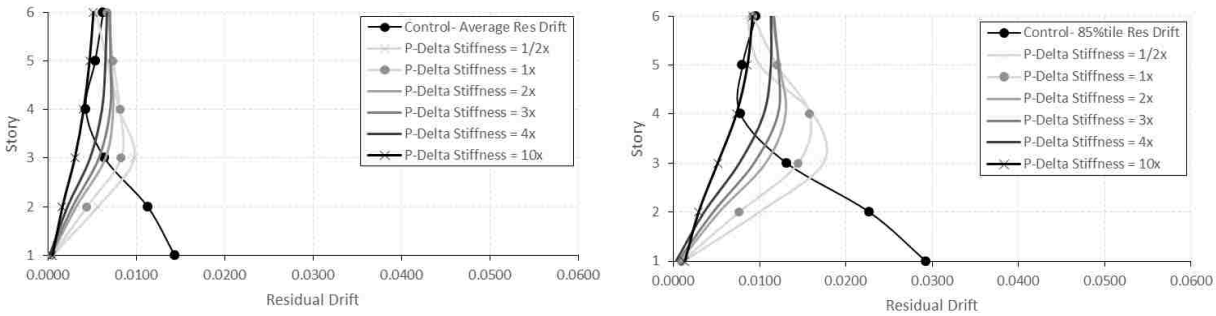

Figure D-19. Average & 85%tile residual drifts for 3× ES at level 1, 6S.

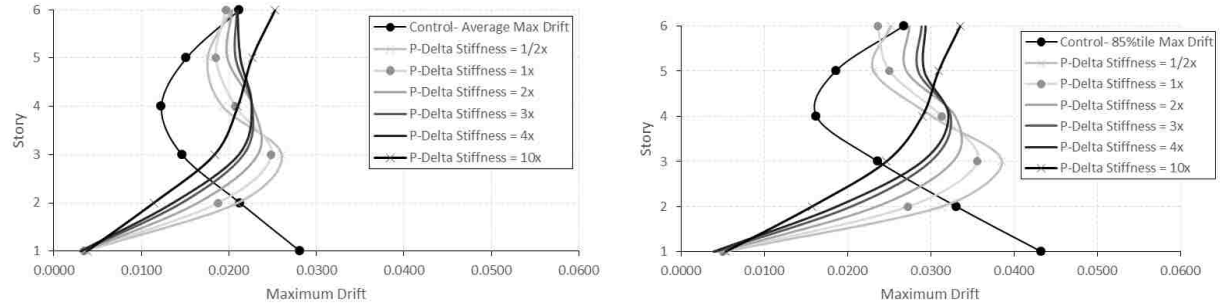

Figure D-20. Average & 85%tile maximum drifts for 3× ES at level 1, 6S.

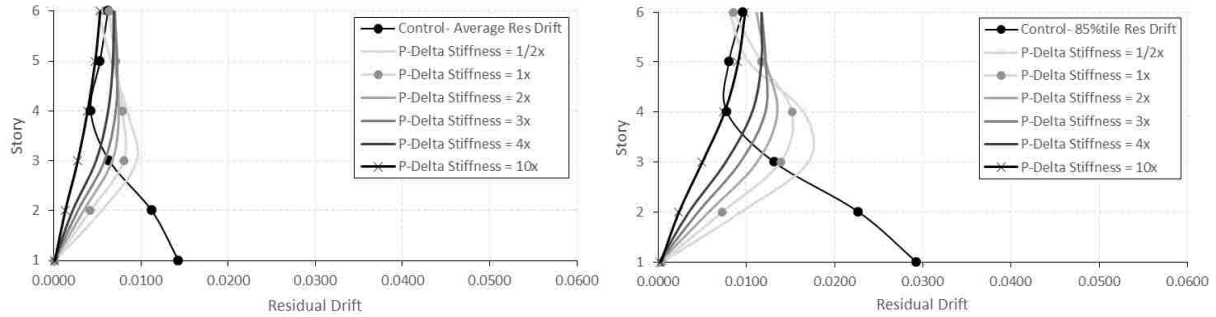

Figure D-21. Average & 85%tile residual drifts for 4× ES at level 1, 6S.

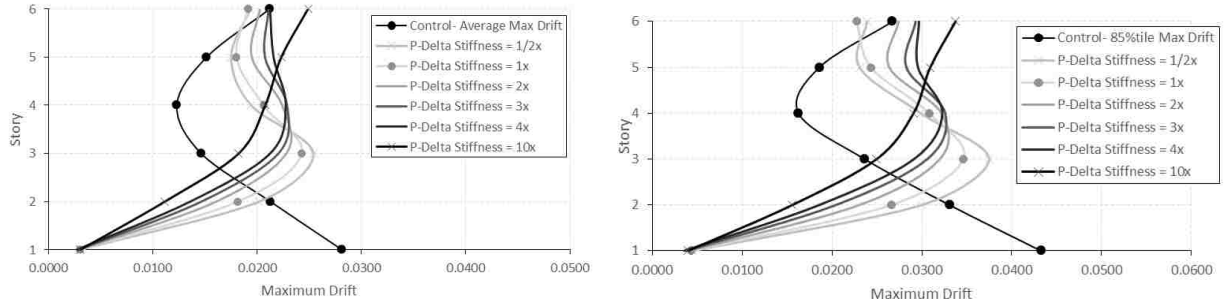

Figure D-22. Average & 85%tile maximum drifts for 4× ES at level 1, 6S.

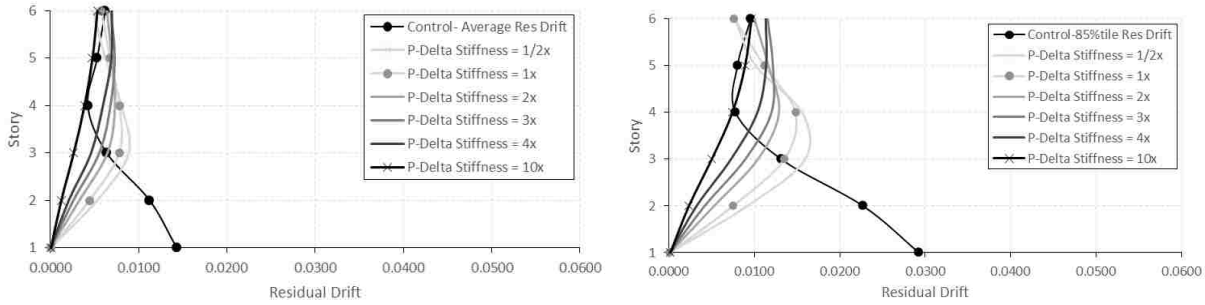

Figure D-23. Average & 85%tile residual drifts for 10× ES at level 1, 6S.

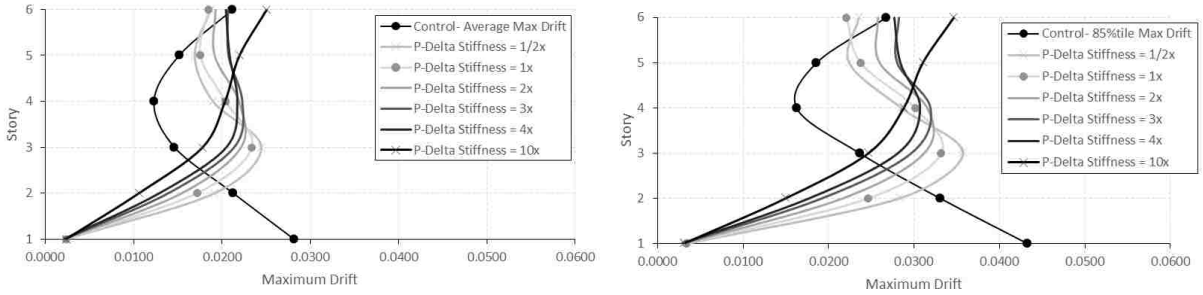

Figure D-24. Average & 85%tile maximum drifts for 10× ES at level 1, 6S

D.4 Elastic Story at Level 2

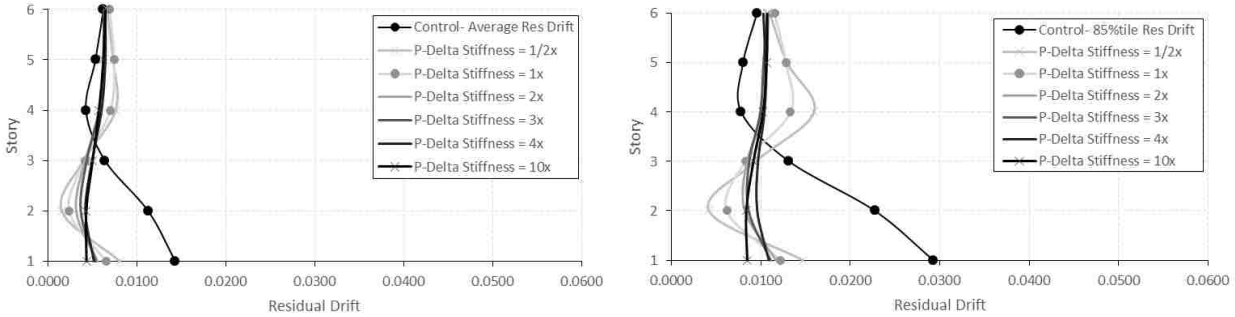

Figure D-25. Average & 85%tile residual drifts for 2× ES at level 2, 6S.

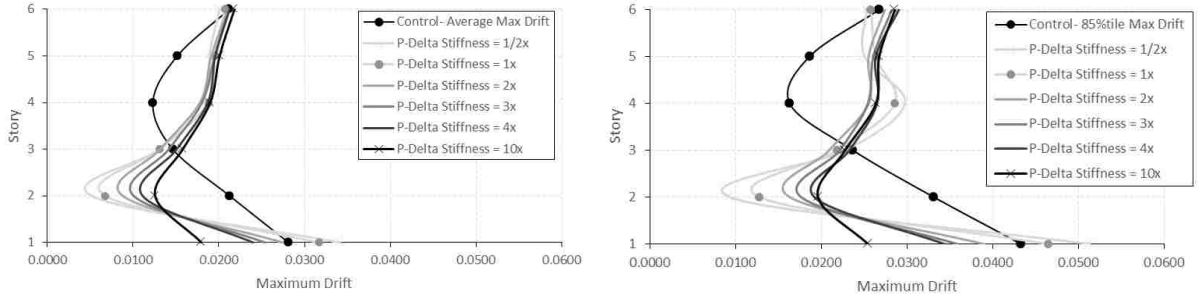

Figure D-26. Average & 85%tile maximum drifts for 2× ES at level 2, 6S.

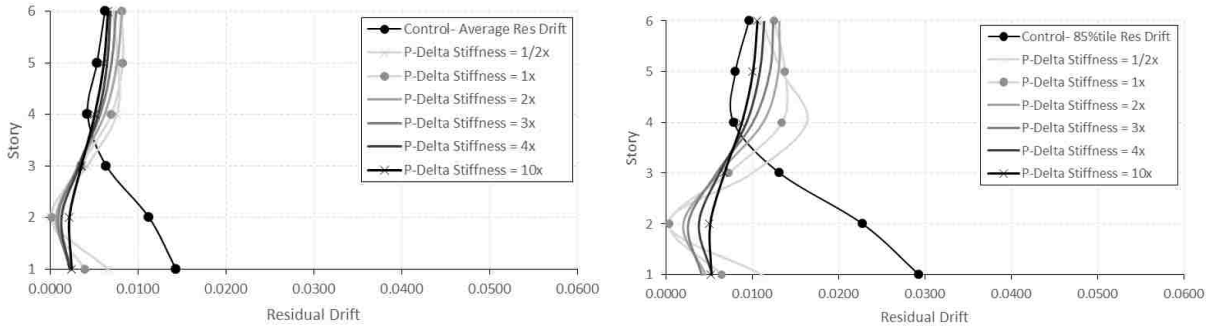

Figure D-27. Average & 85%tile residual drifts for 3× ES at level 2, 6S.

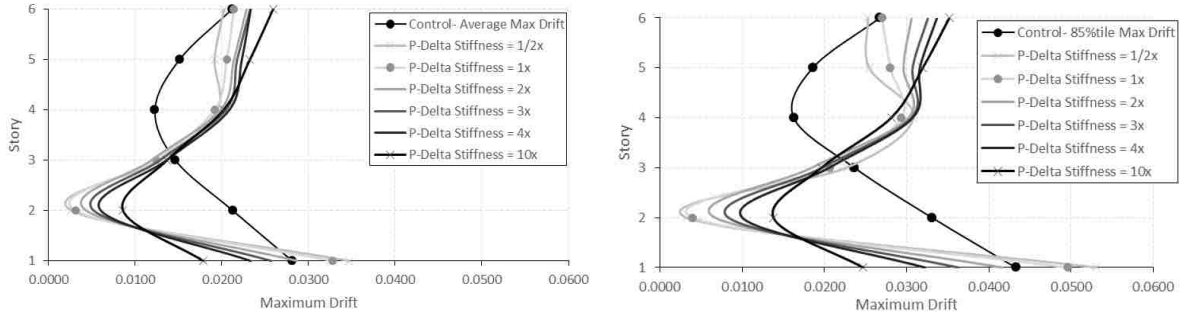

Figure D-28. Average & 85%tile maximum drifts for 3× ES at level 2, 6S.

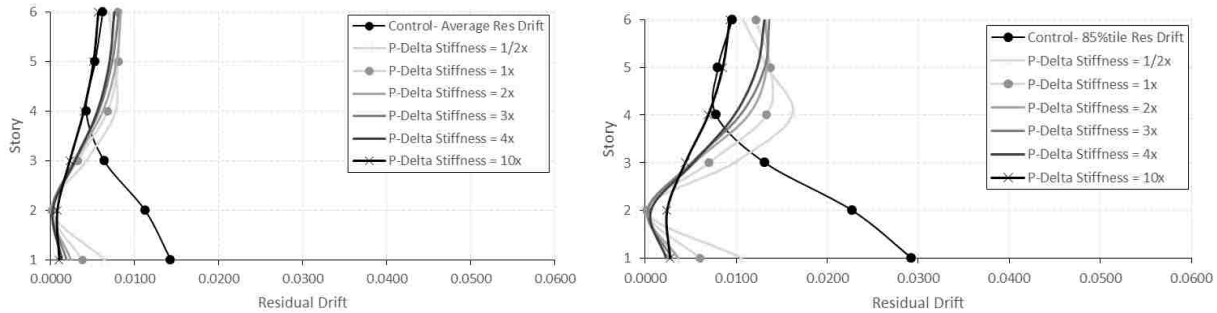

Figure D-29. Average & 85%tile residual drifts for 4× ES at level 2, 6S.

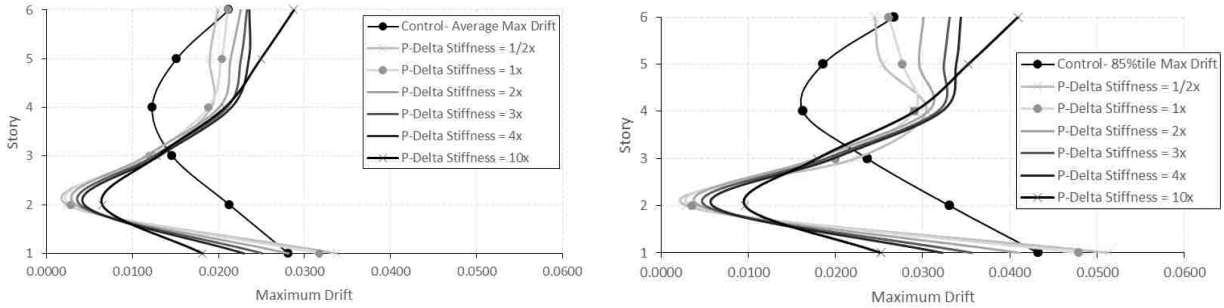

Figure D-30. Average & 85%tile maximum drifts for 4× ES at level 2, 6S.

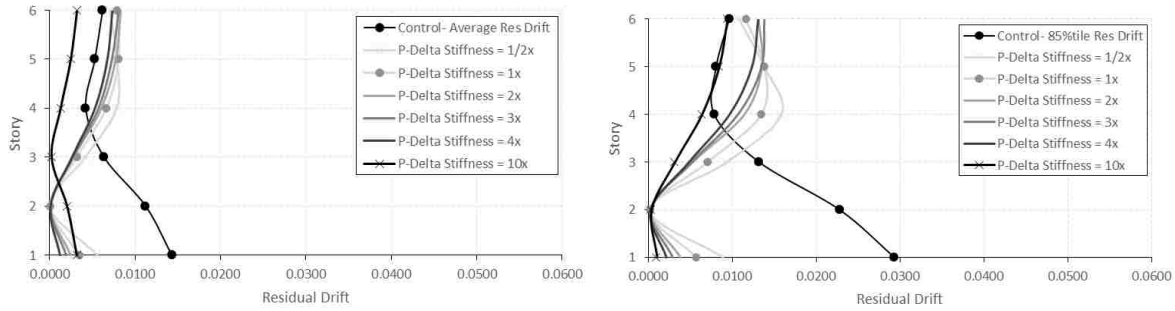

Figure D-31. Average & 85%tile residual drifts for 10× ES at level 2, 6S.

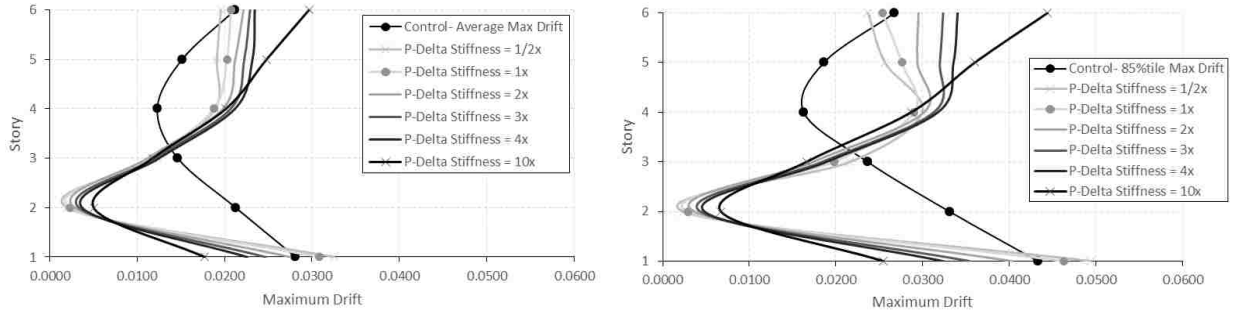

Figure D-32. Average & 85%tile maximum drifts for 10× ES at level 2, 6S.

D.5 Elastic Story at Level 3

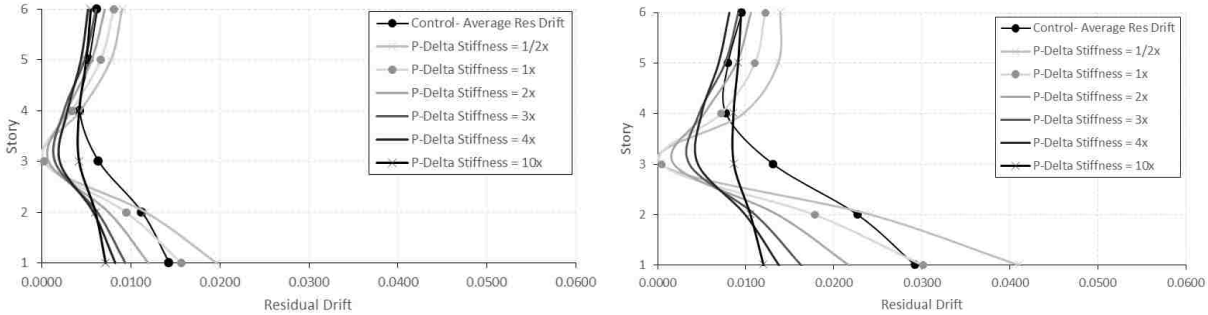

Figure D-33. Average & 85%tile residual drifts for 2× ES at level 3, 6S.

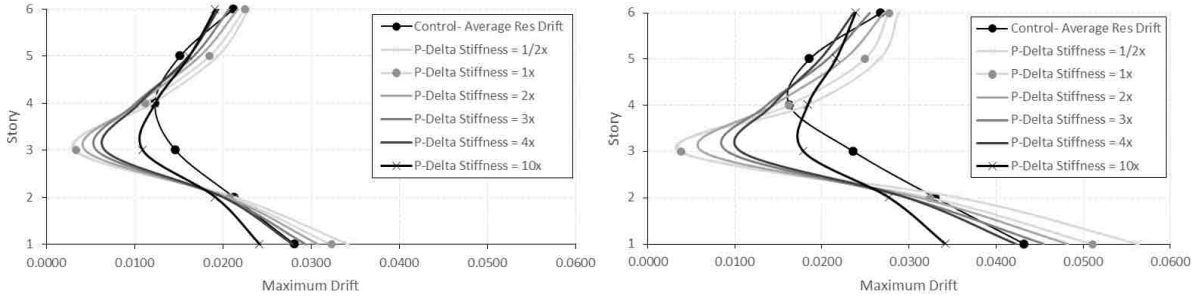

Figure D-34. Average & 85%tile maximum drifts for 2× ES at level 3, 6S.

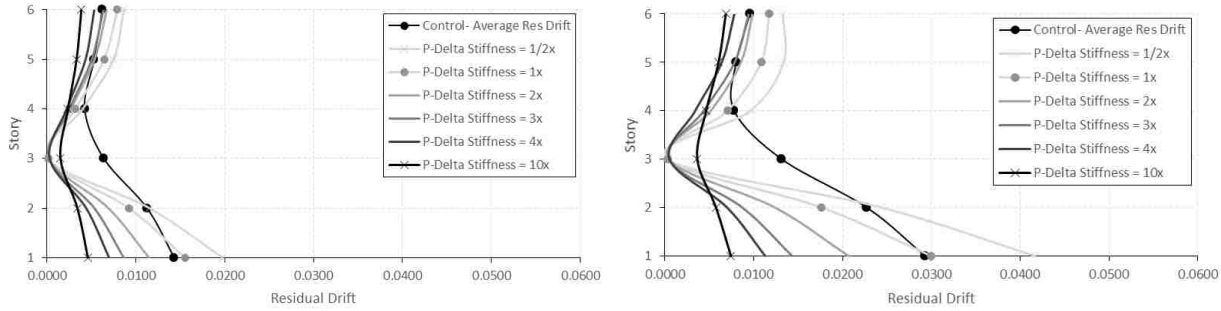

Figure D-35. Average & 85%tile residual drifts for 3× ES at level 3, 6S.

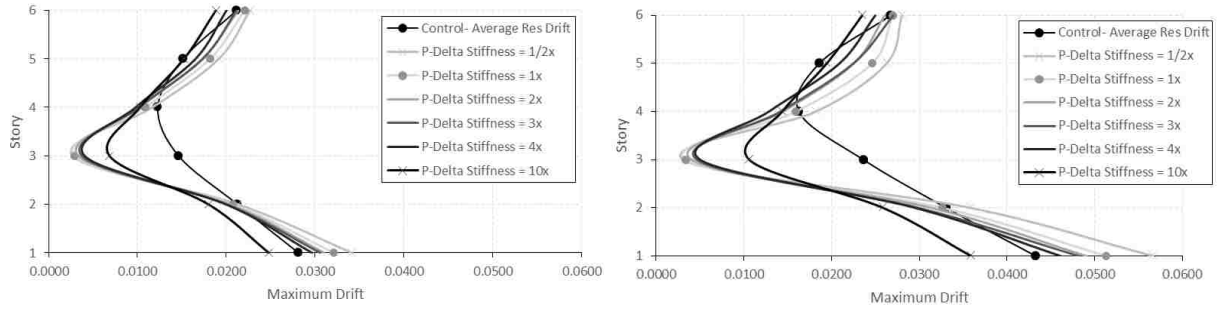

Figure D-36. Average & 85%tile maximum drifts for 3× ES at level 3, 6S.

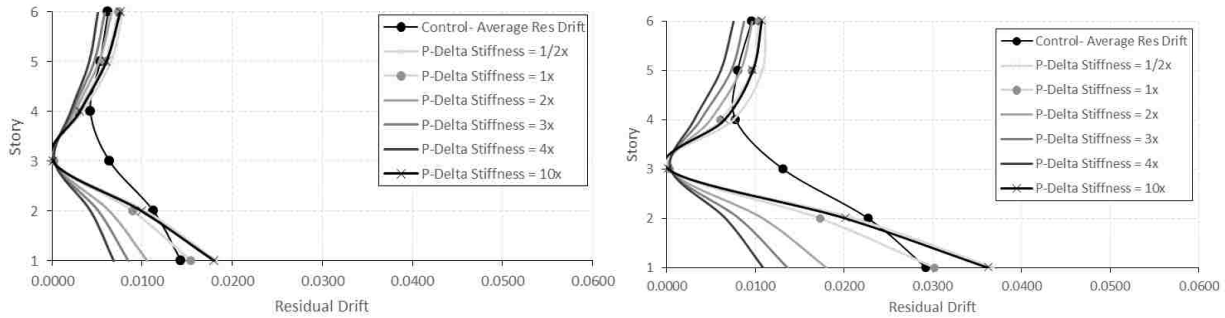

Figure D-37. Average & 85%tile residual drifts for 4× ES at level 3, 6S.

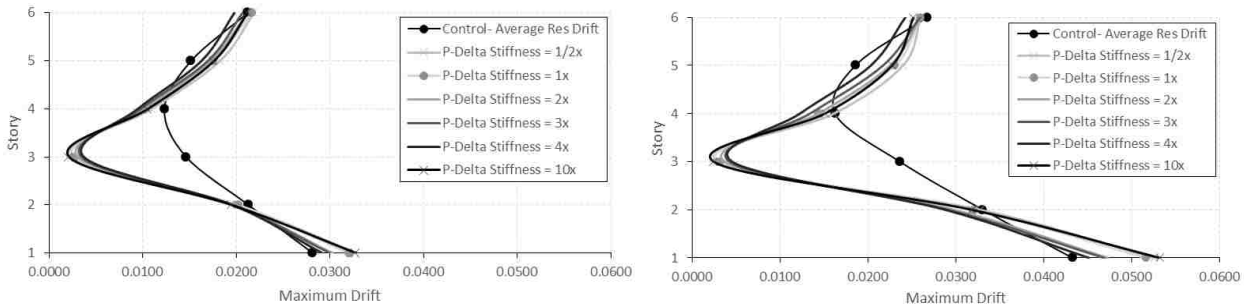

Figure D-38. Average & 85%tile maximum drifts for 4× ES at level 3, 6S.

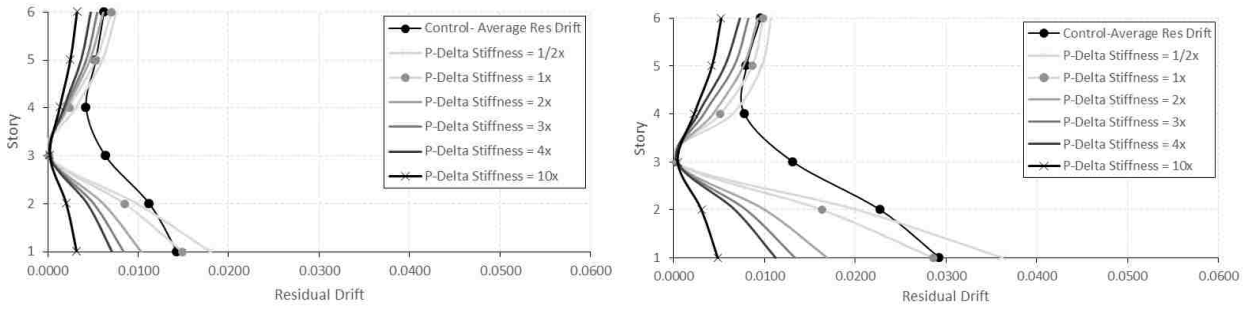

Figure D-39. Average & 85%tile residual drifts for 10× ES at level 3, 6S.

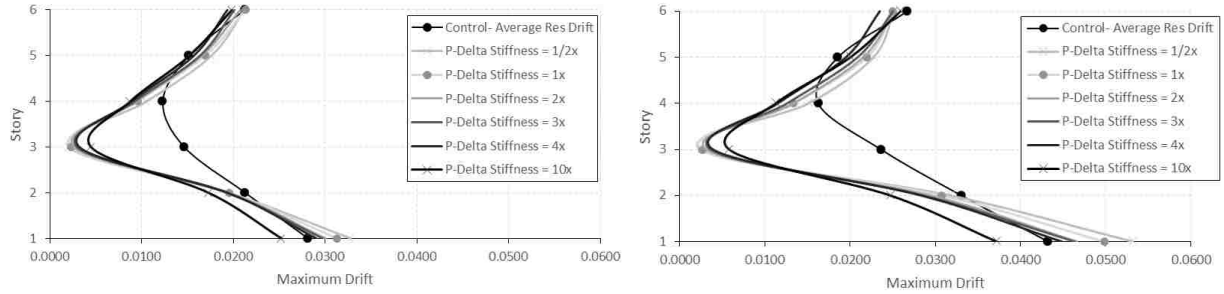

Figure D-40. Average & 85%tile maximum drifts for 10× ES at level 3, 6S.

D.6 Elastic Story at Level 4

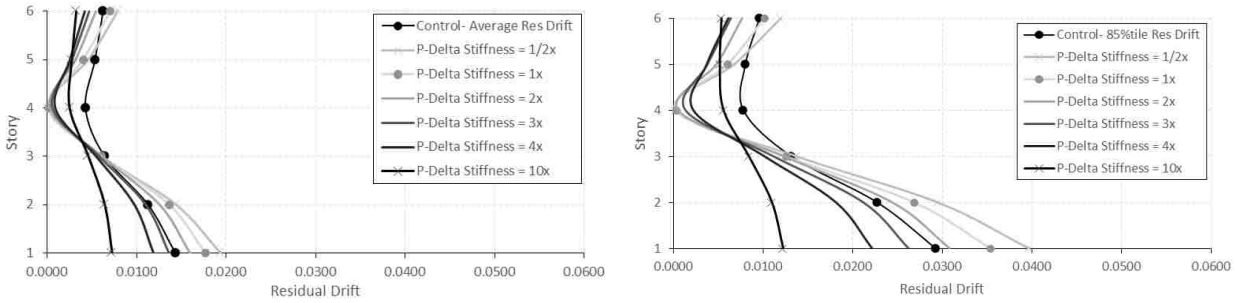

Figure D-41. Average & 85%tile residual drifts for 2× ES at level 4, 6S.

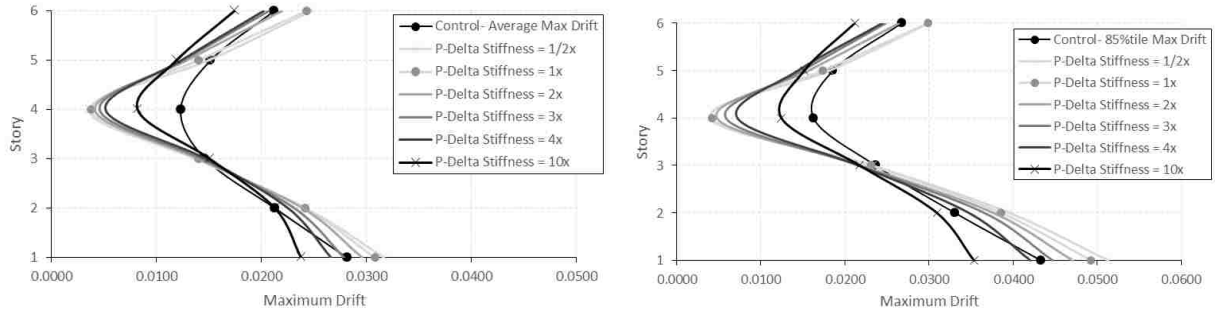

Figure D-42. Average & 85%tile maximum drifts for 2× ES at level 4, 6S.

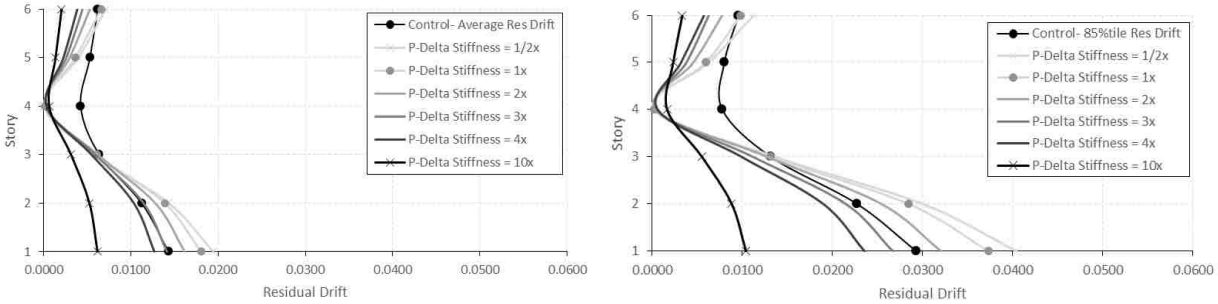

Figure D-43. Average & 85%tile residual drifts for 3× ES at level 4, 6S.

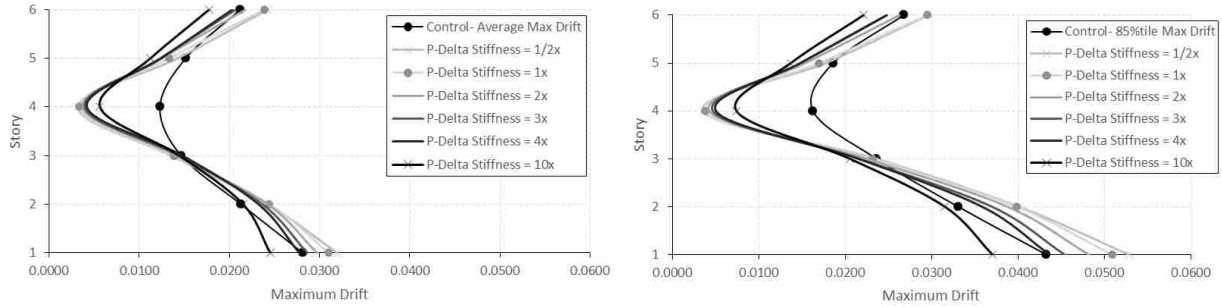

Figure D-44. Average & 85%tile maximum drifts for 3× ES at level 4, 6S.

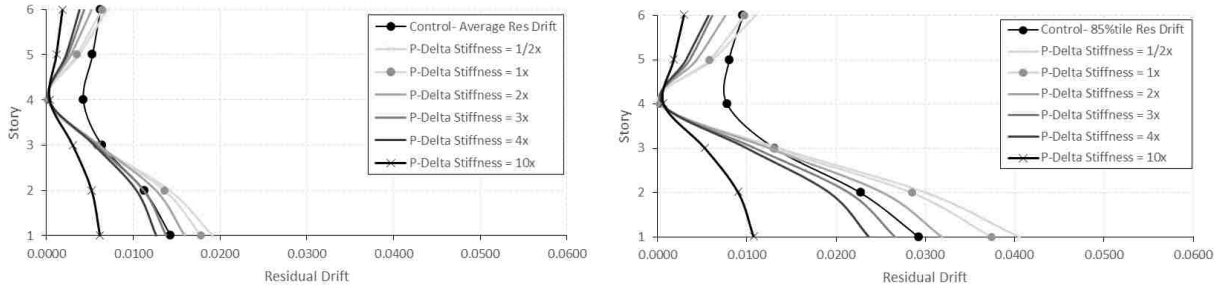

Figure D-45. Average & 85%tile residual drifts for 4× ES at level 4, 6S.

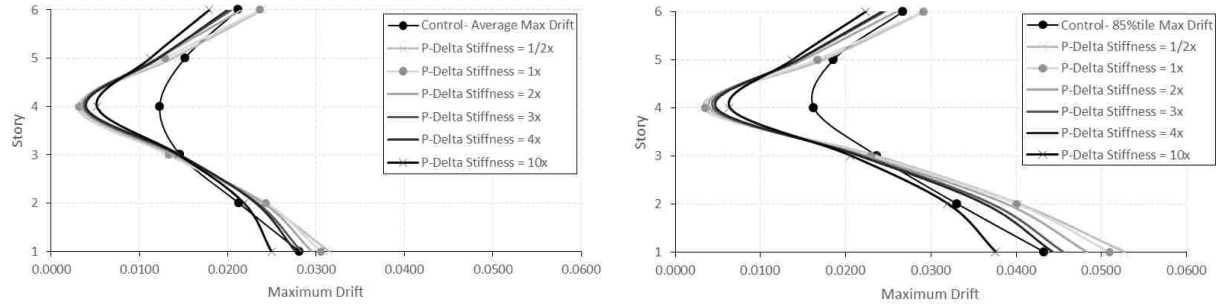

Figure D-46. Average & 85%tile maximum drifts for 4× ES at level 4, 6S.

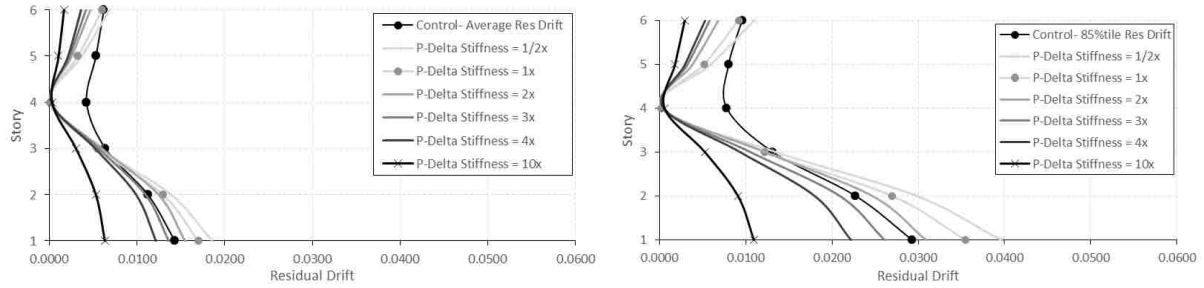

Figure D-47. Average & 85%tile residual drifts for 10× ES at level 4, 6S.

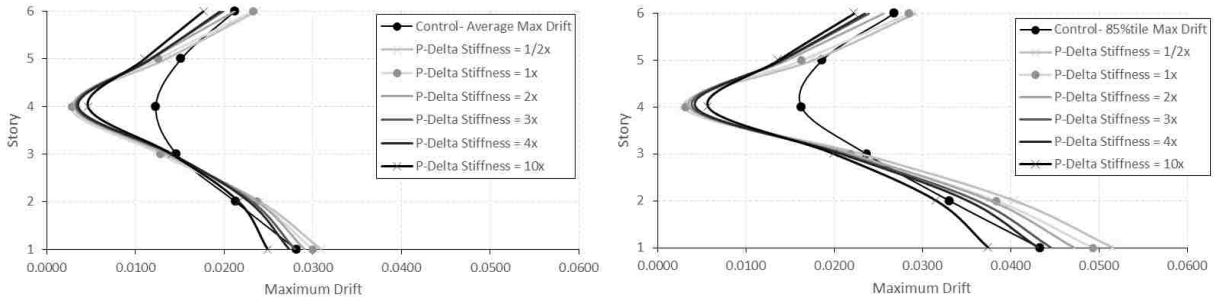

Figure D-48. Average & 85%tile maximum drifts for 10× ES at level 4, 6S.

D.7 Elastic Story at Level 5

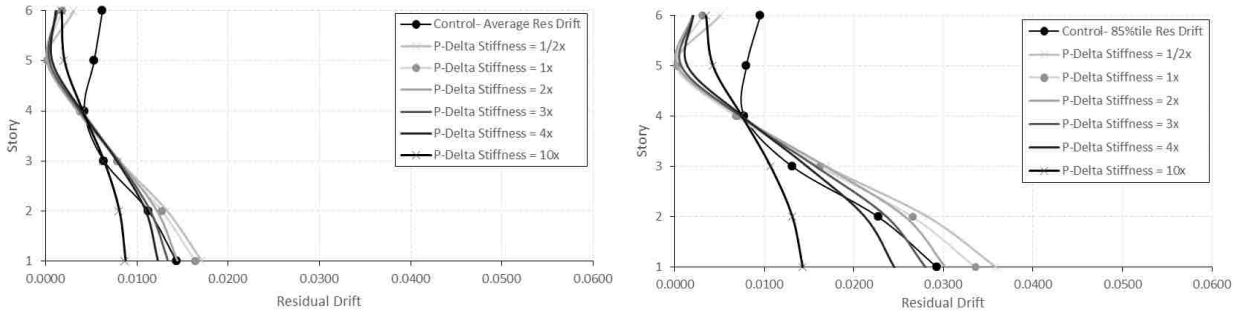

Figure D-49. Average & 85%tile residual drifts for 2× ES at level 5, 6S.

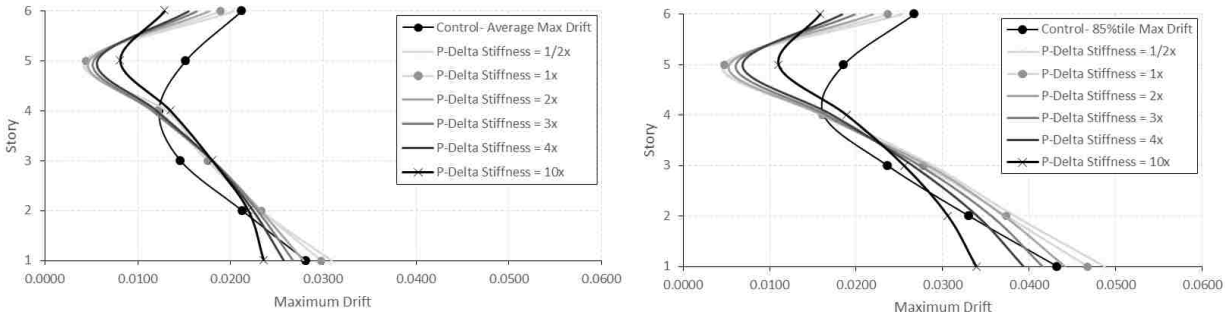

Figure D-50. Average & 85%tile maximum drifts for 2× ES at level 5, 6S.

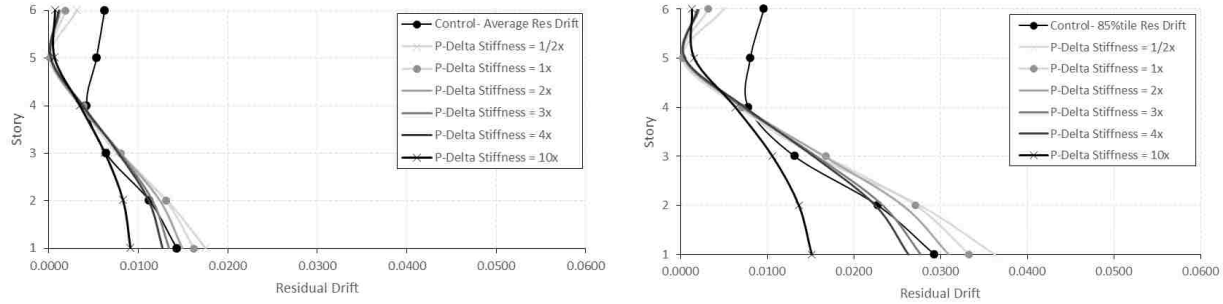

Figure D-51. Average & 85%tile residual drifts for 3× ES at level 5, 6S.

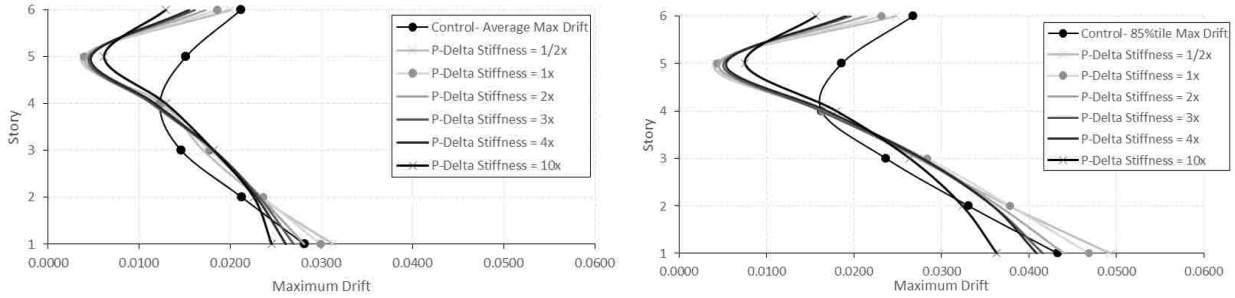

Figure D-52. Average & 85%tile maximum drifts for 3× ES at level 5, 6S.

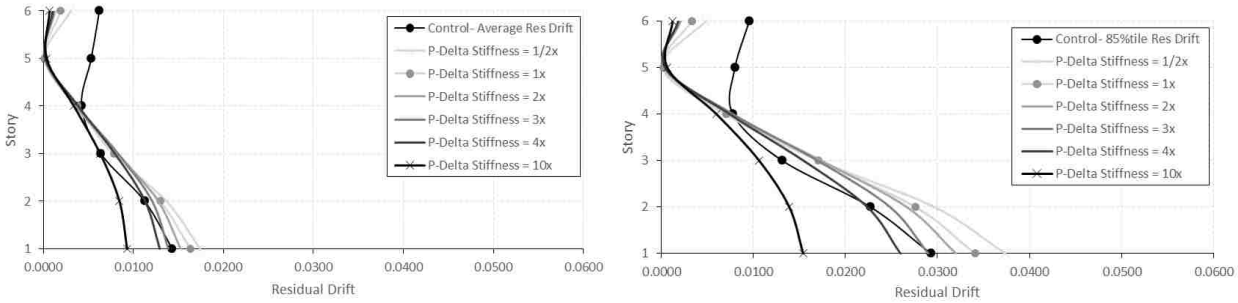

Figure D-53. Average & 85%tile residual drifts for 4× ES at level 5, 6S.

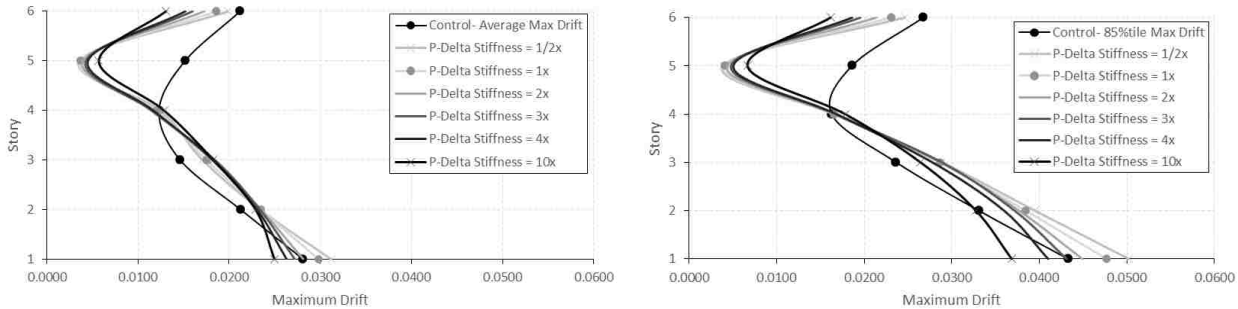

Figure D-54. Average & 85%tile maximum drifts for 4× ES at level 5, 6S.

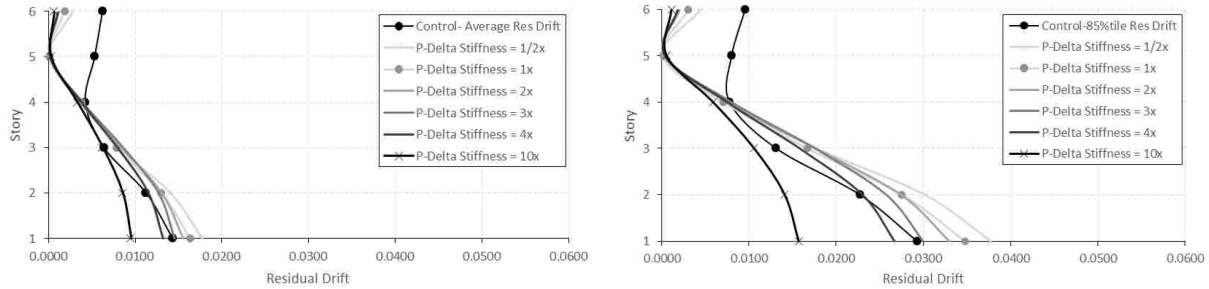

Figure D-55. Average & 85%tile residual Drifts for 10× ES at level 5, 6S.

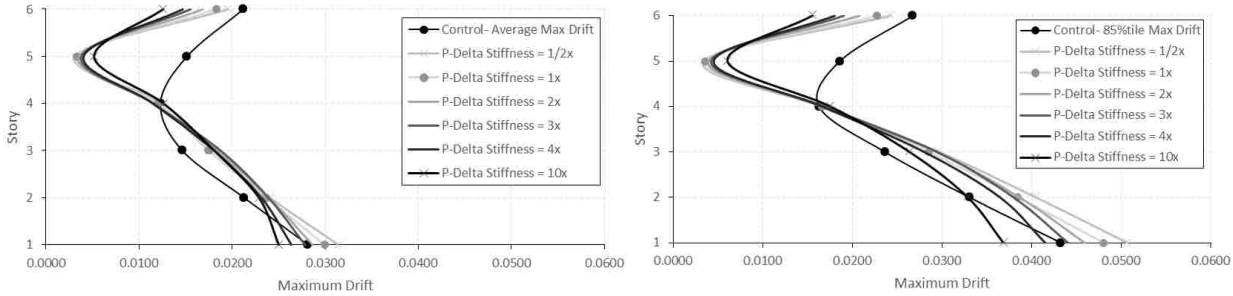

Figure D-56. Average & 85%tile maximum drifts for 10× ES at level 5, 6S.

D.8 Elastic Story at Level 6

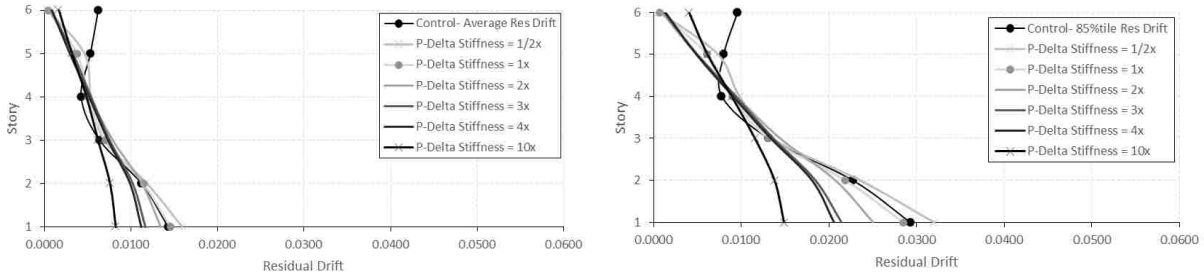

Figure D-57. Average & 85%tile residual drifts for 2× ES at level 6, 6S.

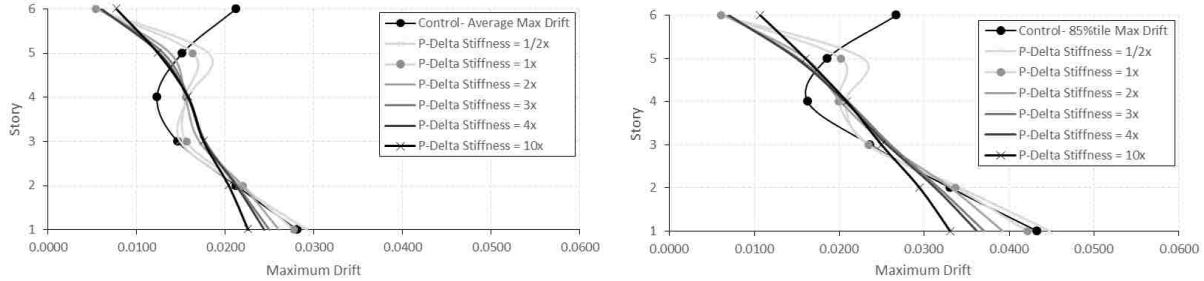

Figure D-58. Average & 85%tile maximum drifts for 2× ES at level 6, 6S.

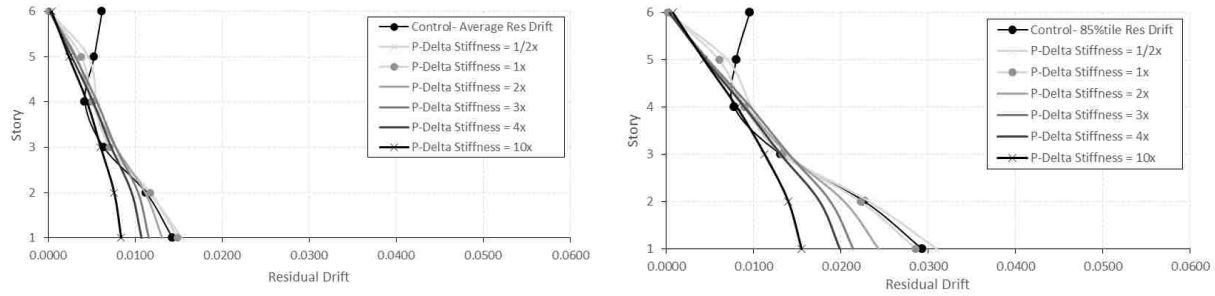

Figure D-59. Average & 85%tile residual drifts for 3× ES at level 6, 6S.

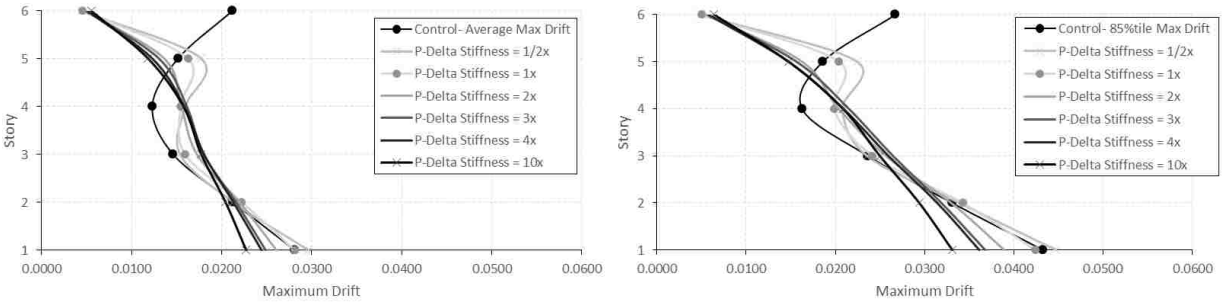

Figure D-60. Average & 85%tile maximum drifts for 3× ES at level 6, 6S.

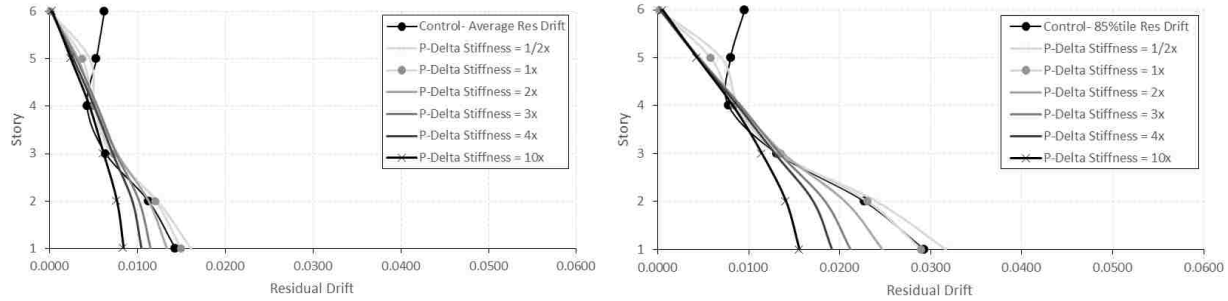

Figure D-61. Average & 85%tile residual drifts for 4× ES at level 6, 6S.

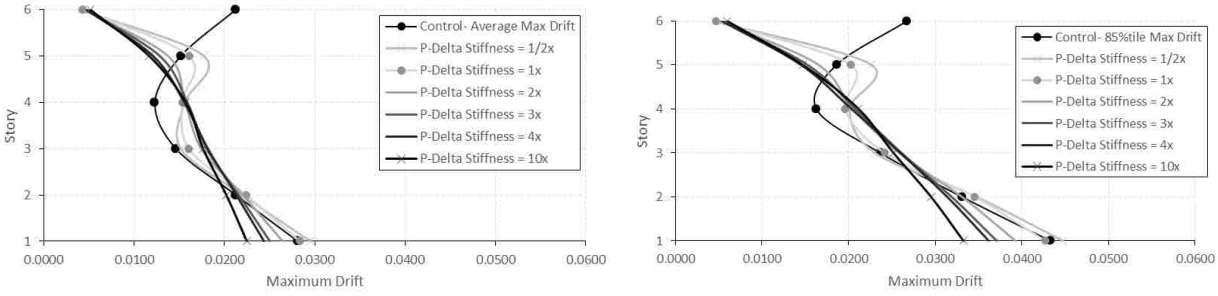

Figure D-62. Average & 85%tile maximum drifts for 4× ES at level 6, 6S.

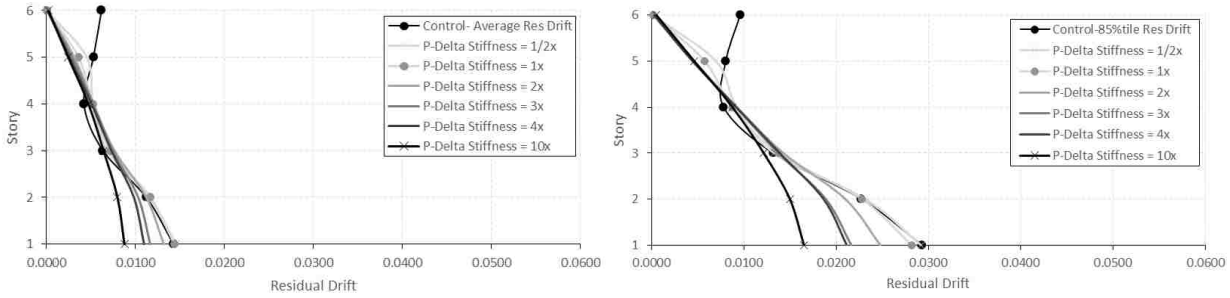

Figure D-63. Average & 85%tile residual drifts for 10× ES at level 6, 6S.

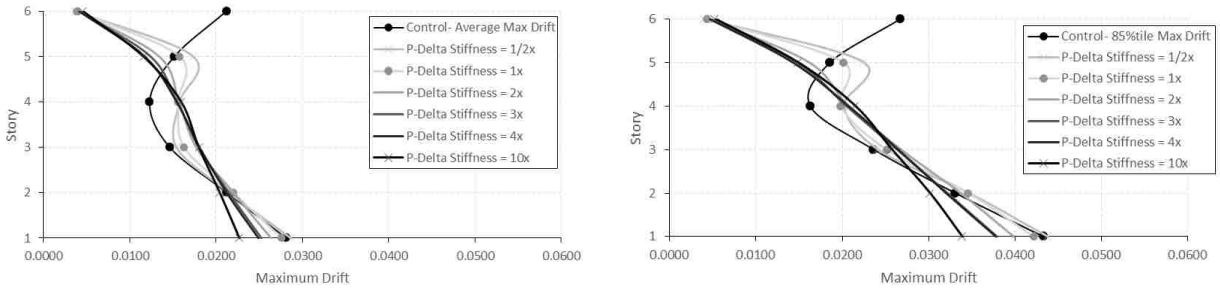

Figure D-64. Average & 85%tile maximum drifts for 10× ES at level 6, 6S.

APPENDIX E. GRAPH OF 8-STORY BUILDINGS

The following graphs show all results of residual and maximum drifts for 8-story (8S) buildings with elastic stories at different levels.

E.1 Elastic Story at Level 1&5

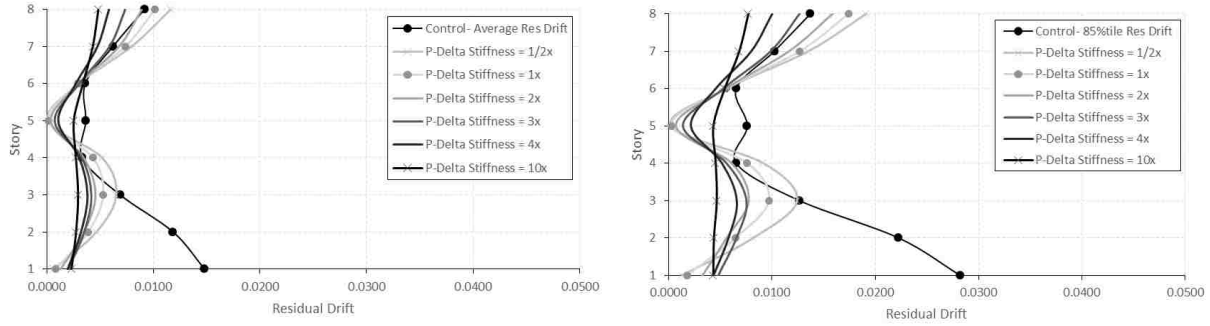

Figure E-1. Average & 85%tile residual drifts for 2× ES at level 1&5, 8S.

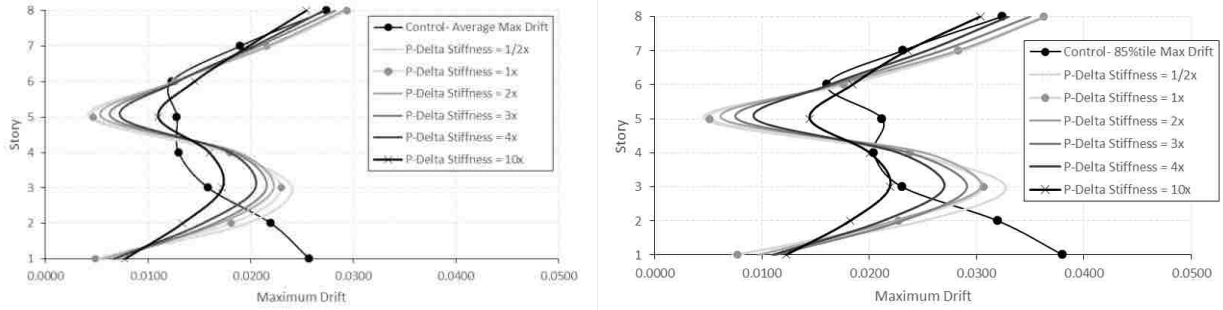

Figure E-2. Average & 85%tile maximum drifts for 2× ES at level 1&5, 8S.

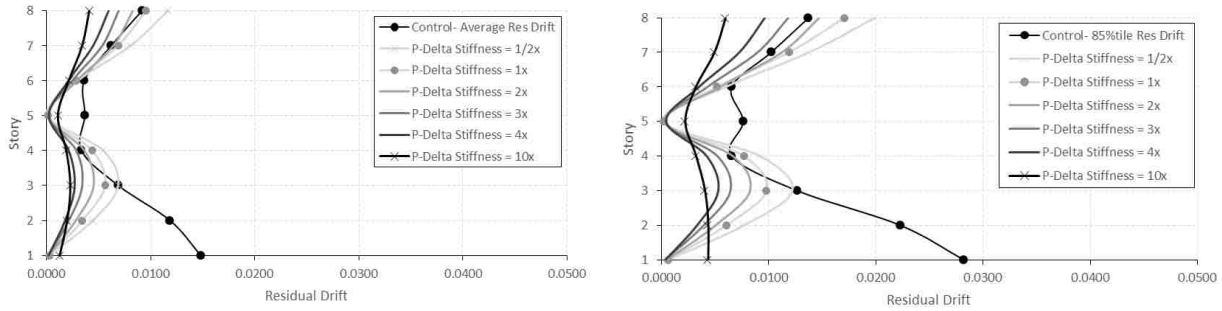

Figure E-3. Average & 85%tile residual drifts for 3× ES at level 1&5, 8S.

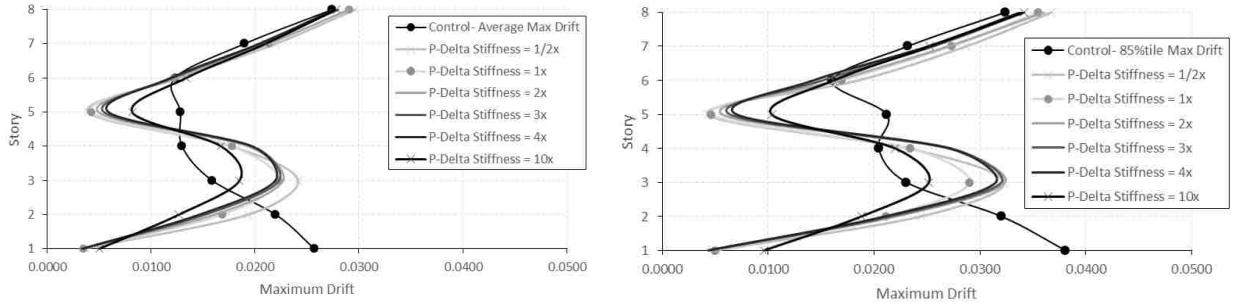

Figure E-4. Average & 85%tile maximum drifts for 3× ES at level 1&5, 8S.

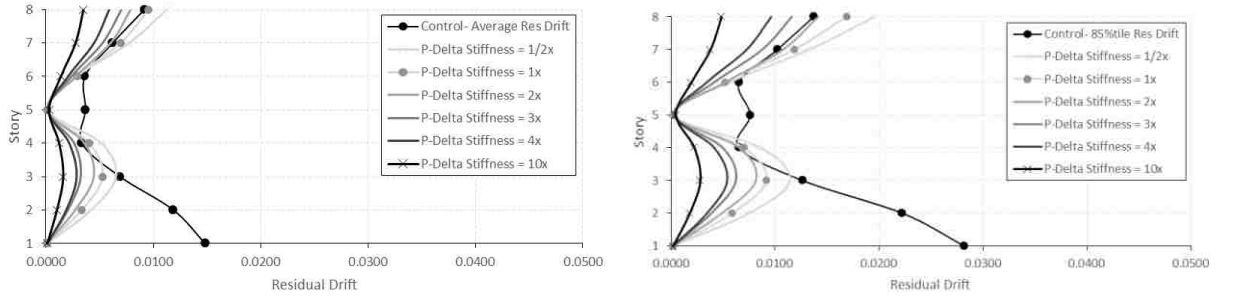

Figure E-5. Average & 85%tile residual drifts for 4× ES at level 1&5, 8S.

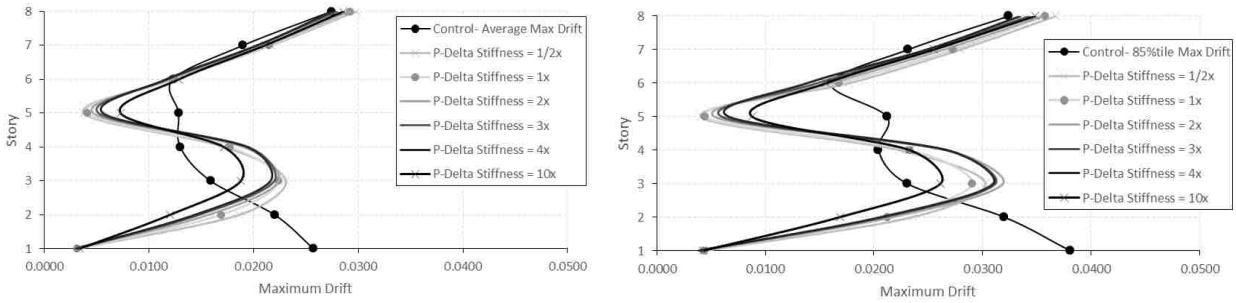

Figure E-6. Average & 85%tile maximum drifts for 4× ES at level 1&5, 8S

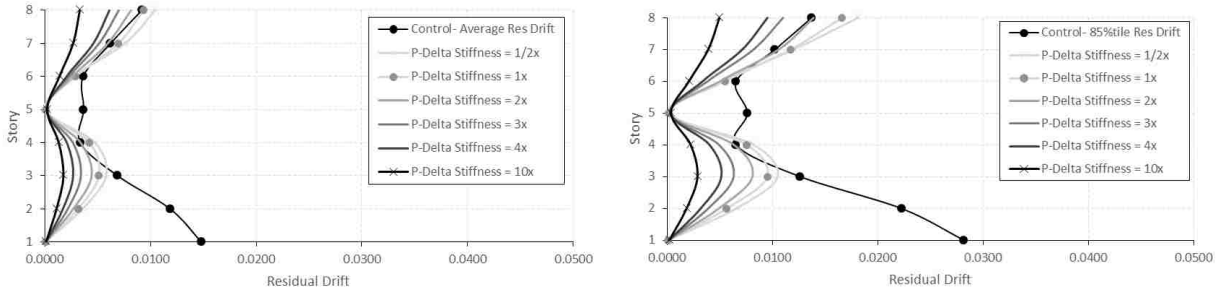

Figure E-7. Average & 85%tile residual drifts for 10× ES at level 1&5, 8S.

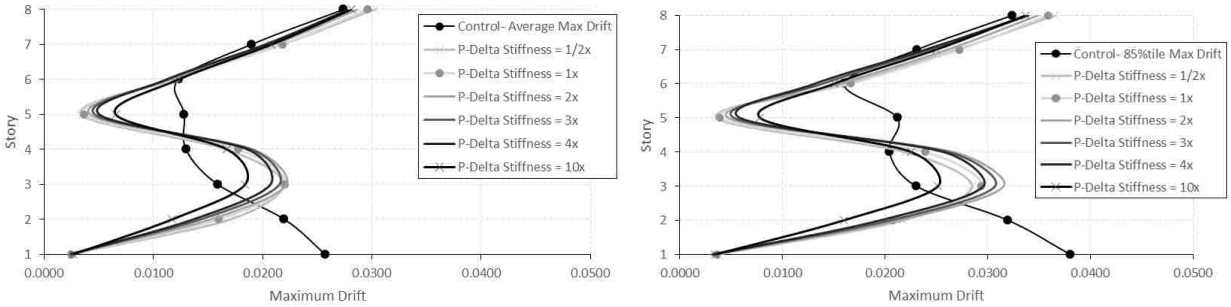

Figure E-8. Average & 85%tile maximum drifts for 10× ES at level 1&5, 8S.

E.2 Elastic Story at Level 4&8

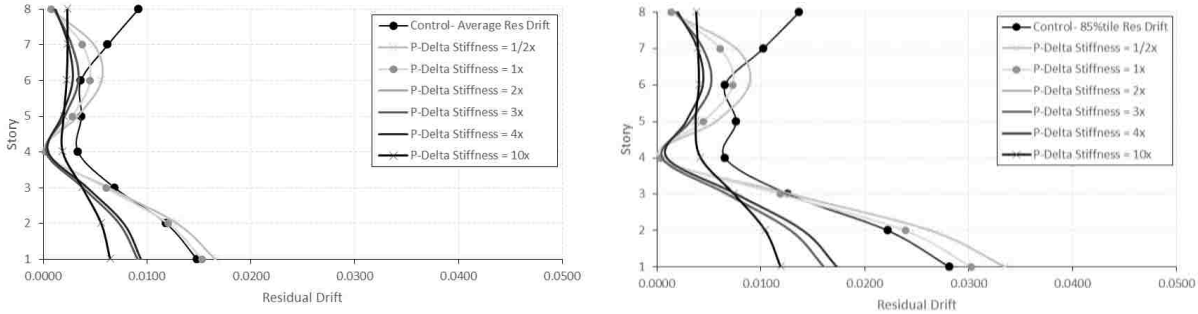

Figure E-9. Average & 85%tile residual drifts for 2× ES at level 4&8, 8S.

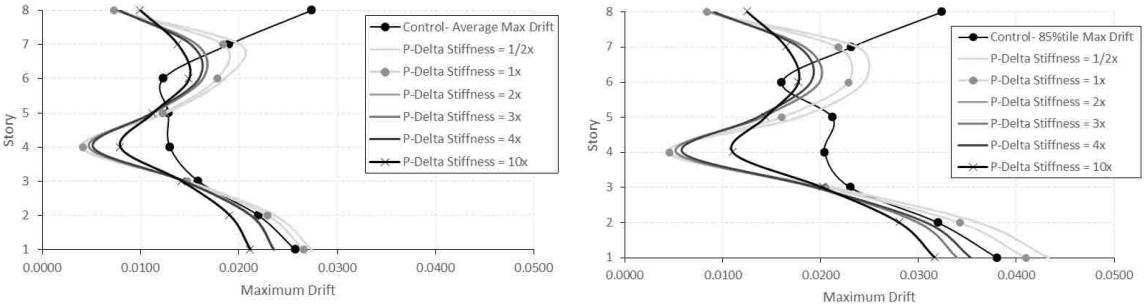

Figure E-10. Average & 85%tile maximum drifts for 2× ES at level 4&8, 8S.

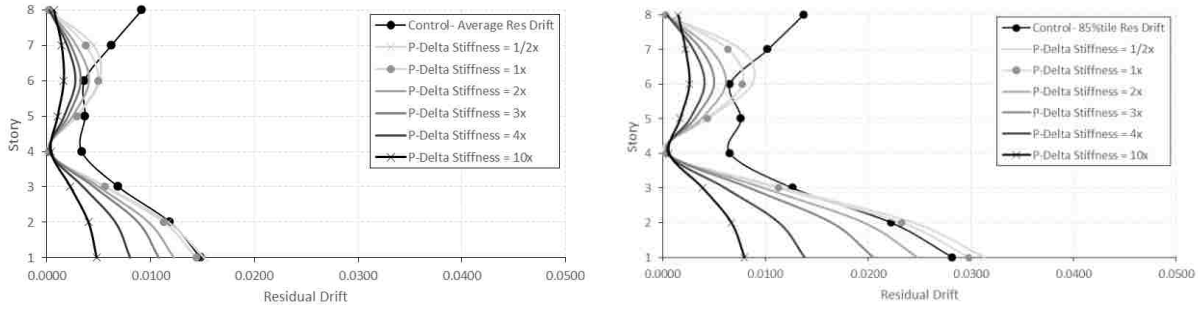

Figure E-11. Average & 85%tile residual drifts for 3× ES at level 4&8, 8S.

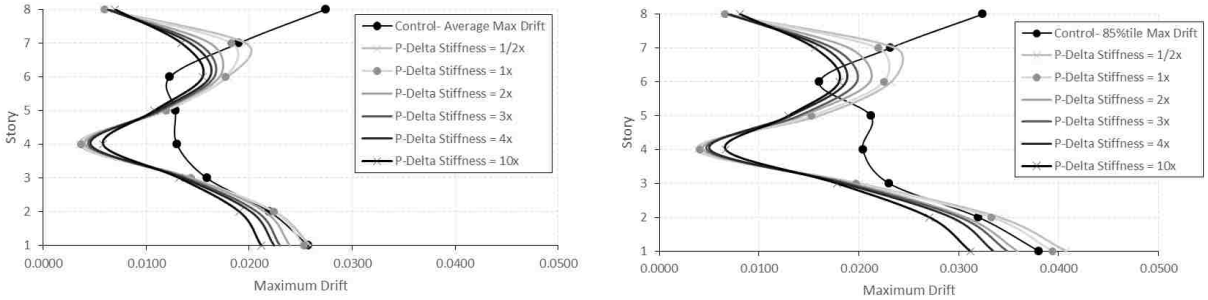

Figure E-12. Average & 85%tile maximum drifts for 3× ES at level 4&8, 8S.

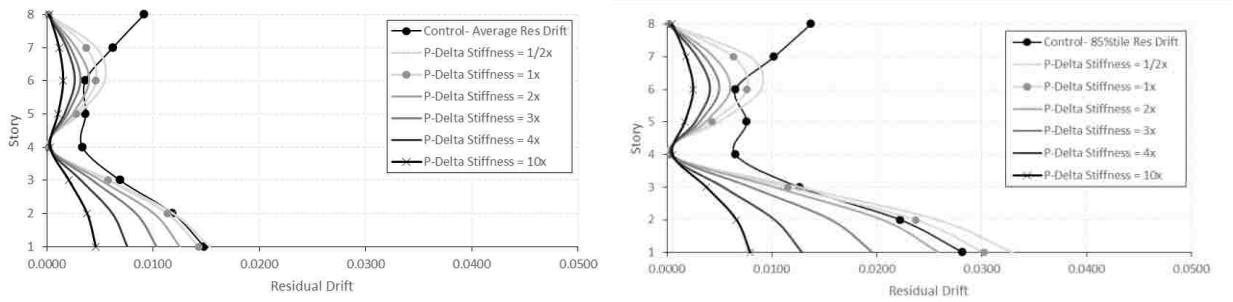

Figure E-13. Average & 85%tile residual drifts for 4× ES at level 4&8, 8S.

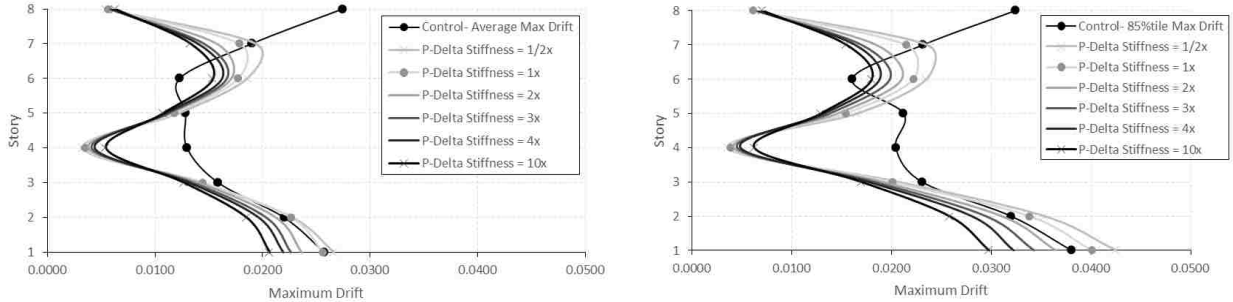

Figure E-14. Average & 85%tile maximum drifts for 4× ES at level 4&8, 8S.

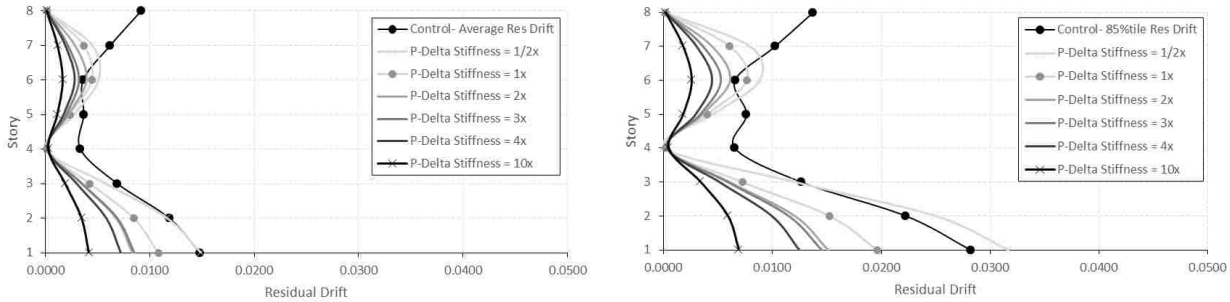

Figure E-15. Average & 85%tile residual drifts for 10× ES at level 4&8, 8S.

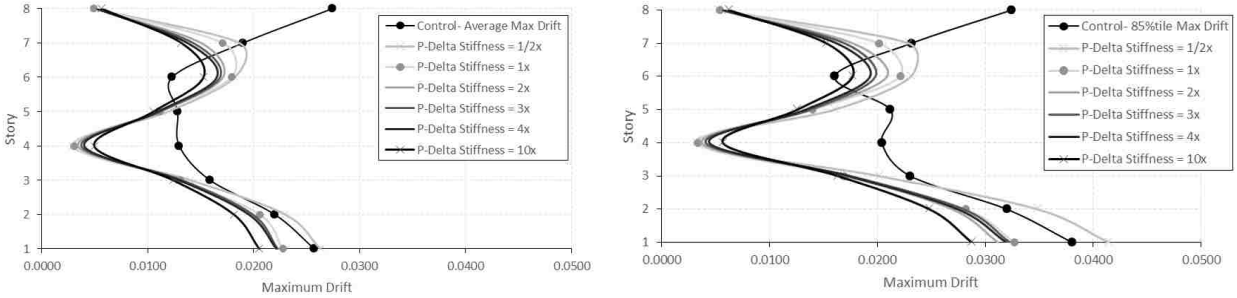

Figure E-16. Average & 85%tile maximum drifts for 10× ES at level 4&8, 8S.

APPENDIX F. GRAPH OF 12-STORY BUILDINGS

The following graphs show all results of residual and maximum drifts for 12-story (12S) buildings with elastic stories at different levels.

F.1 Elastic Story at Level 1, 5, & 9

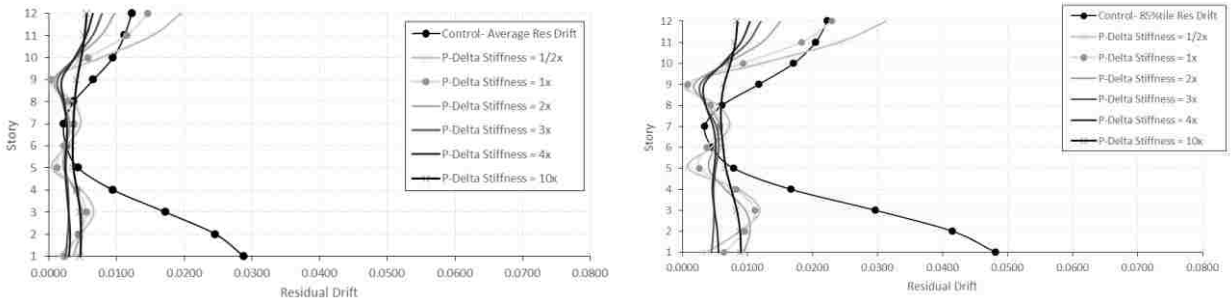

Figure F-1. Average & 85%tile residual drifts for 2× ES at level 1, 5, &9, 12S.

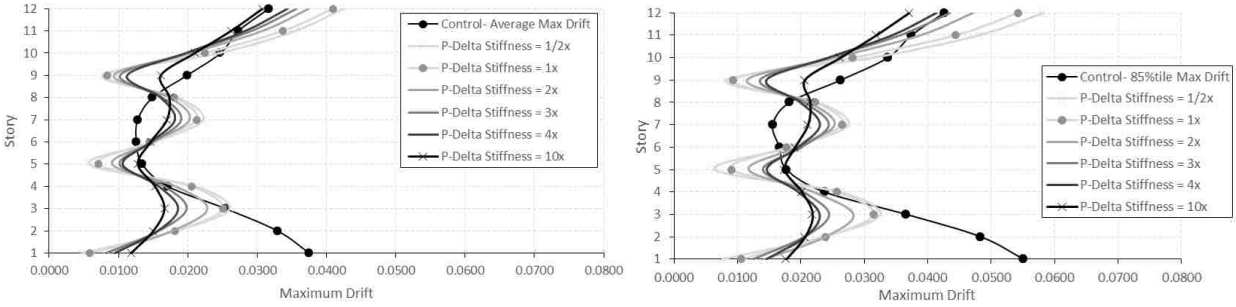

Figure F-2. Average & 85%tile maximum drifts for 2× ES at level 1, 5, &9, 12S.

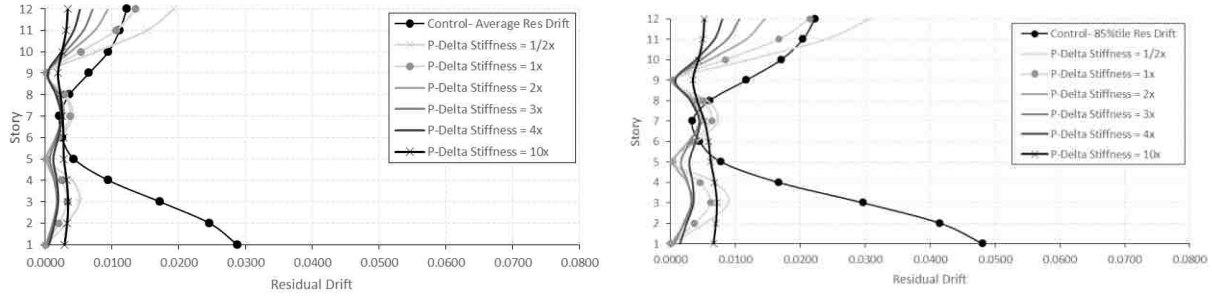

Figure F-3. Average & 85%tile residual drifts for 3× ES at level 1, 5, &9, 12S.

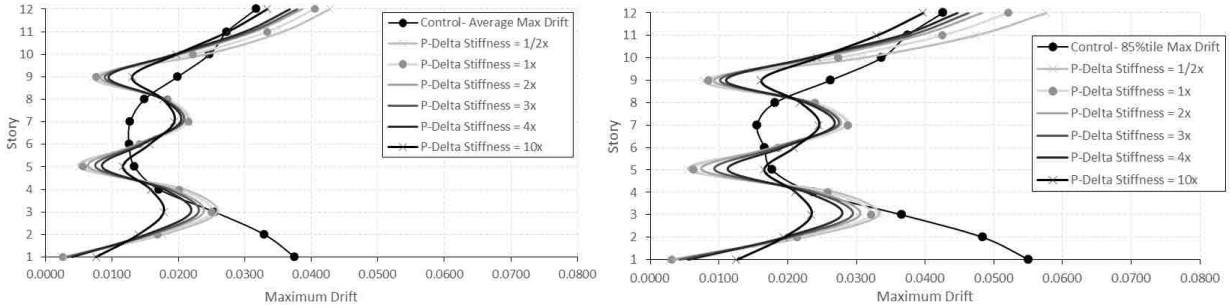

Figure F-4. Average & 85%tile maximum drifts for 3× ES at level 1, 5, &9, 12S.

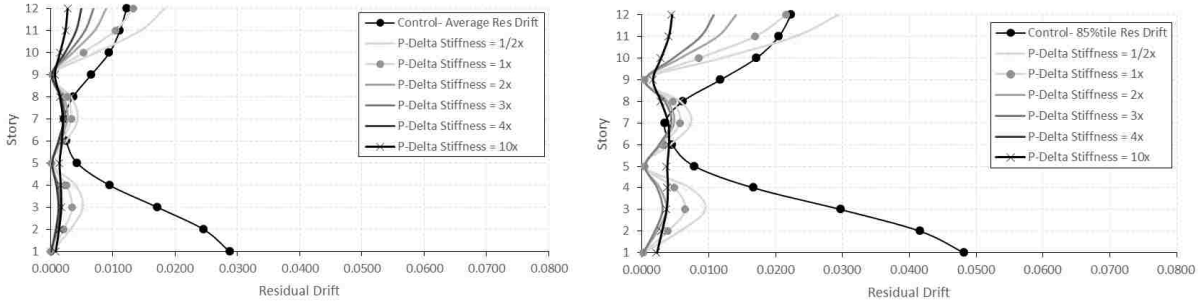

Figure F-5. Average & 85%tile residual drifts for 4× ES at level 1, 5, &9, 12S.

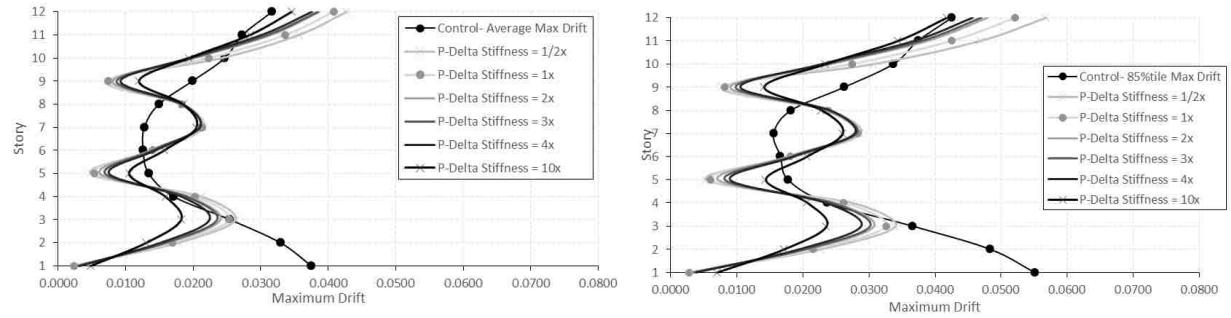

Figure F-6. Average & 85%tile maximum drifts for 4× ES at level 1, 5, &9, 12S.

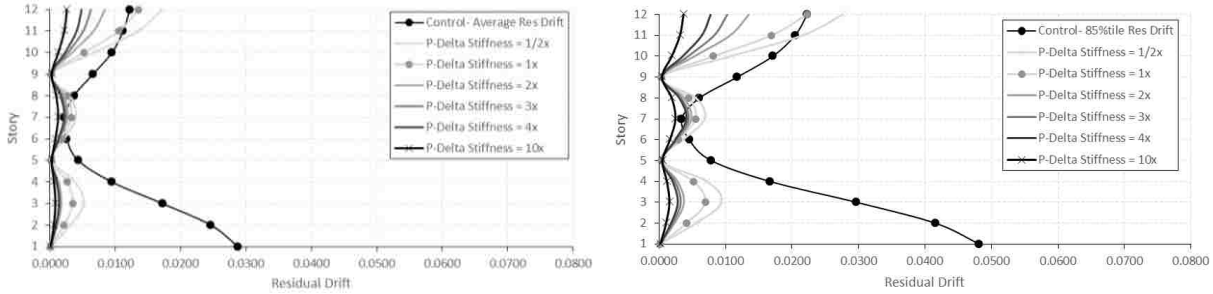

Figure F-7. Average & 85%tile residual drifts for 10× ES at level 1, 5, &9, 12S.

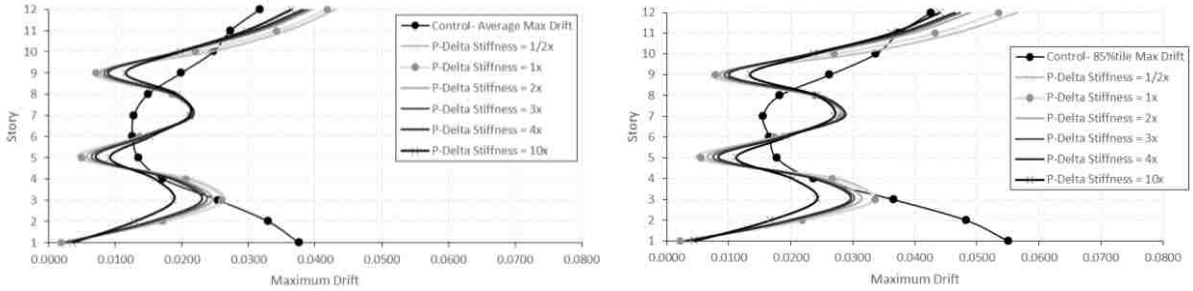

Figure F-8. Average & 85%tile maximum drifts for 10× ES at level 1, 5, &9, 12S.

F.1 Elastic Story at Level 4, 8, & 12

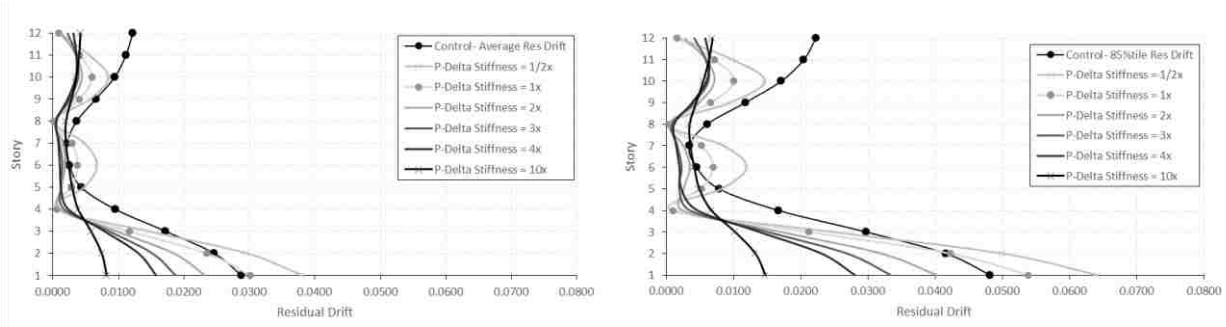

Figure F-9. Average & 85%tile residual drifts for 2× ES at level 4, 8, &12, 12S.

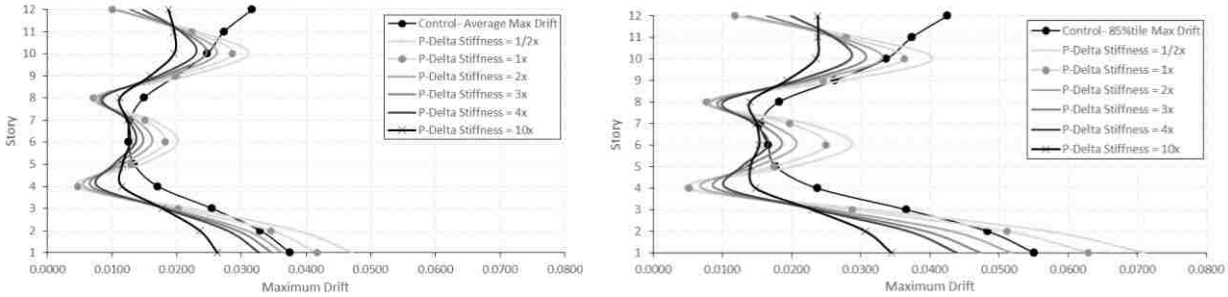

Figure F-10. Average & 85%tile maximum drifts for 2× ES at level 4, 8, &12, 12S.

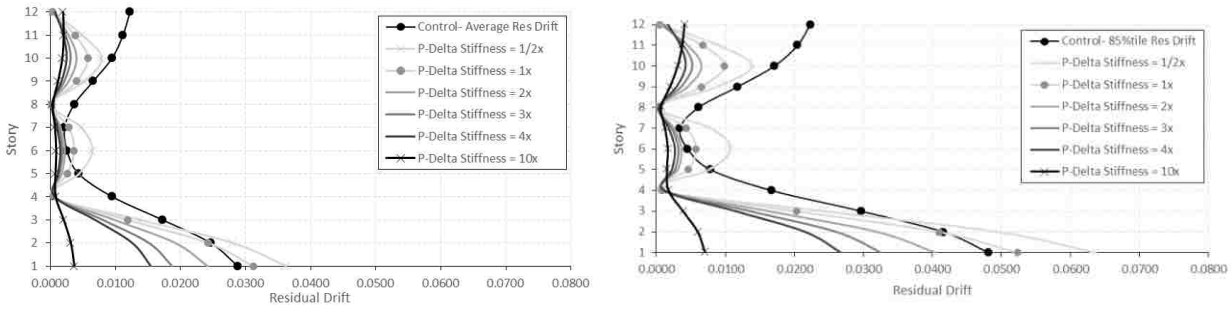

Figure F-11 Average & 85%tile residual drifts for 3× ES at level 4, 8, &12, 12S.

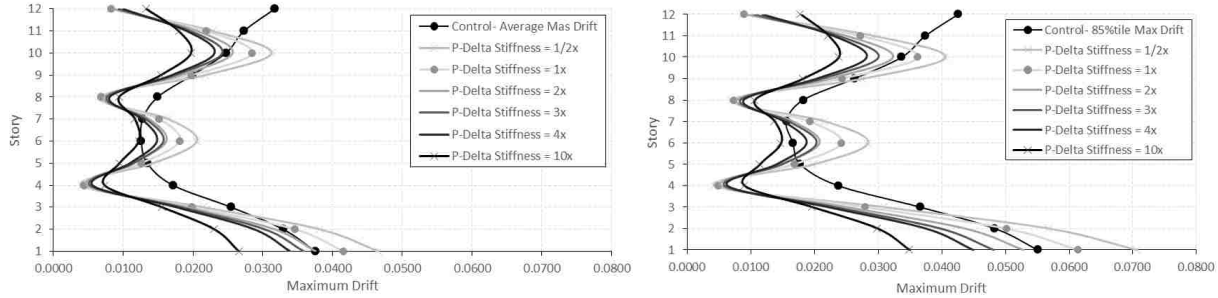

Figure F-12. Average & 85%tile maximum drifts for 3× ES at level 4, 8, &12, 12S.

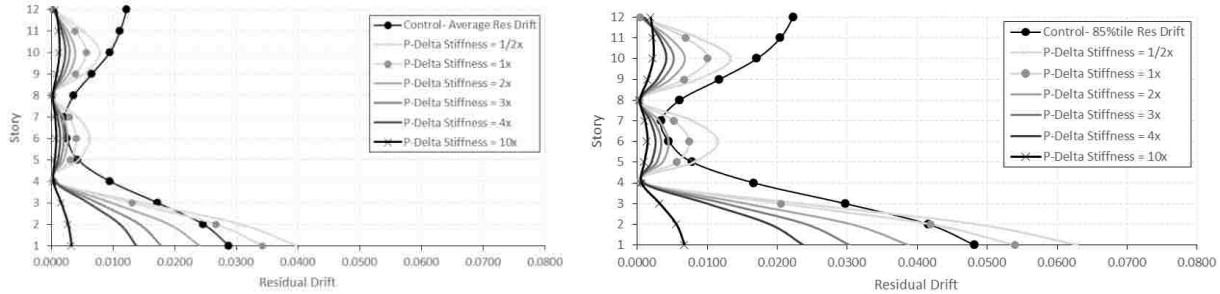

Figure F-13. Average & 85%tile residual drifts for 4× ES at level 4, 8, &12, 12S.

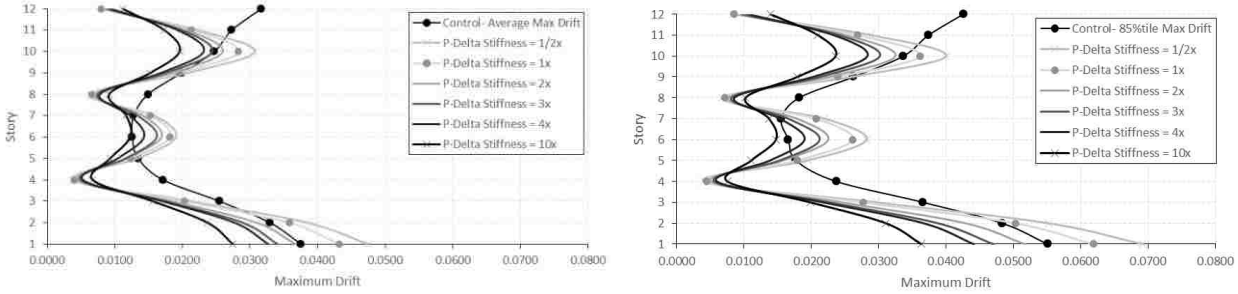

Figure F-14. Average & 85%tile maximum drifts for 4× ES at level 4, 8, &12, 12S.

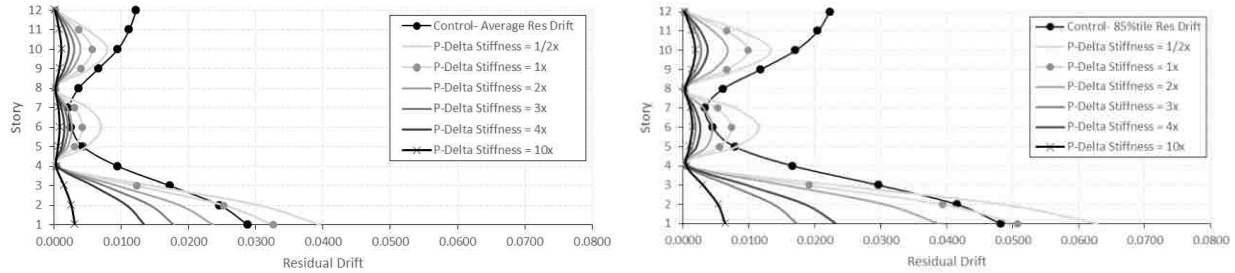

Figure F-15. Average & 85%tile residual drifts for10× ES at level 4, 8, &12, 12S.

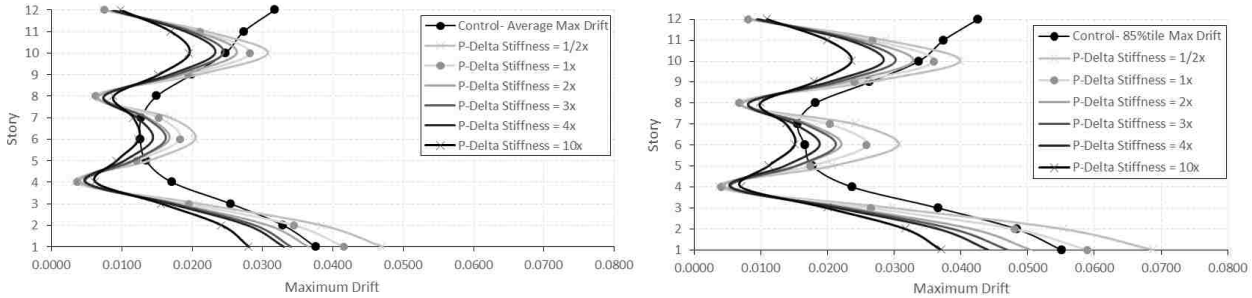

Figure F-16. Average & 85%tile maximum drifts for 10× ES at level 4, 8, &12, 12S.

APPENDIX G. GRAPH OF 16-STORY BUILDINGS

The following graphs show all results of residual and maximum drifts for 16-story (16S) buildings with elastic stories at different levels.

G.1 Elastic Story at Level 1, 5, 9, & 13

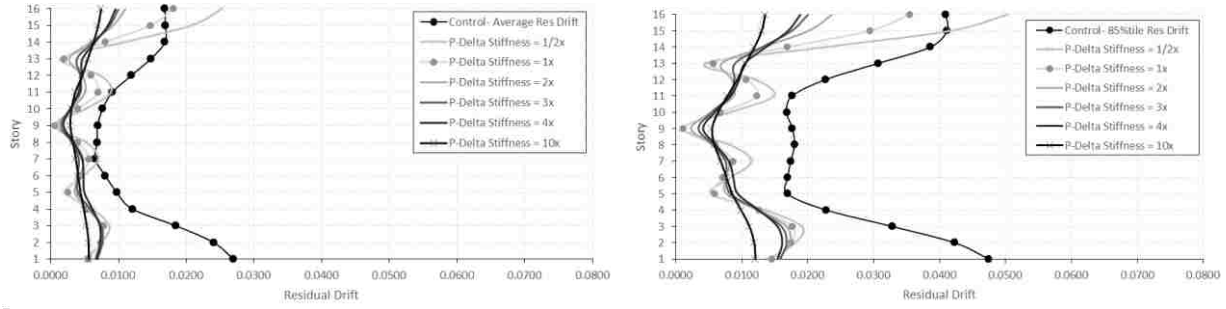

Figure G-1. Average & 85%tile residual drifts for 2× ES at level 1, 5, 9, &13, 16S.

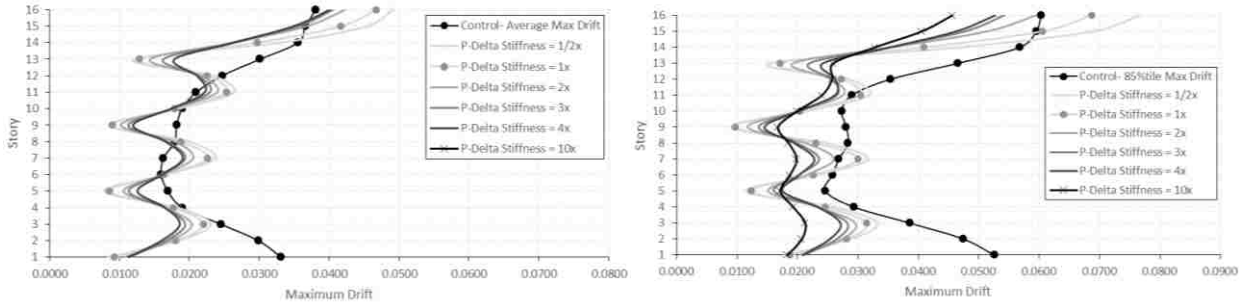

Figure G-2. Average & 85%tile maximum drifts for 2× ES at level 1, 5, 9, &13, 16S.

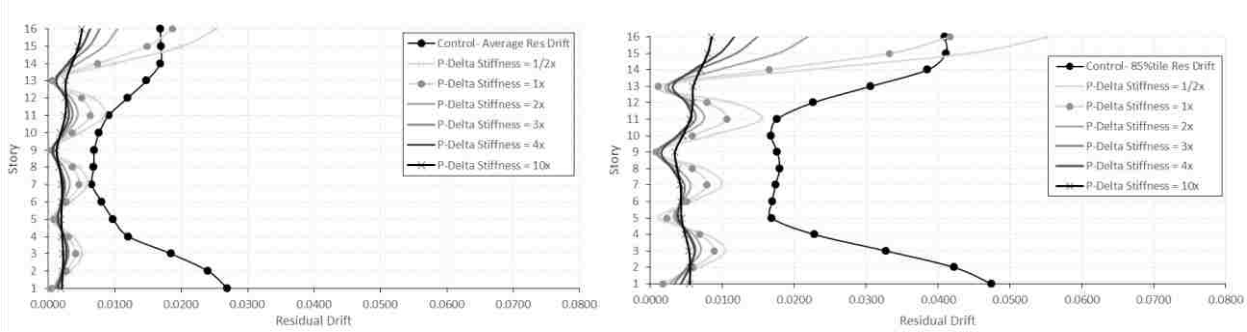

Figure G-3. Average & 85%tile residual drifts for 3× ES at level 1, 5, 9, &13, 16S.

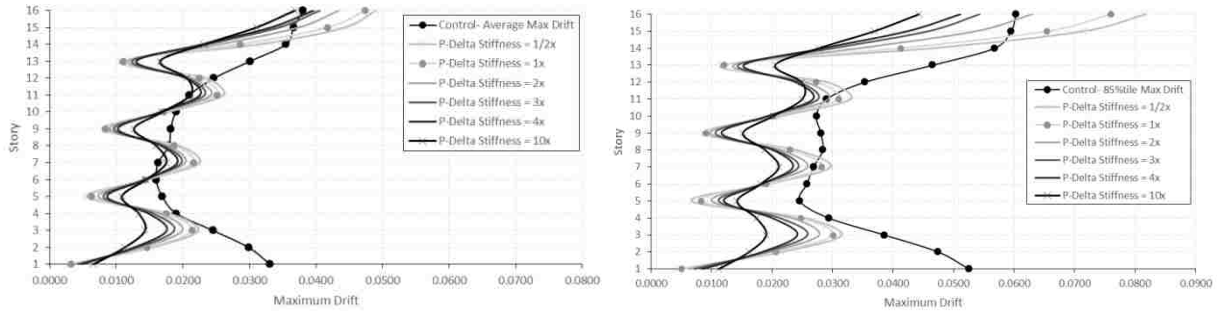

Figure G-4. Average & 85%tile maximum drifts for 3× ES at level 1, 5, 9, &13, 16S.

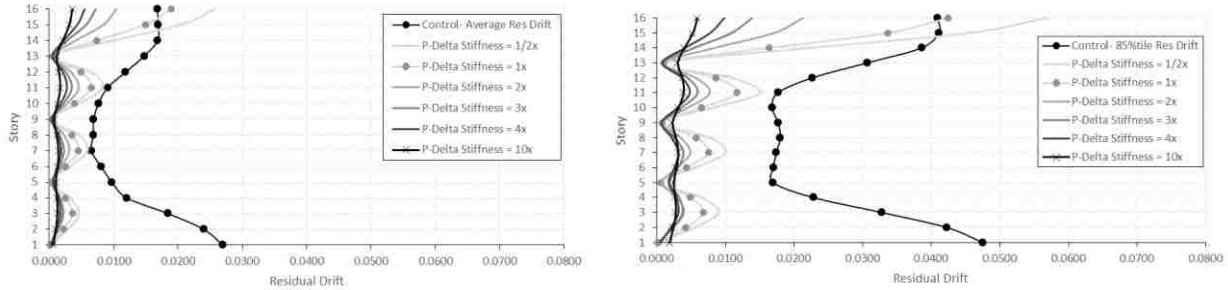

Figure G-5. Average & 85%tile residual drifts for 4× ES at level 1, 5, 9, &13, 16S.

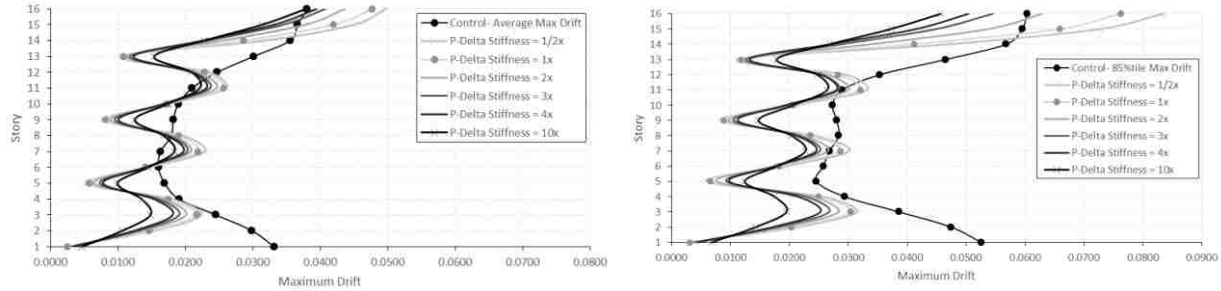

Figure G-6. Average & 85%tile maximum drifts for 4× ES at level 1, 5, 9, &13, 16S.

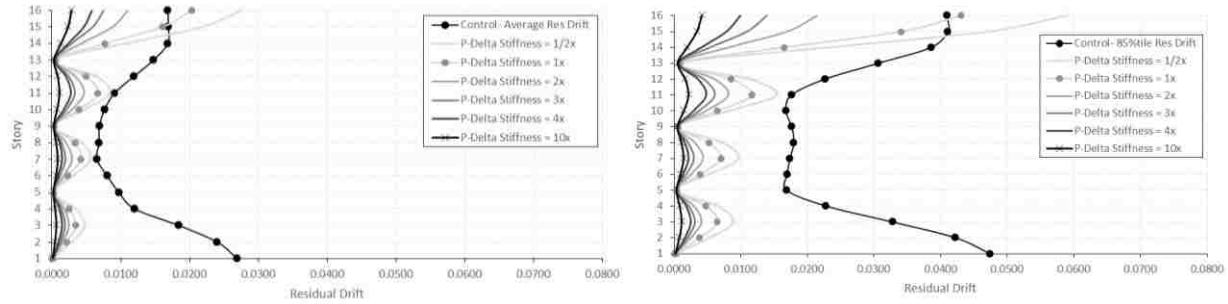

Figure G-7. Average & 85%tile residual drifts for 10× ES at level 1, 5, 9, &13, 16S.

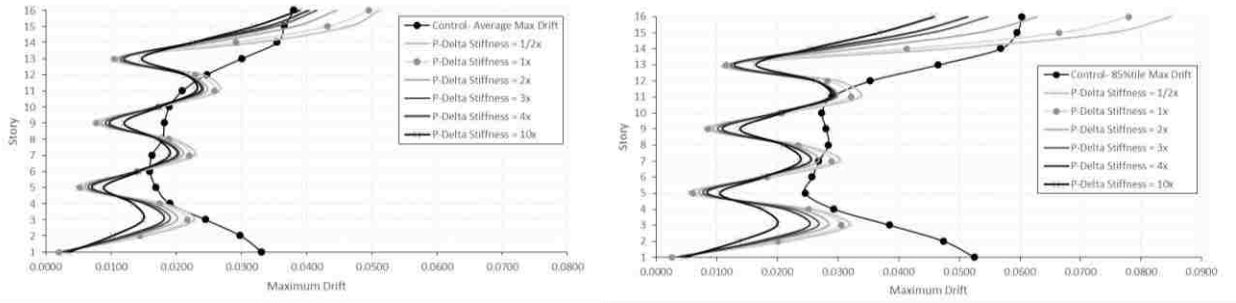

Figure G-8. Average & 85%tile maximum drifts for 10× ES at level 1, 5, 9, &13, 16S.

G.2 Elastic Story at Level 4, 8, 12, & 16

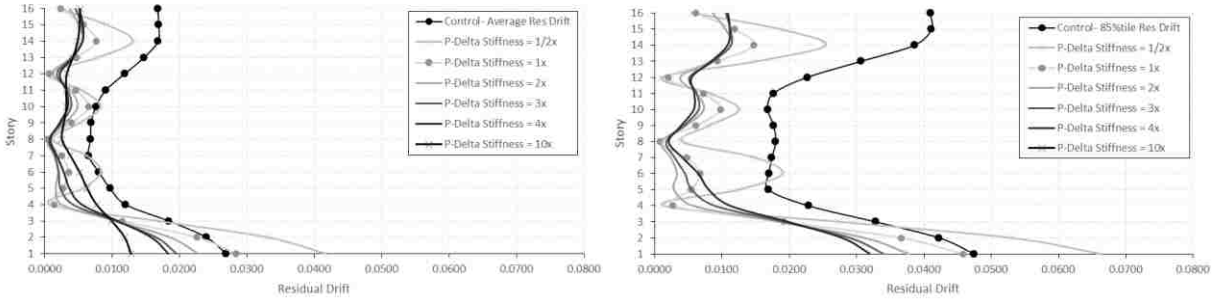

Figure G-9. Average & 85%tile residual drifts for 2× ES at level 4, 8, 12, &16, 16S.

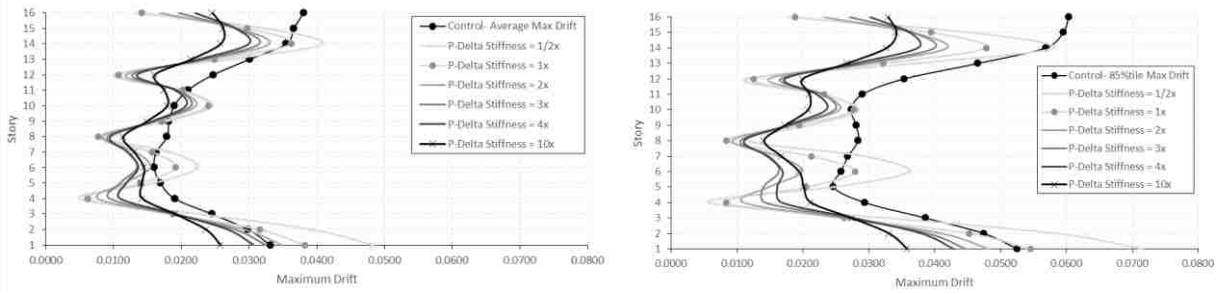

Figure G-10. Average & 85%tile maximum drifts for 2× ES at level 4, 8, 12, &16, 16S.

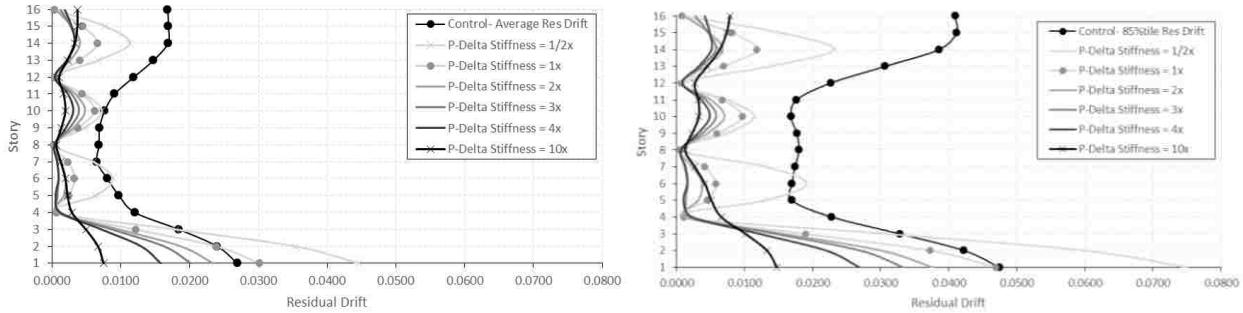

Figure G-11. Average & 85%tile residual drifts for 3× ES at level 4, 8, 12, &16, 16S.

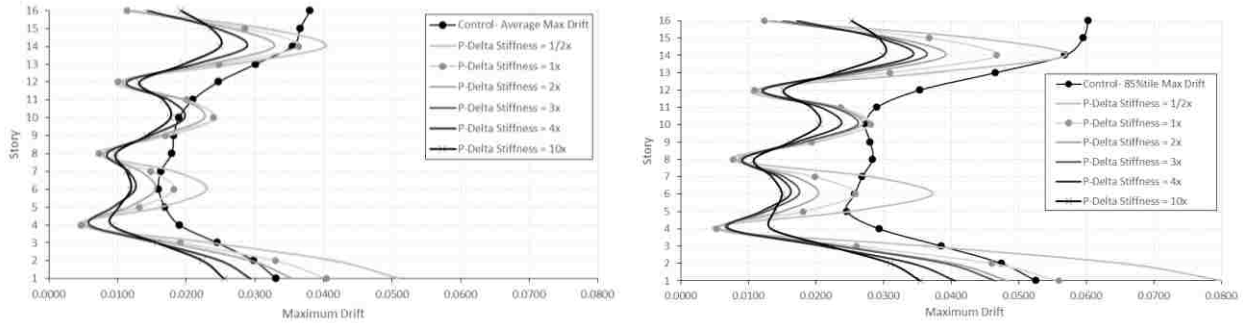

Figure G-12. Average & 85%tile maximum drifts for 3× ES at level 4, 8, 12, &16, 16S.

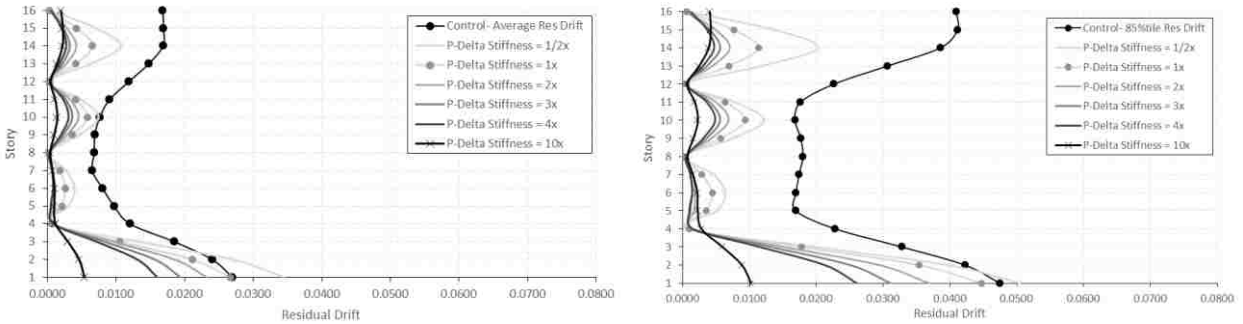

Figure G-13. Average & 85%tile residual drifts for 4× ES at level 4, 8, 12, &16, 16S.

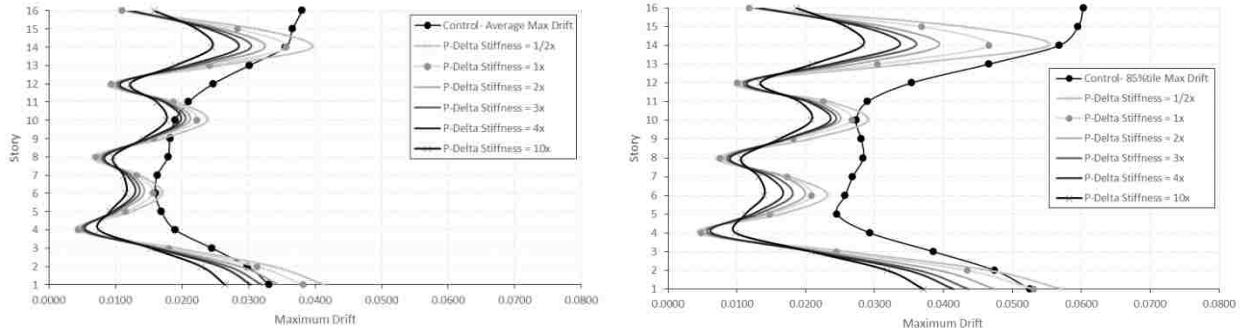

Figure G-14. Average & 85%tile maximum drifts for 4× ES at level 4, 8, 12, &16, 16S.

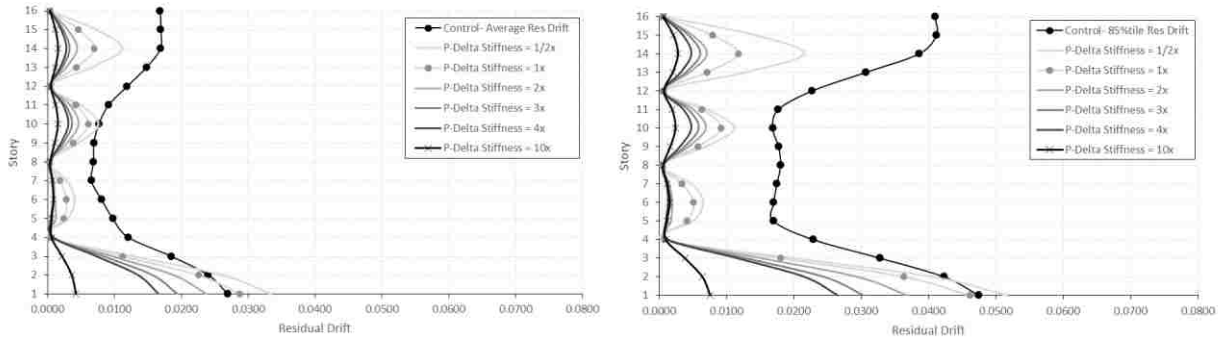

Figure G-15. Average & 85%tile residual drifts for 10× ES at level 4, 8, 12, &16, 16S.

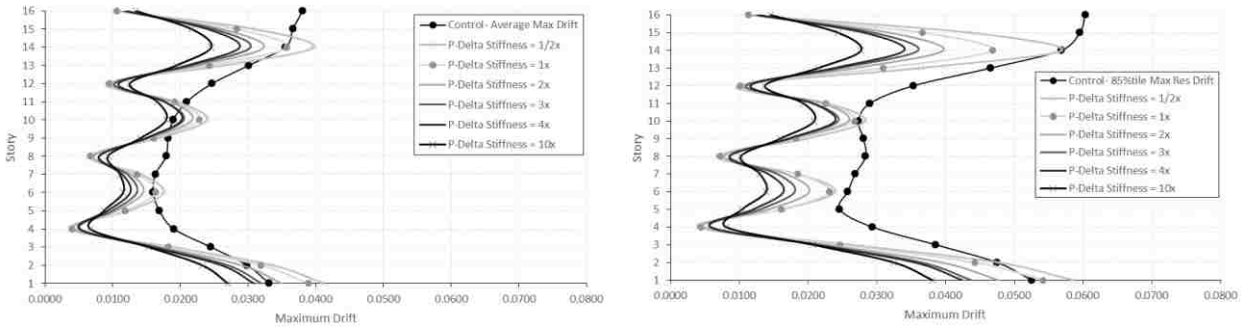

Figure G-16. Average & 85%tile maximum drifts for 10× ES at level 4, 8, 12, &16, 16S.